To the Graduate Council:

I am submitting herewith a thesis written by Hari Prasad Nadella entitled "The Effect of Melt Spinning and Drawing Variables on the Structure and Mechanical Properties of Isotactic Polypropylenes." I recommend that it be accepted in partial fulfillment of the requirements for the degree of Master of Science, with a major in Chemical Engineering.

Joseph E. Spruiell

Joseph E. Spruiell, Major Professor

We have read this thesis and recommend its acceptance:

John L. White

Edward S. Clark

Accepted for the Council

Hilton A. Smith

Vice Chancellor
Graduate Studies and Research

THE EFFECT OF MELT SPINNING AND DRAWING VARIABLES ON THE STRUCTURE AND MECHANICAL PROPERTIES OF ISOTACTIC POLYPROPYLENES

A Thesis

Presented for the

Master of Science

Degree

The University of Tennessee, Knoxville

Hari Prasad Nadella

August 1976

1288923

ACKNOWLEDGEMENTS

The author wishes to express his deepest and sincere appreciation to both Dr. J. E. Spruiell and Dr. J. L. White, his advisors, for their advice and guidance throughout this research study. Gratitude is also extended to Dr. E. S. Clark for his interest and advice in this program. Thanks are extended to the entire Chemical and Metallurgical Engineering faculty and staff for their cooperation and assistance.

The author is grateful to the Hercules and Tennessee Eastman for providing the polymer for the research. Financial assistance provided by the Chemical and Metallurgical Engineering Department is gratefully acknowledged.

Finally, special thanks are extended to my brother-in-law and sister, without whose help and guidance I would not be where I am now.

ABSTRACT

The purpose of this experimental study was to investigate the effect of spinline and drawing variables on the structure and properties of isotactic polypropylene fibers. Hercules Profax® (6323, 6423, 6823) and Tennessee Eastman Tenite® (4241, 4221) polypropylenes having a range of melt flow indices (0.42 - 12.0) were selected for the experimental study. These polypropylenes were melt spun under various spinning conditions at an extrusion temperature of 230°C. The structures of the spun filaments were characterized using wide angle x-ray diffraction, small angle x-ray scattering, birefringence and density measurements. The tensile mechanical properties were also measured for the spun filaments.

Selected fibers were drawn in an Instron tensile testing machine. Two drawing processes were examined; cold drawing followed by annealing at 140°C and hot drawing at 140°C. The structures and mechanical properties of the drawn fibers were also characterized.

The spinnability of the polypropylenes decreased with increased molecular weight and decreased flow rate. The structure of the spun filaments varied according to the spinline variables considered. Spinning polypropylene into cold water at low stresses resulted in a paracrystalline (smectic) structure, whereas spun samples spun into ambient air have a monoclinic crystal structure. For samples spun into air, the structure and morphology of the filaments could be correlated with the stress under which the crystallization occurred. Changes in variables which produced greater spinline stress such as increased take-up velocity,

decreased extrusion rate, and increased molecular weight produced increases in both crystalline and amorphous orientation and a change from a spherulitic to a row nucleated morphology. The tensile strength and elastic modulus increased and the elongation to break decreased as the spinline stress increased.

The drawn fibers showed improvements in mechanical properties over the spun fibers. The hot-drawn fibers generally showed higher levels of birefringence (average molecular orientation) and slightly better mechanical properties than the cold drawn and annealed fibers. Under the experimental conditions investigated, the mechanical properties of the drawn fibers (both cold and hot drawn) correlated with the birefringence.

This correlation with birefringence was extended to include the spun fibers as well as the drawn filaments. It is significant that the correlation seemed valid independent of the molecular weight of the polymer and the spinning and/or drawing conditions.

TABLE OF CONTENTS

CHAPTER		PAGE
I.	INTRODUCTION	1
II.	BACKGROUND AND REVIEW OF LITERATURE	4
	The Structure of Unoriented Polypropylene	4
	Crystallization Kinetics of Polypropylene in the Absence of Molecular Orientation	13
	Techniques for Characterization of Oriented Polymers	15
	The Development of Crystallinity and Orientation During Melt Spinning	20
	The Morphology of Melt Spun Fibers	25
	Structural Changes During Drawing and Heat Setting of Fibers	28
	Mechanical Properties of the Spun and Drawn Fibers	33
III.	EXPERIMENTAL DETAILS	37
	Materials	37
	Melt Spinning of Filaments	39
	Characterization of Fiber Samples	41
	Mechanical and Thermal Processing	48
	Mechanical Property Measurements	49
IV.	STRUCTURE DEVELOPMENT IN MELT SPUN FIBERS	52
	The Melt Spinning Process	52
	Structural Characterization of Melt Spun Filaments	58

CHAPTER PAGE

Discussion of Melt Spun Fibers 73

V. TENSILE PROPERTIES OF MELT SPUN FIBERS 80

Typical Tensile Curves 80

Tensile Properties and Spinline Variables--Results . . 80

Tensile Properties and Structural Variables--Results . 92

Discussion of Tensile Properties 92

VI. DRAWING AND HEAT TREATMENT OF MELT SPUN FIBERS 105

Structural Changes in the Filaments Subjected to Mechanical and Thermal Treatment 105

Mechanical Properties of Drawn Fibers. 117

VII. PROPERTIES OF SPUN AND DRAWN FIBERS. 125

VIII. CONCLUSIONS AND RECOMMENDATIONS. 130

BIBLIOGRAPHY. 134

APPENDICES. 141

Appendix A. 142

Appendix B. 144

VITA. 147

LIST OF TABLES

TABLE		PAGE
I.	As-Received Polymer Properties	38
II.	Spinning Conditions for Polypropylenes	53
III.	Characterization of Spun Polypropylene Fibers.	56
IV.	Percent Crystallinity for Polypropylenes at Various Take-up Velocities	65
V.	Characteristics of Spun Fibers Selected for Drawing Studies and Draw Ratios.	106
VI.	Estimated Values of Crystalline Orientation Factors of the Drawn Fibers.	143
VII.	Experimental Data of Polypropylene Fibers Spun at 230°C Extrusion Temperature.	145
VIII.	Experimental Data on Drawn Polypropylene Fibers.	146

LIST OF FIGURES

FIGURE		PAGE
1.	Schematic Representation of (a) Isotactic, (b) Syndiotactic and (c) Atactic Polypropylene Chain Segments . .	6
2.	Projection on (001) of the Structure of Polypropylene Assuming the Cc Space Group	8
3.	Schematic Diagram of Melt Spinning Equipment.	40
4.	Fiber Sample Holder Attachment for Obtaining WAXS Patterns.	43
5.	Schematic Arrangement of X-Ray Equipment for Orientation Factor Measurements.	47
6.	Fiber Sample Holder Used for Annealing Studies.	50
7.	Plot of Reduced Viscosity Versus Concentration Yielding Intrinsic Viscosities for Melt Spun and As-Received Polypropylenes. Measurements Were Made at 137°C in Decalin	55
8.	Effect of Take-up Velocity and Mass Flow Rate on Spinline Stress for Polypropylene Monofilaments	57
9.	Effect of Take-up Velocity and Cooling Medium on WAXS Patterns of Melt Spun H-0660 (a) 50 Meters/Min, (b) 200 Meters/Min, (c) 550 Meters/Min, (d) 25 Meters/Min, (e) 100 Meters/Min, (f) 300 Meters/Min. . .	59
10.	Effect of Molecular Weight and Melt Flow Rate on Crystalline Orientation at 200 Meters/Min Take-up	

FIGURE PAGE

Velocity, (a) H-1200, (b) T-900, (c) T-0255, (d) H-0042 (0.5 gm/min) 61

11. WAXS Pattern Showing Bimodal Orientation, (a) in Spun Fiber and the Lack of It (b) in Drawn Fiber 62

12. Effect of Spinline Stress on SAXS for Melt Spun Polypropylenes, (a) T-0255-50 (σ_L = 0.3 x 10^6 dynes/cm^2), (b) T-0255-200 (σ_L = 12.0 x 10^6 dynes/cm^2), (c) H-0042-50 (σ_L = 15.5 x 10^6 dynes/cm^2), (d) H-0042-200 (σ_L = 55.1 x 10^6 dynes/cm^2) 63

13. Changes in Percent Crystallinity with Spinline Stress for Polypropylene Fibers. 66

14. Crystalline Orientation Factor (f_c) as a Function of Take-Up Velocity in Polypropylene Fibers. 67

15. Orientation Functions ($f_{a'}$, f_b, and f_c) of Polypropylene Filaments as a Function of Spinline Stress. 69

16. Birefringence in Polypropylene Filaments as a Function of Take-up Velocity 71

17. Total and Amorphous Birefringence of Polypropylene Filaments as a Function of Spinline Stress. 72

18. Crystalline and Amorphous Orientation Factors (f_c and f_{am}) of Polypropylene Filaments as a Function of Spinline Stress 74

19. Comparison of Orientation Factors Obtained by Henson (36) for Three Different Spinning Temperatures on H-0660 to

FIGURE PAGE

the Present Results for Different Polypropylenes 76

20. Morphological Model for Bimodal Orientation of Polypropylene 78

21. Typical Tensile Curves for Polypropylene Filaments 81

22. Modulus Versus Take-up Velocity of Polypropylene Filaments. 82

23. Yield Strength Versus Take-up Velocity of Polypropylene Filaments. 83

24. Tensile Strength Versus Take-up Velocity of Polypropylene Filaments. 84

25. Percent Elongation to Break Versus Take-up Velocity of Polypropylene Filaments. 85

26. Elastic Modulus Versus Spinline Stress of Polypropylene Filaments. 87

27. Yield Strength Versus Spinline Stress of Polypropylene Filaments. 88

28. Tensile Strength Versus Spinline Stress of Polypropylene Filaments. 89

29. Percent Elongation to Break Versus Spinline Stress of Polypropylene Filaments. 90

30. Percent Elastic Recovery on the Second Cycle at 100 Percent Extension Versus Spinline Stress of As-Spun Unannealed Polypropylene Filaments 91

31. Modulus Versus Birefringence of Spun Polypropylene Filaments. 93

FIGURE PAGE

32. Yield Strength Versus Birefringence of Polypropylene Filaments 94

33. Tensile Strength Versus Birefringence of Polypropylene Filaments 95

34. Percent Elongation to Break Versus Birefringence of Polypropylene Filaments 96

35. Modulus Versus Crystalline Orientation Factor, f_c, of Melt Spun Polypropylene Filaments 97

36. Yield Strength Versus Crystalline Orientation Factor, f_c, of Melt Spun Polypropylene Filaments. 98

37. Tensile Strength Versus Crystalline Orientation Factor, f_c, of Melt Spun Polypropylene Filaments. 99

38. Percent Elongation to Break Versus Crystalline Orientation Factor, f_c, for Melt Spun Polypropylene Filaments 100

39. Tensile Strength Versus Amorphous Orientation Factor, f_{am}, of Melt Spun Polypropylene Filaments. 101

40. Percent Elongation to Break Versus Amorphous Orientation Factor, f_{am}, of Melt Spun Polypropylene Filaments 102

41. Effect of Cold Drawing on Melt Spun Fiber, (a) Melt Spun and (b) Cold Drawn Fiber (Before Annealing) 107

42. WAXS Patterns for Low Molecular Weight Polypropylene Filaments (H-1200) Spun at 200 Meters/Min Showing the Effects of Either Cold Drawing at 140°C, (a) As-Melt Spun, (b) DI, Draw Ratio = 4.0, (c) DII, Draw Ratio = 6.8, (d) DIII, Draw Ratio = 9.5, (e) TI, Draw

FIGURE PAGE

Ratio = 6.4, (f) TII, Draw Ratio = 6.8, (g) TIII, Draw Ratio = 9.5 108

43. WAXS Patterns for High Molecular Weight Polypropylene Filaments (H-0042) Spun at 50 Meters/Min Showing the Effects of Either Cold Drawing and Annealing at 140°C (b through d) or Hot Drawing at 140°C (e through g), (a) As-Melt Spun, (b) DI, Draw Ratio = 2.0, (c) DII Draw Ratio = 4.1, (d) DIII, Draw Ratio = 6.2, (e) TI, Draw Ratio = 2.0, (f) TII, Draw Ratio = 4.1, (g) DIII, Draw Ratio = 6.2. 110

44. WAXS Patterns for High Molecular Weight Polypropylene Filaments (H-0042) Spun at 550 Meters/Min Showing the Effects of Either Cold Drawing and Annealing at 140°C (b through d) or Hot Drawing at 140°C (e through g), (a) As-Melt Spun, (b) DI, Draw Ratio = 2.0, (c) DII, Draw Ratio = 2.9, (d) DIII, Draw Ratio = 3.8, (e) TI, Draw Ratio = 2.0, (f) TII, Draw Ratio = 2.9, (g) TIII, Draw Ratio = 3.8. 111

45. SAXS Patterns for As-Spun and Drawn (Draw Ratio = 6.8) H-1200-200 Fibers, (a) As-Spun, (b) Cold Drawn, (c) Cold Drawn, Annealed at 140°C for 15 Minutes, (d) Hot Drawn at 140°C (Time Taken for Drawing ∿ Seven Minutes). 113

46. Birefringence Versus Draw Ratio of As-Spun, Cold Drawn and Annealed and Hot Drawn Polypropylene Fibers 114

FIGURE PAGE

47. Typical Stress-Strain Curves for Drawn and As-Spun Polypropylene Fibers 118

48. Tensile Strength Versus Draw Ratio of Cold Drawn and Annealed and Hot Drawn Polypropylene Fibers. 119

49. Modulus Versus Birefringence of Cold Drawn and Annealed and Hot Drawn Polypropylene Fibers 121

50. Tensile Strength Versus Birefringence of Cold Drawn and Annealed and Hot Drawn Polypropylene Fibers. 122

51. Percent Elongation Versus Birefringence of Cold Drawn and Hot Drawn Polyproylene Fibers. 123

52. Elastic Modulus Versus Birefringence for Polypropylene Fibers. Variables Include Polymer Molecular Weight, Spinning Conditions (Flow Rate, Take-Up Velocity) and Drawing Procedures 126

53. Tensile Strength Versus Birefringence for Polypropylene Fibers. Variables Include Polymer Molecular Weight, Spinning Conditions (Flow Rate, Take-Up Velocity) and Drawing Procedures 127

54. Percent Elongation to Break Versus Birefringence for Polypropylene Fibers. Variables Include Polymer Molecular Weight, Spinning Conditions (Flow Rate, Take-Up Velocity) and Drawing Procedures 128

CHAPTER I

INTRODUCTION

Isotactic polypropylene is a crystalline thermoplastic polyolefin. It assumes a special position because of its stereo regular structure. Isotactic polypropylene entered the stage of large scale production in 1957, and since then it has grown at a phenomenal rate, especially since 1963 (26).

Polypropylene (PP) is tied in very closely both technically and commercially with linear polyethylene. The entire technology of polypropylene manufacture is based on the methods developed by Ziegler to make linear polyethylene (58). During the early and mid 1950's, Natta (68) at the Instituto Di Chimica Industriale Politecnico, Milan, discovered that PP and higher α-olefins can be polymerized by the use of coordination catalysts ($TiCl_3$-$Al(C_2H_5)_3$). This led to the concept of stereo specific polymerization and stereo regularity in polymer chains, i.e., various states of tacticity (atactic, isotactic and syndiotactic). The crystallizability of the stereo regular polymers result in properties of commercial interest (13), especially for the isotactic material.

Isotactic polypropylene has become both an important thermoplastic and fiber in recent years. It is its fiber-forming properties which are the primary concern of this thesis. The final properties of the fibers produced from isotactic polypropylene depend upon their molecular orientation, crystallinity and morphological structure.

These characteristics are controlled by the methods and conditions of fiber formation (84).

Melt spinning and drawing processes are to be considered in this thesis. Melt spinning, first considered by Carothers and Hill (16), consists of feeding the solid polymer to an extruder. The extruder serves to melt and homogenize the polymer and delivers it to a set of small orifices (spinneret). A metering pump is frequently provided to give a stable constant flow rate. The melt emerging from the die decends vertically, is solidified and taken up on a godet. In the drawing operation the spun fibers are made to pass between two rolls which rotate at different speeds, thereby stretching the fiber.

Carothers and Hill (16) first investigated the relationship between the spinning conditions and the structure and the properties of the fiber (linear alphatic polyester) produced. These studies of optical and x-ray scattering characteristics of the fibers indicate an increase in the molecular orientation, hence the tensile strength, with increasing drawdown tension in the fiber. Later studies of Ziabicki and Kedzierska (104, 105, 106, 107, 108) indicate that orientation is a direct function of spinline stress and an inverse function of the difference between the take-up and extrusion velocities and diameter of the filament.

In polyolefins such as polyethylene and polypropylene, crystallization and some orientation occur during spinning, while further orientation occurs during subsequent processing. The effect of various conditions of melt spinning, drawing and annealing on structural parameters and the relationship between the structural

parameters and the mechanical properties for polypropylene fibers has been considered, though incompletely, by Sheehan and Cole (84) and Samuels (78, 79, 81).

The present research is a continuation of research work on fiber processing carried out in the Department of Chemical and Metallurgical Engineering, The University of Tennessee, Knoxville. Earlier studies on polyethylene included investigation of melt spinning dynamics, melt rheological characteristics and heat transfer from monofilament fibers (3, 17), development of crystallinity and orientation along the spinline (1, 2, 22), interaction of spinning and drawing variables on polyethylene fiber crystallinity, orientation and mechanical properties (23, 100). Research work recently completed (36) includes studies of development of structure, orientation and crystallinity along the spinline during the melt spinning of one type of polypropylene monofilaments.

The purpose of the present research project is twofold. First the effect of varying the molecular weight and the resin manufacturer (tacticity, molecular weight distribution) on the resulting structure and properties of melt spun polypropylene monofilaments was to be investigated and compared to the previous work. The second area involved an investigation of the drawing of the several melt spun polypropylenes and the interaction of drawing and spinning variables on the structure and properties of the final drawn filaments.

CHAPTER II

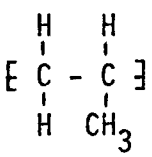
BACKGROUND AND REVIEW OF LITERATURE

A. THE STRUCTURE OF UNORIENTED POLYPROPYLENE

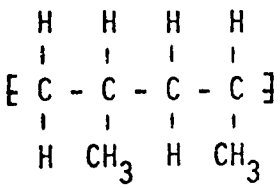
A complete description of the structural characteristics of polypropylene includes specification of its molecular configuration, studies of its various polymorphic forms (including molecular conformation and packing) and a description of its commonly observed morphological features. In this first section of Chapter II these features are considered for the case that molecular orientation is absent. The nature of molecular orientation and its significance in fiber processing are considered in later sections.

Molecular Configuration

The chemical repeat unit of polypropylene is



These units normally repeat in head to tail fashion as follows:



Polypropylene can be synthesized in a wide range of tacticities, including highly stereo specific isotactic and syndiotactic forms as well as the atactic form. These tactic forms are illustrated schematically in Figure 1. In the isotactic case the substituent methyl groups are all on the same side of the main carbon chain when the chains are fully extended whereas in the syndiotactic form the pendent methyl groups alternate regularly (6). In the atactic form the methyl groups possess a considerable degree of randomness in their location relative to the carbon chain backbone (83).

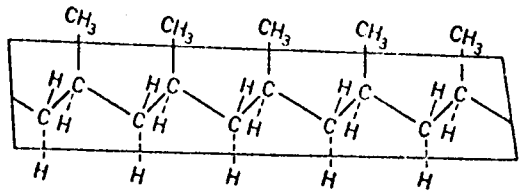
Both isotactic and syndiotactic polypropylenes are partially crystalline whereas the atactic form, because of its lack of stereoregularity along the molecule, is necessarily amorphous. Commercial polypropylenes are highly isotactic and have high crystallinity; these are of particular interest in this research. Most of the discussion in the remainder of this section relates to the isotactic form.

Polypropylene Phases

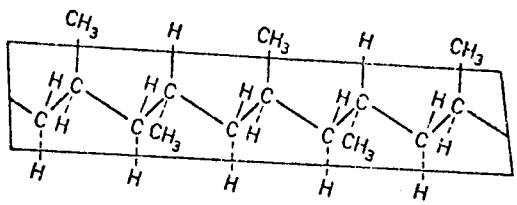
A number of phases exist for isotactic polypropylene including an amorphous phase, three different crystalline forms (α, β, γ), and a so-called paracrystalline form (4, 62, 66, 70). The occurrence of the various forms is dependent on the molecular weight, degree of isotacticity and the thermal and mechanical history of the sample.

The α- or monoclinic form is the crystalline form generally observed for both melt and solution crystallized samples prepared at atmospheric pressure (62).

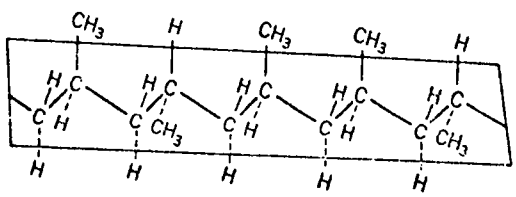
A structure determination was carried out on the α-phase isotactic



(a)



(b)



(c)

Figure 1. Schematic Representation of (a) Isotactic, (b) Syndiotactic and (c) Atactic Polypropylene Chain Segments

polypropylene by Natta and Corradini (71) and Turner Jones, et al. (97). From wide angle x-ray diffraction (71), the identity period on the c-axis was found to be 6.5Å. From this it was concluded that the chains have a threefold helical configuration (3_1 helix), which corresponds to a regular alternation of trans and gauche bonds $(tg)_n$. The x-ray studies of Natta and Corradini (71) established monoclinic symmetry for the unit cell. The values of the unit cell constants are

$a = 6.65 \pm 0.5$Å $\qquad b = 20.96 \pm 0.15$Å

$c = 6.50 \pm 0.64$Å $\qquad \beta = 99° 20' \pm 1°$

The unit cell volume contains twelve monomeric units (chemical repeat units). The absence of hkl reflections (71) with $h + k = 2n \pm 1$ confirms that the whole crystal lattice is c-centered. According to Natta and Corradini (71) the most probable space group for polypropylene is Cc. Assuming this space group, the crystal structure of the α-form is as shown in Figure 2.

The β-form is obtained by rapidly quenching the polymers from the melt to below 130°C (97). X-ray diffraction study of the β-form suggests that the unit cell is hexagonal. Keith and Padden (48) suggested a hexagonal unit cell with constants a = 12.71Å and b = 6.35Å.

The γ-form is only obtained by cooling from the melt. It frequently occurs in small amounts in specimens of unfractionated polypropylene as shown by the presence of a weak line at 4.42Å. It is characterized by five strong x-ray reflections, four of which lie very close to the four of the five strong reflections of the α-form given by

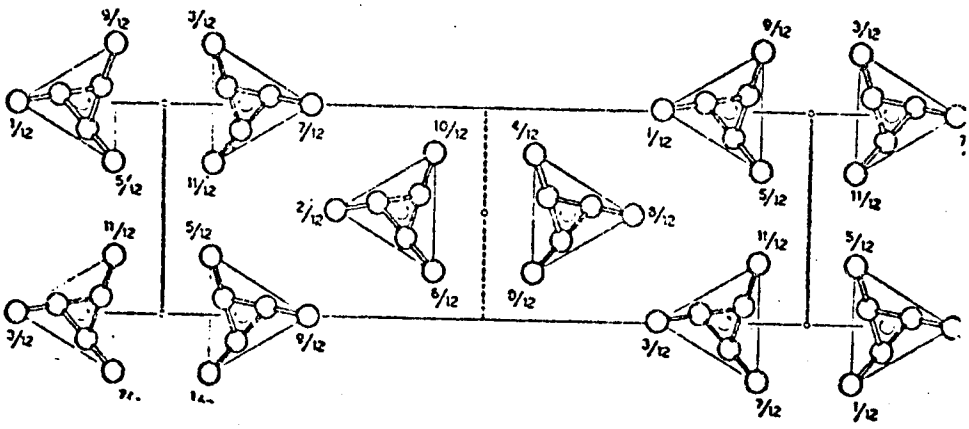


Figure 2. Projection on (001) of the Structure of Polypropylene Assuming the Cc Space Group

Source: G. Natta and P. Corradini, Nuovo Cimento, 15, 40 (1960).

unoriented specimens. The line at 4.77Å of the α-form is replaced by the line at 4.42Å.

Addink and Bientema (4) observed the γ-modification in specimens of low molecular weight. They also observed a lesser crystalline form, δ-modification in specimens of highly amorphous materials separated from the bulk isotactic material by extraction.

Though isotactic polypropylene is capable of crystallizing in three main polymorphic forms, α-phase (monoclinic) is the normal form found in isotactic polypropylene. The β-phase (hexagonal) is metastable in character and it reverts to α-phase by deformation or by recrystallization. The γ-modification is either metastable or stable depending on conditions of sample preparation.

Allowing a melt of isotactic polypropylene to cool slowly yields a mixture of two phases, amorphous and the α-crystalline form. Rapid cooling by quenching into ice water can produce the paracrystalline, smectic phase (66, 70). This intermediate form, which is neither truly crystalline or amorphous, has been observed by several investigators (31, 43, 84, 103). Hosemann (39) appears to be the first to refer to this intermediate form as "paracrystalline." The presence of this paracrystalline phase in quenched polypropylene has led to the suggestion that the structure might best be interpreted in terms of a two-component three phase model (103). The two components are crystallizable and non-crystallizable parts of the bulk polymer and the three phases are amorphous, paracrystalline and crystalline (31, 103). The relative amounts of these phases are presumed to be very sensitive to the quench conditions (31, 43). According to this interpretation the unoriented

halo does not change much with thermal treatment, illustrating the non-crystallizability of this component. The amorphous phase comprises 25 percent to 30 percent of the bulk compared to the 5.8 percent heptane extractables (103). In this interpretation the paracrystalline phase is presumed to result from a highly disordered part of the crystallizable polymer and is distinct from the non-crystallizable part which is even more disordered. This interpretation is not universally accepted and other investigators have made other suggestions concerning the structure of the quenched polypropylene. Natta (70) termed the structure of a quenched polypropylene as "an unstable crystalline smectic modification." Miller (66), from the x-ray patterns of quenched isotactic polypropylene, concluded that there was complete absence of any indication of crystallinity. Boye, Watson and Patton (14) state that the para-crystalline form is more crystalline than amorphous.

X-ray studies (8, 70) of the unoriented smectic form revealed two strong halos with d-spacings 5.9Å and 4.1Å, respectively. Structural interpretations (39, 66, 70, 103) hold that smectic polypropylene has a short range three-dimensional order with the molecules in the same conformation as the crystalline α-form. Disorder occurs in the packing of chains perpendicular to their axes (39, 66, 70, 103). Several investigators (29, 31, 91) suggested a hexagonal crystal lattice for the smectic polypropylene.

The smectic form converts to the α- (monoclinic) form on heating (66) while the α-form can be converted to the smectic form by cold deformation (84, 103).

Morphology of Solution and Melt Crystallized Polypropylene

Single crystals of isotactic polypropylene have been grown by cooling very dilute solutions of the polymer. Well defined folded-chain, lamellar crystals were obtained from dilute solutions of high molecular weight fractions in α-chloronapthalene.

Khoury (54) studied the development of monoclinic spherulites as they grew from more concentrated solutions. He noted unusual dendritic, precursor crystals from which the spherulites evolve. These appeared to consist of lamellar branches which criss-crossed each other producing a basket-weave appearance.

When a polymer melt is allowed to cool slowly some of the molecules will crystallize into folded-chain lamellae while others will not, resulting in a two-phase crystalline plus amorphous model. The crystalline region is composed of individual crystallites formed from molecules folded back on themselves (30, 74). These lamellae are connected to each other through tie molecules. The amorphous region may consist of less tactic molecules, tie molecules and so on, which contribute to the imperfections and disorder. These crystalline and non-crystalline regions associate into larger ordered arrangements, ultimately forming spherulites and the spherulites in turn are interconnected through interspherulitic fibrillar links (79). The crystals in the interfibrillar links are oriented with their chain axes parallel to the fibrillar axis, whereas the crystals along the radii of the spherulites can have different orientations depending on temperature and growth conditions (30, 47).

Keith and Padden (49) made a survey of spherulites formed by the

isothermal crystallization of polypropylene from the melt in the temperature range of 110-149°C. They distinguished four types of spherulites from the study of optical properties and conditions of growth.

Keith and Padden (48) obtained diffraction patterns with isotactic polypropylene spherulites of types I and II. These patterns show stronger reflections at smaller bragg angles and these all can be identified and indexed as from the monoclinic structure proposed for isotactic polypropylene by Natta and his co-workers (69). Keith and Padden (48) and Van Hans (99) reported that the β-form results from the crystallization of rarer types of spherulites (types III and IV).

The morphology of the quenched form (smectic) of polypropylene was investigated by Gezovich and Geil (31). Thin films of quenched polypropylene consist of small ball-like structures, which are defective hexagonal crystals. In thicker films they aggregate to form spherulites with no observable fine structure. They obtained smectic spherulites by quenching the melt to above 0°C. Quenching the polypropylene melt to below 0°C results in the formation of numerous, isolated monoclinic spherulites with a better defined morphology (31).

Levels of Crystallinity

There are five principal methods which adequately determine the degree of crystallinity:

1. X-ray diffraction
2. Density measurements
3. Heat of fusion measurements
4. Nuclear magnetic resonance

5. Infrared absorption

These methods were discussed by Mears (61) and Samuels (83).

Commercially available crystalline polypropylene samples have levels of crystallinity of order 60 to 80 percent (94). Degree of crystallinity for the spun fibers was found to be about 55 percent by several investigators (36, 83, 84, 103). Sheehan and Cole (84) determined the crystallinities for polypropylenes of varying molecular weights. However, they report an average value of 51 percent for all the samples they investigated.

B. CRYSTALLIZATION KINETICS OF POLYPROPYLENE IN THE ABSENCE OF MOLECULAR ORIENTATION

The rate of crystallization is a major factor in determining the extent of crystallization in a particular sample. Indeed polymers which crystallize slowly can often be quenched rapidly enough to retain the amorphous, super-cooled liquid phase, while other polymers which crystallize rapidly (polyethylene) cannot be prevented from crystallizing during quenching. This suggests that there is an important interaction between crystallization kinetics and the structure resulting from various processing operations. Further, the physical properties of a polymer are closely related to its detailed structural state and the conditions under which this state was approached (33). For these reasons crystallization kinetics are of primary importance in studies of structure-properties-processing relations.

Avrami (9) developed an expression for the kinetics of crystallization under isothermal conditions. His theory leads to the expression:

$$x = 1 - \exp(-Kt^n) \qquad (1)$$

where x is the fraction crystallized, K is a constant containing nucleation and growth rate parameters and n is an exponent whose value depends on the mechanism of nucleation and on the form of crystal growth. This quantity (n) can be determined experimentally.

Much work has been done in developing nucleation rate theories. Turnbull and Fisher (72) developed an expression for the absolute rate of nucleation in condensed systems. Mandelkern, Quinn and Flory (60) extended the above work of Avrami and Turnbull and Fisher to describe the kinetics of polymer systems. In this treatment they accounted for the fact that the ultimate crystallinity of polymers never approaches 100 percent, unlike low molecular weight substances.

Griffith and Ranby (33) studied the crystallization kinetics of Hercules polypropylenes between 133°C and 155°C using dilatometers. They applied the Avrami expression for isothermal crystallization in the form

$$(V_t - V_f)/(V_o - V_f) = \exp(-Kt^n) \qquad (2)$$

where V_t is the specific volume at time t, V_f final specific volume, V_o specific volume at t = 0, n and K are the Avrami exponent and an overall crystallization rate constant.

Griffith and Ranby (33) obtained crystallization rate data for a commercial sample containing stabilizer and 9 percent extractable polymer (degree of polymerization (DP) = 10,000), an experimentally

extracted sample containing no stabilizer (DP = 7,500) and thermally degraded experimentally extracted sample (DP = 1,200). Their results indicate that crystallization rates are higher for low molecular weight (thermally degraded) samples and lower for samples with atactic content and stabilizer.

Hoshino, et al. (40) studied the crystallization kinetics of polypropylene fractions of varying tacticities using dilatometric techniques. These results were supplemented with studies using the optical microscope and x-ray diffraction. Their results are consistent with a two-stage process of crystallization: (a) radial growth at the spherulitic interface described by an Avrami equation characterized by n = 3.9 in its earlier stages (primary crystallization) and (b) secondary crystallization within the spherulite described by an Avrami equation with an exponent of 1.8.

Hoshino, et al. (40) reported that for samples of very low tacticity spherulitic structures are "frustrated" in growth at very early stages of development, and a larger part of the crystallization is of the secondary type.

C. TECHNIQUES FOR CHARACTERIZATION OF ORIENTED POLYMERS

Crystalline Orientation

Orientation of molecules and crystallites relative to arbitrarily chosen reference axes embedded in the polymer produces anisotropy in its mechanical, optical and physical properties (110). Orientation is normally produced by deformation of either the solidified polymer or of the molten mass as it is being cooled and frozen.

A quantitative expression for the average orientation of polymer chains in uniaxially oriented samples was given by P. H. Hermans and coworkers (37). For rigid crystallites the Hermans' orientation factor is,

$$f = 1 - \frac{3}{2}\overline{\sin^2 \phi_{c,z}} = [3\overline{\cos^2 \phi_{c,z}} - 1]/2 \qquad (3)$$

where $\phi_{c,z}$ is the angle between the stretch direction and the crystallographic axis parallel to the polymer chain, $\overline{\cos^2 \phi_{c,z}}$ indicates the average value of $\cos^2 \phi_{c,z}$.

Stein (89) generalized equation (3) for three crystallographic axes.

$$f_a = [3\overline{\cos^2 \phi_{a,z}} - 1]/2 \qquad (4)$$

$$f_b = [3\overline{\cos^2 \phi_{b,z}} - 1]/2 \qquad (5)$$

$$f_c = [3\overline{\cos^2 \phi_{c,z}} - 1]/2 \qquad (5)$$

where f_c corresponds to Hermans' orientation function for the crystalline regions.

From the above equations it can be seen that the orientation function for a given crystal axis has a value of +1 for parallel orientation, a value of 0 for random orientation and -1/2 for the perpendicular orientation with respect to the stretch direction. For

crystals with orthogonal axes,

$$\overline{\cos^2 \phi_{c,z}} + \overline{\cos^2 \phi_{b,z}} + \overline{\cos^2 \phi_{a,z}} = 1.0 \qquad (7)$$

and

$$f_a + f_b + f_c = 0 \qquad (8)$$

In monoclinic polypropylene there is no set of reflecting planes which is perpendicular to the c-axis. Further, since the a, b and c axes are not mutually orthogonal the above relation between f_a, f_b and f_c does not hold. Wilchinsky (101, 102) derived equations relating variation of intensity with azimuthal angle of the 110, 040 and 130 reflections in polypropylene to the orientation function parameters which characterize the b and c axes.

$$\overline{\cos^2 \phi} = 1 - \left[\frac{(1 - 2 \sin^2 \rho_2)\, \overline{\cos^2 \phi_1} - (1 - 2 \sin^2 \rho_1)\, \overline{\cos^2 \phi_2}}{\sin^2 \rho_1 - \sin^2 \rho_2}\right] \qquad (9)$$

where the subscripts refer to the respective planes. ρ is the angle between the plane normal and b-axis and can be calculated from the unit cell dimensions. ϕ is the angle between the reference direction and x-axis.

Birefringence

Birefringence is a measure of the overall state of preferred

orientation including both crystalline and amorphous contributions (6). For a uniaxially oriented specimen, it is defined as the difference between the principal refractive index parallel (n_{11}) and perpendicular ($n_{\underline{1}}$) to the stretch direction. The refractive index is related to the polarizability of the molecular chains.

For a uniaxially oriented, polycrystalline polymer the measured birefringence, Δn_T, may be defined as a combination of contributions from the crystalline and amorphous phases (neglecting the form birefringence) (85).

$$\Delta n_T = x\, \Delta n_c^\circ\, f_c + (1 - x)\, \Delta n_{am}^\circ\, f_{am} \qquad (10)$$

where Δn_c° and Δn_{am}° are intrinsic birefringence of perfectly oriented crystalline and amorphous regions respectively, f_c and f_{am} are the crystalline and amorphous orientation functions and x is the crystalline fraction.

Amorphous Orientation

The Hermans-Stein orientation functions discussed earlier relate to the crystal regions in the polymer. The original Hermans orientation factor can be used to quantitatively describe the degree of orientation in the amorphous regions, but this quantity is not easily obtained from x-ray diffraction measurements. To measure the orientation in the amorphous regions it is common to use a physical property which is highly dependent on the orientation in the sample. If the sample is partially crystalline, the amorphous orientation function is obtained by

difference using an expression similar to Equation (10). In this case the crystalline contribution is evaluated by techniques described previously, and the difference between the average property and the crystalline contribution gives an amorphous contribution from which f_{am} can be obtained.

Millberg (65) explained the use of x-ray methods and infrared measurements in determining the amorphous orientations. Samuels (83) used birefringence and sonic modulus in the determination of the amorphous orientation function. In the present research birefringence, crystalline fraction, crystalline orientation functions, Δn_c° and Δn_{am}° were used in Equation (15) to calculate the amorphous orientation function.

Morphology

Small angle x-ray scattering (SAXS) is measured by both photographic and diffractometric techniques. The SAXS measurements provide information about variations of electron density in the sample, which are in the range of tens to hundreds of angstrom units. Frequently the only cooperative reflections that appear in the SAXS pattern occur as a consequence of periodic arrangement of crystal lamellae and intercrystalline disordered regions. Measurement of the position of the interference maximum allows direct calculation of this so-called long period or the distance between crystal centers. Since the long period spacing measures the distance between crystal centers, it can be considered equal to the sum of the thickness of the crystalline and amorphous or intercrystalline regions (83).

D. THE DEVELOPMENT OF CRYSTALLINITY AND ORIENTATION DURING MELT SPINNING

In this section fundamental studies of oriented crystallization kinetics and of the development of orientation and crystallinity during melt spinning are considered. Detailed considerations of the morphology of spun filaments are reviewed in the next section. Before proceeding, it is worth noting at this point that a review paper on the subject of "Structure Development During Melt Spinning" has been published recently by Spruiell and White (88).

Keller (50, 51) did much work concerning orientation and crystallization in polymers. He reported that under certain conditions the extrusion process can produce a characteristic perpendicular orientation of the crystallites.

Ziabicki and Kedzierska (104, 107, 108) studied orientation in Nylon-6 fibers by means of birefringence and x-ray diffraction and found that orientation by spinning is not accompanied by structural transformation as occurs during cold drawing of this polymer. They concluded that the development of orientation in Nylon-6 fibers occurs along the spinline while the polymer is still molten and is a result of the simultaneous action of the velocity gradient and thermal relaxation. Ziabicki and Kedzierska (105, 106) found orientation to increase monotonically with difference between take-up and extrusion velocities and with the reciprocal of fiber diameter.

Crystallization as it occurs during melt spinning takes place in a non-isothermal environment under molecular orientation. Ziabicki

(109) has dealt with the process in a theoretical treatment of melt spinning and has proposed a new parameter called the "kinetic crystallizability." By using the parameter he (109) related the crystallinity of as-spun filaments to the polymer characteristics and cooling conditions. This model adequately predicts the fact that some polymers will not crystallize during spinning due to rapid cooling rates and slow crystallization kinetics. Ishibashi, Aoki and Ishii (42) have investigated non-isothermal crystallization taking place in the course of solidification process of Nylon-6. Both the above treatments take no account of the heat of crystallization. Nakamura, Watanabe and Katayama (67) considered the effect of heat of crystallization and developed an explicit expression for the rate of crystallization. Katayama, et al. (46) obtained an expression for the ultimate percentage crystallinity. All the above studies have neglected the influence of applied stress on crystallization rates during processing.

Katayama, Amano and Nakamura (46), Dees and Spruiell (22) and Henson (36) have made on-line studies of the development of crystallinity in the spinline for high density polyethylene and polypropylene fibers using on-line WAXS measurements. Their observations showed the important effect on crystallization kinetics of molecular orientation resulting from the elongational flow and draw down forces (stress). Spruiell and White (88) prepared continuous cooling transformation curves (CCT) to compare the kinetics of crystallization during melt spinning for polyethylene and polypropylene to those for quiescent melts of the same polymers. They concluded that the stress and the accompanying molecular orientation decreases the free energy of

formation of crystal nuclei, and it is primarily this fact which leads to the crystallization rates.

The variation in the level of crystallinity in melt spun polyethylene fibers as a function of take-up velocity has been studied by Kitao, Ohya, Furakawa and Yamashita (56), Abbott and White (1), Dees and Spruiell (22) and White, Dharod and Clark (100). They found that the ultimate crystallinity in the spun fibers decreases with take-up velocity. Such variation in crystallinity has been explained by Ziabicki, Abbott and White and White, et al. Ziabicki (109) and Abbott and White (1) suggest that it is the result of increased cooling rates due to the higher ratio of surface area to mass in the fiber at higher take-up velocities which leads to smaller residence time in the region of maximum crystallization rates. This view seems questionable because of the rapid crystallization rate of polyethylene not too far below its melting temperature. White, et al. (100) offer an alternative view which is perhaps more useful: "There seems to be no amorphous regions in high density polyethylene in the classical sense. Application of tensile stress greatly increases the rate of crystallization which in turn gives rise to greater levels of crystalline disorder. There is insufficient time for conformational adjustment of the chains to produce the high level or order often found in single crystals carefully grown from solution, resulting in lower crystallinity."

Katayama, et al. (46), Kitao, et al. (56), Abbott and White (1), Dees and Spruiell (22) and White, et al. (100) studied the crystalline orientation in melt spun polyethylene fibers. All of these investigators except Katayama, et al. (28) determined crystalline orientation factors as a function of take-up velocity. These results show a nearly

random orientation at low take-up velocity ($f_a = f_b = f_c \sim 0$). At higher take-up velocities, the a and b crystallographic axes tend to become perpendicular to the fiber axis ($f_a \sim -0.40$, $f_b \sim -0.45$), while the chain axis (c-axis) becomes increasingly parallel to the fiber axis ($f_c \sim .85$) (56). Dees and Spruiell (22) also observed the on-line development of orientation in polyethylene and interpreted their results as evidence for a skin-core fiber structure under certain spinning conditions.

The effect of molecular weight on the interaction of fiber crystallinity and orientation was studied by Abbott and White (1) and White, et al. (100). For a given set of spinning conditions they found a higher order of orientation in high molecular weight polymer. However, they observed a similar trend of orientation with spinning conditions in high density high molecular weight and high density low molecular weight polyethylenes.

Studies of orientation development in polypropylene were conducted by Katayama, et al. (46), Kitao, et al. (56), Hoshino, et al. (41), Sheehan and Cole (84), Samuels (81, 82), Henson (36) and Spruiell and White (88).

Sheehan and Cole (84) observed x-ray patterns for undrawn polypropylene filaments made by spinning polymers of different molecular weights under different conditions of extrusion and quenching temperature. The x-ray patterns of filaments cooled rapidly by quenching into water showed that these materials were the smectic form of polypropylene. Fibers spun into air were the monoclinic form. The orientation was shown to be a function of spinning conditions, but quantitative orientation

measurements were not made.

Katayama, et al. (46) reported for polypropylene, polyethylene and polybutene a monotonic increase in birefringence which starts prior to crystallization but increases rapidly as crystallization proceeds. There is also a decrease in the diameter and surface temperature of the fiber.

The manner in which the orientation of the crystal axes are changing with processing conditions can be represented by an orientation function triangle (89). Kitao, et al. (56) presents an orientation function triangle diagram for polypropylene as-spun fibers which are in agreement with data obtained by Samuels (82) (melt-spun fibers) and Hoshino, et al. (41).

Hoshino, et al. (41) used birefringence measurements to characterize the total orientation as well as that of crystalline and of less ordered regions.

Henson (36) and Spruiell and White (88) studied the effect of melt temperature, take-up velocity and spinline stress on the development of orientation during melt spinning of isotactic polypropylene through WAXS. The general trend in the orientation functions versus take-up velocity plots were similar to those observed for polyethylene. The c-axis orientation factor increases with take-up velocity ($f_c \sim 0.6$), the value being higher for lower melt temperature, yielding three different curves for the three different temperatures studied (200°C, 230°C, 260°C). The orientation function when plotted against the spinline stress showed no independent effect of melt temperature but increased monotonically with spinline stress.

Inspite of its overall apparent similarity to polyethylene, the crystalline orientation developed in melt-spun oriented polypropylene is complicated by the existence of bimodal distribution of the unit cell orientations. In one population of crystals, termed as the c-axis oriented population, the c-axis is approximately parallel to the fiber axis with the b and a axes cylindrically disposed about this axis. In the other population of crystals, termed a'-axis oriented population, the a'-axis (a'-axis is perpendicular to b and c crystallographic axes) is parallel to the fiber axis, with b and c cylindrically disposed about this axis (88). Morphological interpretations of these results are discussed in the next section.

The contributions by the amorphous chains to the total orientation in melt-spun polypropylene fibers was evaluated by Kitao, et al. (56) and Samuels (83). They both concluded that the orientation developed in the amorphous chains during melt spinning is less compared to the orientation developed in the crystalline regions.

E. THE MORPHOLOGY OF MELT SPUN FIBERS

The organization of the sub-structure within the spun fiber at all morphological levels is complex. Its particular character will depend on spinning conditions (24, 83).

The importance of spinning conditions on the fiber structure was realized in the original studies of Carothers and Hill (16). Keller (50, 51) in the mid 1950's followed by Ziabicki and Kedzierska (104, 107, 108) published their work on the structures of melt spun fibers. Keller (50, 51) reported a characteristic perpendicular orientation of

the crystallites which correspond to two types of structures in the extruded samples.

In the more recent work, Keller and Machin (52) state that there is a lamellar crystal growth, normal to the stress direction nucleated along direction parallel to the stress direction. An a-axis orientation ($a = 7.4\text{Å}$) was found to exist in polyethylene fibers.

Samuels (83) discussed the structure of oriented melt spun polypropylene fibers (no details on the melt spinning were given). H_VSALS patterns indicated that the spun fibers were composed of 0.7-μ spherulites whose long axes were normal to the fiber axis direction. The spun fiber was assumed to be composed of inhomogeneously deformed spherulites and interspherulitic fibrillar links.

The work of Katayama, et al. (46) combined measurements of filament surface temperature, diameter, birefringence and both WAXS and SAXS to study structure formation in polyethylene, polypropylene and polybutene-1. Their results were interpreted to indicate a morphology consisting of lamellar and interlamellar regions stacked normal to the fiber axis. The SAXS especially indicated this morphology and pointed to similarities between polypropylene and polyethylene.

Based on their experimental studies and the suggestion of Kellar and Machin (52), Dees and Spruiell (22) proposed a detailed morphological model for melt spun linear polyethylene. This work together with other extensive experimental studies of structural development during the melt spinning of polyethylene (1, 22, 100), polyoxymethylene (53) and polypropylene (36) fibers were reviewed by Spruiell and White (88). They concluded that the morphologies developed in polyethylene,

polyoxymethylene and polypropylene with increasing take-up velocity and stress exhibit numerous similarities. At low spinline stress, the fibers have an unoriented lamellar super structure, probably a spherulitic structure which develops into a row nucleated structure at high spinline stresses.

As noted previously, melt spun polypropylene fibers often show bimodal orientation. Clark (19), Clark and Spruiell (21) and Anderson and Carr (7) have proposed morphological models for flow crystallized polypropylene. The interpretation of bimodal orientation by Clark (19) and Clark and Spruiell (21) consists of a row structure of planar lamellae interconnected by tie molecules, which give rise to the c-axis oriented contribution. The a'-axis oriented contribution is suggested to arise from interlamellar crystals which grow with a special epitaxial relationship with the primary row structure.

Highly crystalline polymers such as polypropylene and polyoxymethylene when allowed to crystallize from the melt under very high stress, produce remarkably elastic fibers and films. These elastic fibers are termed "hard" elastic materials to distinguish them from elastomers (87). Clark (20) and Sprague (87) have proposed detailed models of morphology of such "hard" elastic fibers and films. These models have considered these highly elastic fibers and films to have a well developed row structure morphology. Evidence for this structure includes SAXS and transmission electron microscopy.

Additional ordering of the initial row structured material can be achieved by annealing at elevated temperatures. These "hard" elastic fibers have moderate to high degree of orientation. SAXS

patterns show an average long period of about 140Å for celcon (polyoxymethylene) and 130 to 140Å for polypropylene (87).

F. STRUCTURAL CHANGES DURING DRAWING AND HEAT SETTING OF FIBERS

In polyolefins such as polyethylene and polypropylene crystallization and some orientation occurs during melt spinning but further orientation occurs during drawing. The spun fiber often has a low degree of anistropy, relatively unoriented molecular state and low mechanical strength. Drawing of the spun fiber results in a reorganization of the sub-structure which transforms this structure with low anisotropy into a highly anisotropic and highly oriented fiber structure with high elastic modulus and tensile strength. The character of reorganization during the drawing step not only depends on the environmental drawing conditions but also on the original structure present in the spun fiber as well. A further rearrangement of the sub-structure of the drawn fiber occurs during any subsequent heat setting process (83).

During cold drawing polymeric fibers usually form necks and shoulders. The cross section is reduced in a localized region (necks) which then travel along the length of the fiber. Carothers and Hill (16) in their early work stated that their synthetic fibers exhibited cold drawing and necking phenomena, during which the fiber is transformed from an unoriented molecular structure to an oriented one.

Fankuchen and Mark (25) analyzed the necked zone in cold drawn nylon-66. From micro beam x-ray diagrams they described orientation in necked and unnecked regions. Miklowitz (64) carried out a study of the mechanical factors influencing the initiation and the propagation of

of the plastic zone in nylon-66.

Kasai and Kakudo (44) examined the continuous structure change in the necking zone of cold drawn polyethylene using wide and small angle x-ray patterns. They also presented a series of plausible models for continuous structure change in necking.

Stein (89) studied uniaxial orientation in stretched polyethylene by x-ray diffraction, birefringence and infrared dichroism. He concluded that the amorphous orientation is somewhat lower than that of the crystallites. Dharod (23) and White, Dharod and Clark (100) studied the drawing operation of high and low density polyethylenes. They observed necking on cold drawing with higher degree of crystallinity and orientation in the necked region in the HDPE. They also found that the crystalline orientation factor in the necked region and unnecked regions remained essentially unchanged with increasing total draw ratio.

Sheehan and Cole (84) carried out their drawing operation on polypropylene filaments in glycerine at 135°C followed by annealing at 100°C for 15 minutes. Their studies showed that filaments with para-crystalline (smectic) structure orient more rapidly and can be drawn more easily than filaments with the monoclinic crystal structure. But beyond a draw ratio of about 25 the crystals were completely oriented regardless of the type of the crystalline structure, crystallite orientation and molecular weight of the starting material.

Studies on polypropylene by Samuels (79) indicate that cold drawn fibers annealed very close to the crystal melting temperature have yielded bi-axial orientation. Samuels (78) also examined the morphological changes of fiber structure during the drawing of spun

fiber at 90°C and compared them with the same fiber after subsequent heat setting at 140°C. He concluded that morphological transformations were different in the high and low ranges of extension. In the low draw region the major deformation occurred in the polar regions of spherulites (assuming the poles of the spherulites are parallel to the fiber axis). In the high draw region slip, cleavage and molecular unfolding convert the spherulitic structure into a microfibrillar structure. During further drawing, the highly oriented crystals resist cleavage or further orientation and the non-crystalline region orients. On heat setting the non-crystalline region relaxes slightly by allowing the lamellae to be carefully oriented by crystal cleavage and slip processes (83).

The deformation behavior in films of polypropylene drawn at 135°C is similar but not identical to that occurring during 110°C extension (83). Samuels (83) reported that the lamellae are larger and more perfect at high temperature (135°C) and thus less deformable and the non-crystalline molecules are more mobile. This leads to diminished internal disruption within the spherulite during drawing, as relaxation processes within the non-crystalline regions result in deformation processes that are non-orienting in character.

Wyckoff (103) presented a two-phase model of the molecular organization for quenching, cold drawing and annealing of polypropylene. He also observed that extensive cold drawing produced severe molecular disorder in addition to excellent orientation.

Transformation from the monoclinic crystalline structure to the paracrystalline state (smectic) upon cold drawing was observed by Sobue

and Tabata (85) and Wyckoff (103). Sobue and Tabata (85) noted that on drawing completely oriented isotactic polypropylene filaments in water at 70°C, the crystalline structure is transformed to the paracrystalline structure. Complete conversion of the crystalline state to the paracrystalline state on cold drawing to a draw ratio of seven was observed by Wyckoff (103).

Annealing (103) highly drawn films of polypropylene did not change the orientation of crystallites under the various annealing conditions, but isometric annealing showed marked improvements in samples with poor orientation of the crystallites. The conversion of paracrystalline to crystalline state started at 70°C, reached the halfway point at 110°C and was largely complete at 145°C.

A decrease in the density of polyethylene during cold drawing was observed by Bertleheim and Stein (12), Glenz, Peterlin and Wilkes (32) and recently by White, et al. (100).

Formation of microvoids in polypropylene films during stretching was observed by Wyckoff (103). His small angle x-ray photographs indicated that the visual whiteness produced during cold drawing was related to lamellar voids elongated in the draw direction.

Samuels (81) found microvoids in the drawn fibers by using dark field microscopy, which suggests that deformation in polypropylene fibers is accompanied by void formation. Fibers drawn at 90°C and heat set at 140°C formed microvoids which oriented transversely at low extensions and longitudinally at high extensions.

Drawing of extremely thin polypropylene films was studied by Sakaoku and Peterlin (77). "At small draw ratio, microfibrils with

lateral dimensions of about 200Å, originating in micronecks at the crack boundaries of the original crystal lamellae, were obtained in isolated areas exhibiting maximum local strain separated by large regions of much less deformed material. The necked regions grow at increased draw ratio at the expense of the unnecked structure. The inhomogeneity of adjacent bundles of microfibrils create a great many longitudinal voids with more or less disoriented microfibrils bridging the gap. Annealing of the drawn sample produced a surface roughness similar to polyethylene.

Balta and Peterlin (10) studied the influence of temperature and draw ratio on the axial long period in polypropylene through small angle x-ray scattering. Their results show that in a wide range of drawing temperatures (20 to 150°C) and draw ratios (five to twenty) the axial long period is a unique function of temperature and is independent of the long period of the starting material which was varied within wide limits (125Å - 250Å). Balta and Peterlin interpreted these results to indicate that during plastic deformation in the neck the lamellae are broken into small folded chain blocks which are then incorporated into the microfibril, the basic building element of the fiber structure. The work of deformational forces must so mobilize the chains in the blocks that they get rearranged with a new long period, corresponding to the temperature of drawing.

Peterlin (76) proposed a three stage model to describe the structural changes occurring during drawing. Based on studies of plastic deformation of single crystals, thin layers and bulk samples together with mechanical, x-ray and infrared data he concluded that the cold drawing of crystalline polymers (polyethylene and

polypropylene) proceeds by (1) the plastic deformation of the original spherulitic structure, (2) the discontinuous transformation of the spherulitic into fiber structure by micronecking, and (3) the plastic deformation of the fiber structure.

G. MECHANICAL PROPERTIES OF THE SPUN AND DRAWN FIBERS

The properties of a fiber depend on its morphological structure which is controlled by the methods and conditions of fiber formation.

Melt Spun Fibers

The mechanical properties of synthetic fibers have received considerable study since the work of Carothers and Hill (16). Most of the early work was primarily concerned with the properties of drawn fibers and the effects of drawing variables. Little attention was given to the properties of as-spun fibers nor to the interaction of melt spinning and drawing variables.

In the earlier studies Carothers and Hill (16) first noted that an increase in draw-down tension causes an increase in the fiber strength. Krassig and Kitcheren (57) reported that the tensile strength in rayon increased linearly with the square of Hermans-Stein orientation function.

Higgins and Bryant (38) conducted experiments to relate tensile properties of high density polyethylene fibers with melt spinning variables. They reported that the tenacity and stiffness modulus of melt spun polyethylene yarn are functions of the logarithm of take-up velocity.

Ziabicki (110) found that in undrawn polyamide and polyester

fibers an increase in birefringence led to an increase in tensile strength and a decrease in elongation.

Recently studies of the mechanical properties of melt spun polyethylene fibers have been reported by Abbott and White (1), Dees and Spruiell (22) and White, et al. (100).

Abbott and White (1) and Dees and Spruiell (100) reported that the mechanical properties of the spun fiber of polyethylene depend primarily upon the orientation rather than the crystallinity level. Their studies indicate an increase in the modulus and tensile strength and a decrease in the elongation to break as the crystalline c-axis orientation function, f_c, increases.

Dharod (23) and White, et al. (100) observed an increase in tensile strength, Young's tangent modulus and a decrease in fiber elongation with increasing molecular weight.

The "hard" elastic fibers discussed earlier have high recovery (50 to 95 percent) from very high strains (100 percent extension) on the second and succeeding load applications (87). These fibers also have a reversible reduction in density with an enormous increase in pore volume and high deformability with good (rapid) recovery at liquid nitrogen temperature (87). Henson (36) also obtained data for the elastic recovery at 50 percent elongation from the second load cycle for both annealed and unannealed polypropylene fibers spun under a variety of conditions. Her data indicate high elastic recovery for the fibers spun under conditions of high spinline stress, especially after annealing.

Henson (36) and Spruiell and White (88) studied the mechanical properties of melt spun polypropylene fibers. They reported that the

filaments spun at higher stress have higher modulus, tensile strength and lower elongation to break. The behavior in the variation of the tensile strength, modulus and elongation to break with c-axis crystalline orientation (f_c) was found similar to polyethylene. The true stress at fracture decreases with f_c. On the basis of this result, Spruiell and White (88) suggest that higher tensile strengths can be reached in drawn fibers by starting with low orientation filaments with spherulitic structure which are then drawn to very high draw ratios.

Drawn Fibers

Drawing of the melt spun fibers greatly increases the modulus and tensile strength but decreases the elongation to break.

In drawn polyethylene fibers the tensile strength and modulus increase by a factor of about ten over the melt spun fibers (100). White, et al. (100) proposed a model for the structure of drawn fibers according to which the modulus and tensile strength will increase with the fraction of the tie molecules.

Samuels (78, 79, 80, 81, 83) reported a lower tensile modulus in polypropylene fibers drawn at 90°C than in fibers drawn at 90°C and heat set at 140°C under tension. He observed a break in the linearity in the tensile modulus draw ratio curves in the draw range of 2 - 2.5x and concluded from morphological examination that void formation and conversion of the spherulitic to the microfibrillar structure was the primary contributor to the observed modulus behavior. Some other important conclusions from Samuels (83) study are:

1. The average state of orientation in the polymer is a useful

expression for comparing structure-property relationships. Average molecular orientation is defined as $f_{av} = xf_c + (1 - x) f_{am}$.

2. Fabrication true strain is linearly related to the final fabricated orientation.

3. Yield stress increases with increasing molecular orientation, increasing rate and decreasing temperature. It correlates directly with average molecular orientation.

4. Yield strain increases with increasing orientation for spherulitic samples but decreases with microfibrillation.

Sheehan and Cole (84) did extensive study on properties and structure of highly isotactic polypropylene filaments. They reported that

1. Narrow molecular weight distribution and high molecular weight favors tenacity. Also narrower molecular weight distribution favors higher modulus values.

2. The more the filaments oriented during spinning, the lower the tenacity of the drawn fibers.

3. Draw ratio increases tenacity independent of molecular weight.

4. Modulus increases and elongation to break decreases with increasing tenacity and draw ratios.

5. Annealing temperature (100°C or 160°C for 30 minutes) has an effect on the density but not on the elongation to break, modulus and tenacity.

CHAPTER III

EXPERIMENTAL DETAILS

A. MATERIALS

General Characteristics

In the present research five different commercially available polypropylenes of varying tacticities and molecular weights were studied. Two of the polypropylenes were from Tennessee Eastman Company (Tenites ®) and the other three polymers were from Hercules, Inc. (Profaxes ®). The Profax samples were presumed to have somewhat higher tacticities than the Tenites®. Table I gives a detailed description of the polymers including the code names used in the present work.

Molecular Weight Measurements

The specific viscosities of Decalin solutions of polypropylene were determined at 137°C with a Cannon-Ubbelohde viscometer. Reduced viscosities were plotted against concentration using Huggins' empirical equation,

$$\eta_{sp/c} = [\eta]_d + k' [\eta]_d^2 c \qquad (11)$$

Intrinsic viscosities in Decalin ($[\eta]_d$) were calculated by extrapolating the $\eta_{sp/c}$ versus C curves to zero concentration.

The weight average molecular weights were calculated using the equation given by Chiang (18)

TABLE I

AS-RECEIVED POLYMER PROPERTIES

Manufacturer and Commercial Code	Melt Index grams/min	Our Code Name	Intrinsic Viscosity dl/gm	Weight Average Molecular Weight	Tacticity
Hercules Profax® 6823	0.42	H-0042	3.21 (3.25, 3.30*)	4.30×10^5	very high
Hercules Profax® 6423	6.6	H-0660	2.26	2.77×10^5	very high
Hercules Profax® 6323	12.0	H-1200	1.99	2.36×10^5	very high
Tennessee Eastman Tenite® 4241	9.00	T-0900	2.01	2.39×10^5	high
Tennessee Eastman Tenite® 4221	2.55	T-0255	2.71	3.48×10^5	high

*Courtesy of Hercules, Inc.

$$\overline{M}_w = \{[\eta]_d \times 10^4\}^{1.25} \qquad (12)$$

The measured viscosities and the calculated molecular weights of the as-received polymers are presented in Table I.

B. MELT SPINNING OF FILAMENTS

A schematic diagram of the melt spinning equipment is shown in Figure 3. The spinning machine was made by Fourne Associates of West Germany. The polymer pellets were fed into a 13 mm screw extruder through a seven liter hopper. The extruder supplied molten polymer at constant pressure to a gear pump, which provided a constant polymer flow rate to the spinneret. The melt passed through a 325 mesh filter screen and through a one-hole spinneret with capillary dimensions of 0.762 mm diameter by 3.81 mm long. Four separate electric heating zones, provided with controllers maintained the desired temperature around the extruder and the spinning head. The spun fibers were taken up on a feed role rotating at the desired take-up speed. The feed role was a three inch outside diameter cardboard roll mounted on a direct current driven Heller Controller. The take-up speeds ranging up to 550 meters/min could be obtained with the feed roll. From the feed roll the filaments were passed to a Lessona 955 constant tension winder where they were taken up on a 3 9/16 inch outside diameter cardboard take-up bobbin.

A Rothschild Tensiometer with a ten gram measuring head was used to measure the fiber tension. The instrument was calibrated and all the measurements were corrected for the changes in the fiber diameter.

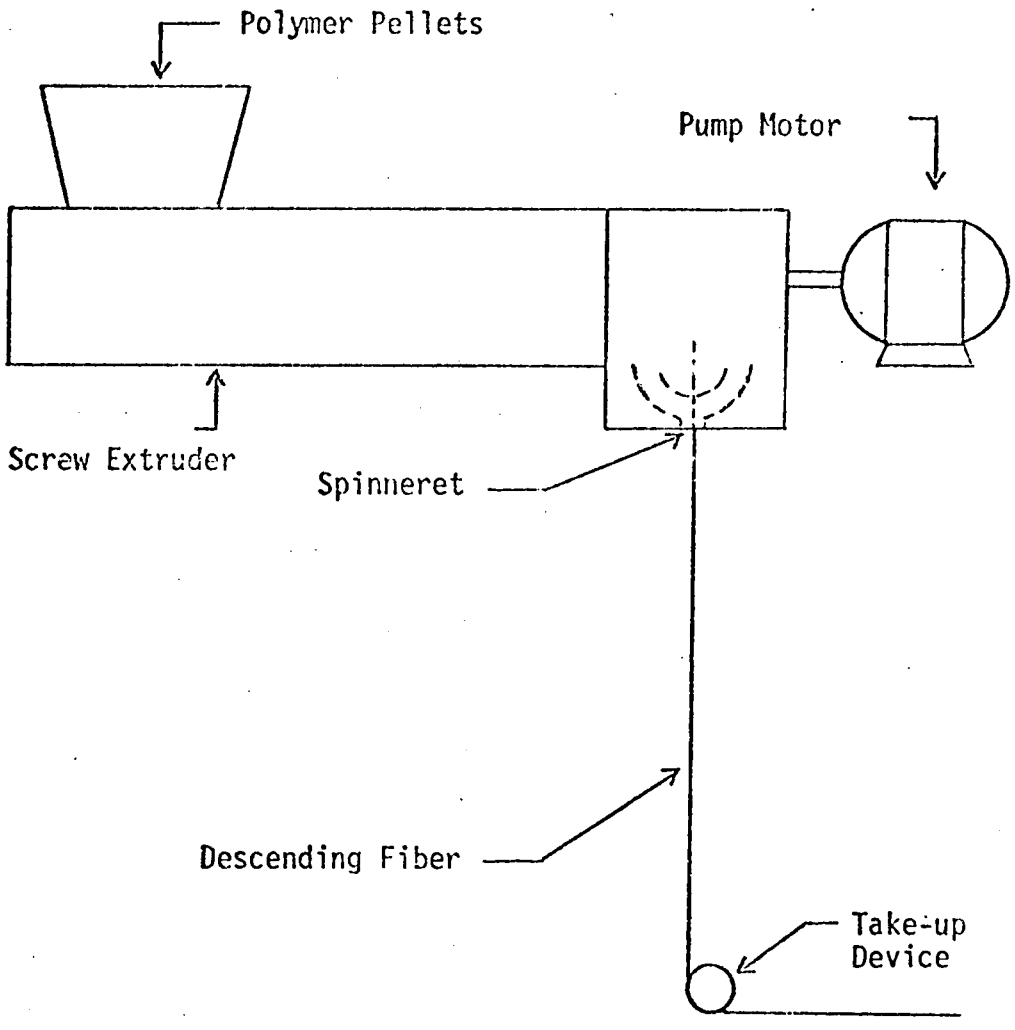


Figure 3. Schematic Diagram of Melt Spinning Equipment

All the experimental runs were made at a constant melt temperature of 230°C. For each of the five polymers in Table I, filaments were spun at speeds of 50, 100, 200, 400 and 550 meters/min. During these runs the mass flow rate was kept at approximately 2.1 grams/min and the spinning medium was ambient air at 21°C. The spin path length was ten feet. Difficulties, in the form of melt fracture, were experienced for the H-0042 polymer under these conditions. To reduce this problem the flow rate per spinneret hole was reduced to 0.5 grams/min by spinning through a four hole spinneret.

Filaments of H-0660 were also spun into a cold water bath at 9°C with a spinneret to bath distance of nine inches. These fibers were taken up at rates between 25-300 meters/min, at 25 meters/min, intervals. Spun samples for H-0660 were provided by a previous researcher, H. Henson (36).

The diameters of fibers were measured with an Optical Microscope provided with a Bausch & Lomb filar Micrometer eyepiece. The diameter data obtained in filar units was converted into microns by multiplying with the appropriate conversion factor for the particular microscope objective used.

C. CHARACTERIZATION OF FIBER SAMPLES

This involves the determination of molecular weight for the spun fiber through dilute solution viscosity measurements, percentage crystallinity through density column and crystal form, orientation and morphology through small and wide angle x-ray diffraction and birefringence studies.

Molecular Weight Determination

The same procedure outlined earlier in this chapter was used for the determination of molecular weight of spun fiber.

Wide Angle X-Ray Scattering (WAXS)

Wide angle x-ray diffraction patterns for the samples (as-spun, drawn, annealed) were obtained using a Philips Norelco x-ray generator and a flat plate camera. The radiation used was Ni filtered Copper K_{α} of wave length 1.542 Angstroms. The x-ray unit was operated at 40 KV and 15 MA. The sample to film distance was 3.71 cm and the sample was fixed on a sample holder which was attached to the beam collimeter by a rubber cap (see Figure 4). Exposure times usually ranged from ten minutes to one hour.

Small Angle X-Ray Scattering (SAXS)

SAXS scattering patterns were obtained on selected fiber samples using a modified Kiessig Camera with pinhole collimation. The camera was mounted on a Rigaku Gereral Electric Rotating anode x-ray generator. Patterns with a resolution of 400Å were obtained with a custom-made collimator. Air scattering was reduced by evacuating the camera with a mechanical pump. The sample to film distance was 400 mm and the exposure time ranged from one half to two hours for spun fibers.

Crystallinity

The percentage crystallinity of the monoclinic spun fibers was determined at 23.2°C using a distilled water isopropyl alcohol density column constructed by the method described by Tung and Taylor (93).



Figure 4. Fiber Sample Holder Attachment for Obtaining WAXS Patterns

The samples were allowed approximately twelve hours to seek their level of displacement. The crystalline fraction was assumed to be given by

$$X = \frac{V_a - V}{V_a - V_c} \tag{13}$$

where V, V_c, and V_a are respectively the specific volumes of the experimental sample, a hypothetical 100 percent crystalline sample, and a 100 percent amorphous sample. The required specific volumes of crystalline and amorphous polypropylene were obtained from the empirical relations developed by Danusso, et al. (24)

$$V_c = 1.059 + 4.25 \times 10^{-4}\ t \tag{14}$$

$$V_a = 1.134 + 9.28 \times 10^{-4}\ t \tag{15}$$

where t is temperature in degrees centigrade.

Birefringence

The total birefringence for the samples was determined on an Orthoplan Polarizing Microscope with a Leitz Berek Compensator. The compensator determines the phase difference (Γ) between two mutually perpendicular plane polarized light waves emerging from the sample. The phase difference is proportional to the birefringence of the sample. The experimental procedure suggested by the manufacturer of the compensator was followed in determining the phase difference or redardation. Total birefringence was calculated from the relation

$$\Delta n_T = \frac{\Gamma}{d}$$

where d is the diameter of the fiber sample and Γ is the retardation.

Orientation

In Chapter II quantitative expressions for the orientation function were given. In this section the utility of Wilchinsky's expression in determining the orientation function for monoclinic polypropylene is examined. In this case there is no set of diffracting planes perpendicular to the c-axis which reveal the c-axis orientation directly. Nevertheless, as noted in Chapter II, the orientation function for the c-axis can be calculated according to Wilchinsky's analysis from the values of $(\overline{\cos^2 \phi_1})$ and $(\overline{\cos^2 \phi_2})$ evaluated for two planes which are parallel to the c-axis (see Equation (9), Chapter II).

The (110) and (040) planes were selected for use in determination of c-axis orientation. For these planes the Wilchinsky equation can be written as

$$\overline{\cos^2 \phi_{c,z}} = 1-\left[\frac{(1-2 \sin^2 \rho_{040})\overline{\cos^2 \phi_{110,z}}-(1-2\sin^2 \rho_{110})\overline{\cos^2 \phi_{040,z}}}{\sin^2 \rho_{110} - \sin^2 \rho_{040}}\right] \tag{16}$$

For a uniaxially oriented sample the average value of the square of the cosine of the angle between the fiber axis and the normal to (hkl) planes is given by

$$\overline{\cos^2\phi}_{hkl} = \frac{\int_0^{\pi/2} I(\phi)\cos^2\phi \sin\phi \, d\phi}{\int_0^{\pi/2} I(\phi)\sin\phi \, d\phi} \qquad (17)$$

where $I(\phi)$ represents the relative value of the intensity of the diffracted beam at angle ϕ.

The numerical values of ρ_{110} and ρ_{040} were calculated from the geometry of the unit cell by Wilchinsky (102). They were found to be $\rho_{040} = 0$ and $\rho_{110} = 72.5$. Substitution of these values in Equation (16) gives,

$$(\overline{\cos^2\phi}_{c,z}) = 1 - 1.099\ \overline{\cos^2\phi}_{110,z} - 0.901\ \overline{\cos^2\phi}_{040,z} \qquad (18)$$

The value for $(\overline{\cos^2\phi}_{c,z})$ was obtained by substituting the experimental values $(\overline{\cos^2\phi}_{110,z})$ and $(\overline{\cos^2\phi}_{040,z})$ into Equation (18). The c-axis crystalline orientation function was calculated from Equation (6).

The quantitative measurement of the intensity distribution of 110 and 040 reflections as a function of the angle χ was carried out on a General Electric XRD-5 x-ray diffractometer system coupled with an ORTEC counting system. The diffraction sample was made up of a sheet of parallel fibers. Figure 5 shows the experimental setup. The intensity data were collected at the (110) and (040) peak positions, which were determined from a 2θ scan. Background intensity was evaluated from the analysis of the 2θ scans at $\chi = 0°$ and 90°. The intensity data were collected on a punched paper tape by a digital ratemeter and are corrected for background intensities. A PDP-15 digital computer was

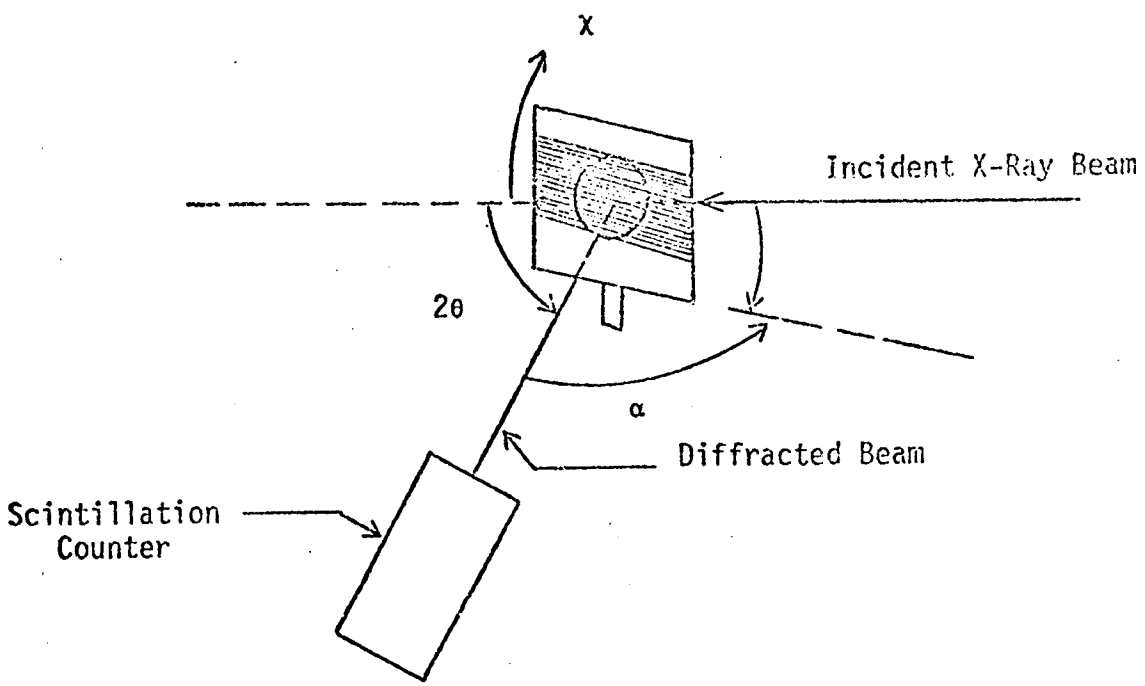


Figure 5. Schematic Arrangement of X-Ray Equipment for Orientation Factor Measurements

Source: M. J. Khokhani, M.S. Thesis, University of Tennessee, Knoxville (1975).

used to carry out integration of Equation (17) with the intensity data obtained at every 5°$_\chi$ angle starting from equatorial position and ending in the meridional position.

The b-axis orientation was obtained directly from (040) plane reflections. For a monoclinic unit cell the orthogonality relationship does not hold. However an a'-axis orientation factor was obtained using an expression similar to Equation (8). In this case, the a'-axis is perpendicular to both the b and c axes of the monoclinic polypropylene unit cell. The a'-axis is approximately 9.3° from the true a-axis since the β-monoclinic angle differs by this much from 90°.

The amorphous contribution to the overall orientation was calculated from Equation (10), using the experimental crystallinity and birefringence together with the intrinsic birefringences for crystalline and amorphous polypropylene given by Samuels (83).

D. MECHANICAL AND THERMAL PROCESSING

Selected spun fibers (H-0042, take-up velocities 50 and 550 meters/min; H-1200, take-up velocity 200 and 550 meters/min) were drawn to the predetermined draw ratios by an Instron Tensile Tester. For each spinning condition three different draw ratios were studied. For each case these were selected so that the draw ratios correspond to the following stages of drawing:

(1) One inch beyond the natural draw ratio as defined by the end of the necking elongation

(2) Approximately one inch before fracture

(3) Intermediate to the above two

A crosshead speed of two inches/min was used for all the samples. For high temperature drawing, the Instron grips were enclosed in a hot dry air oven provided with a temperature controller set at 140°C. The cold drawn fibers were annealed in a temperature controlled drying oven at 140°C for 15 minutes. Figure 6 shows a picture of the fiber sample holder used for annealing. The samples were under tension and slippage was prevented by using Neoprene grips.

E. MECHANICAL PROPERTY MEASUREMENTS

Tensile properties of the fibers were obtained at room temperature with an Instron Tensile Tester. Force versus elongation curves were obtained for all spun samples. These results were used to evaluate the modulus, yield strength, tensile strength and percent elongation to break. A crosshead speed of two inches/minute was used with a fiber gauge length of one inch.

The percent elongation to break was determined from the expression

$$\text{Percent elongation to break} = \frac{l_f - l_o}{l_o} \times 100 \qquad (19)$$

where l_f is the length at fracture and l_o is the initial gauge length.

The elastic recovery from 100 percent elongation was measured on the second loading cycle for the melt spun samples. The starting gauge length was one inch. The relationship used to calculate the elastic recovery is

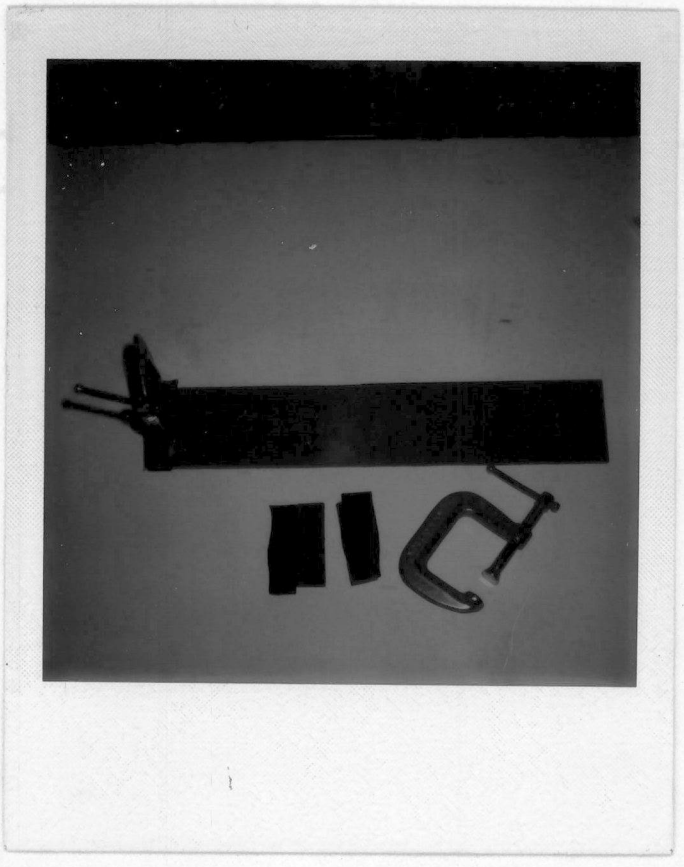


Figure 6. Fiber Sample Holder Used for Annealing Studies

$$ER_{100} = \frac{2.0\ L_\gamma - L_f}{L_\gamma} \qquad (20)$$

where L_γ and L_f are lengths after relaxation of first and second cycles.

The tensile properties for the drawn-annealed and high temperature drawn fibers were determined in a manner similar to that described for the spun fibers. The only difference is that the rate of elongation during testing was only 0.5 inches/minute for the drawn fibers.

CHAPTER IV

STRUCTURE DEVELOPMENT IN MELT SPUN FIBERS

A. THE MELT SPINNING PROCESS

Preparation of Spun Filaments

As noted in Chapter III, polypropylenes from two different suppliers having a range of molecular weights were spun at a single extrusion temperature of 230°C.

Table II gives the spinning conditions used in the preparation of samples for each polymer and some general observations made regarding the spinnability of the polymers.

Spinnability decreased with increased molecular weight. This is especially evident in the melt spinning of polypropylene having a melt index of 0.42 (highest molecular weight specimen under investigation). Melt fracture occurred in this sample at the spinning temperature and flow rate used for all other polymers ($\dot{\gamma}_{w,\ 2.1} \sim 895\ sec^{-1}$). In order to avoid melt fracture, the melt spinning for this specimen was achieved by reducing the flow rate from 2.1 grams/min to 0.5 grams/min ($\dot{\gamma}_{w,0.5} \sim 213\ sec^{-1}$). The Hercules samples could be melt spun at higher take-up speeds (melt draw ratio, $V_L/V_o = 95$) than the Tennessee Eastman polymers (melt draw ratio = 62). This probably could be traced to the fact that the two manufacturers use different catalyst systems in the preparation of polymers. This may result in differences in tacticity and/or molecular weight distribution. The latter effect

TABLE II

SPINNING CONDITIONS FOR POLYPROPYLENES

Sample	Melt Temperature (°C)	Melt Flow Rate (gms/min)	Spinning Medium	Take-up Velocities (m/min)	Comments
H-0042	230	0.5	Ambient	50, 100, 200, 400 550	Melt fracture at higher flow Rates
H-0660	230	2.1	Ambient	50, 100, 200, 400 550	Samples provided by H. Henson
H-1200	230	2.1	Ambient	50, 100, 200, 400 550	Smooth Spinning
T-0255	230	2.1	Ambient	50, 100, 200	Fractured beyond 200 m/min
T-0900	230	2.1	Ambient	50, 100, 200, 400	Fractured beyond 200 m/min
H(Smectic)	230	2.1	Cold water bath at 9 °C	25, 50, 75, 100, 125, 150, 175, 200, 250, 300	Quench bath is nine inches away from spinneret head

may be responsible for the observed differences in spinnability.

Degradation of Polypropylene During Spinning

Molecular weights of the spun fiber were also determined from the intrinsic viscosity measurements of the samples in decalin solution. Figure 7 is a plot of reduced viscosity versus concentration for the polymer solutions. Shown here are the results for the as-received polymer, whose intrinsic viscosities and molecular weights were reported in Chapter III, as well as the results for the spun fibers. The weight average molecular weight of the spun fiber and the degradation due to melt spinning are given in Table III. Degradation due to melt spinning was observed in all the polymers with values ranging from 1 percent to 27 percent. The highest degradation (27 percent) was observed for H-0042, the sample with the highest molecular weight.

The Development of Stress in the Spinline

Figure 8 shows changes of the stress in the spinline with take-up velocity and mass flow rate. The spinline stress was found to increase with the take-up velocity for all the polymers at a specified melt flow rate. At a given take-up velocity, increasing the melt flow rate was found to decrease the spinline stress. Within the range of variables examined the change in melt flow rate seemed to have the greatest effect on spinline stress. The effect of the molecular weight can be observed from the data for samples spun at a melt flow rate of 2.1 grams/min. The samples of T-0255 show higher stress levels at a given take-up velocity than the H-1200 samples and the data on the intermediate molecular weight specimens were scattered between T-0255

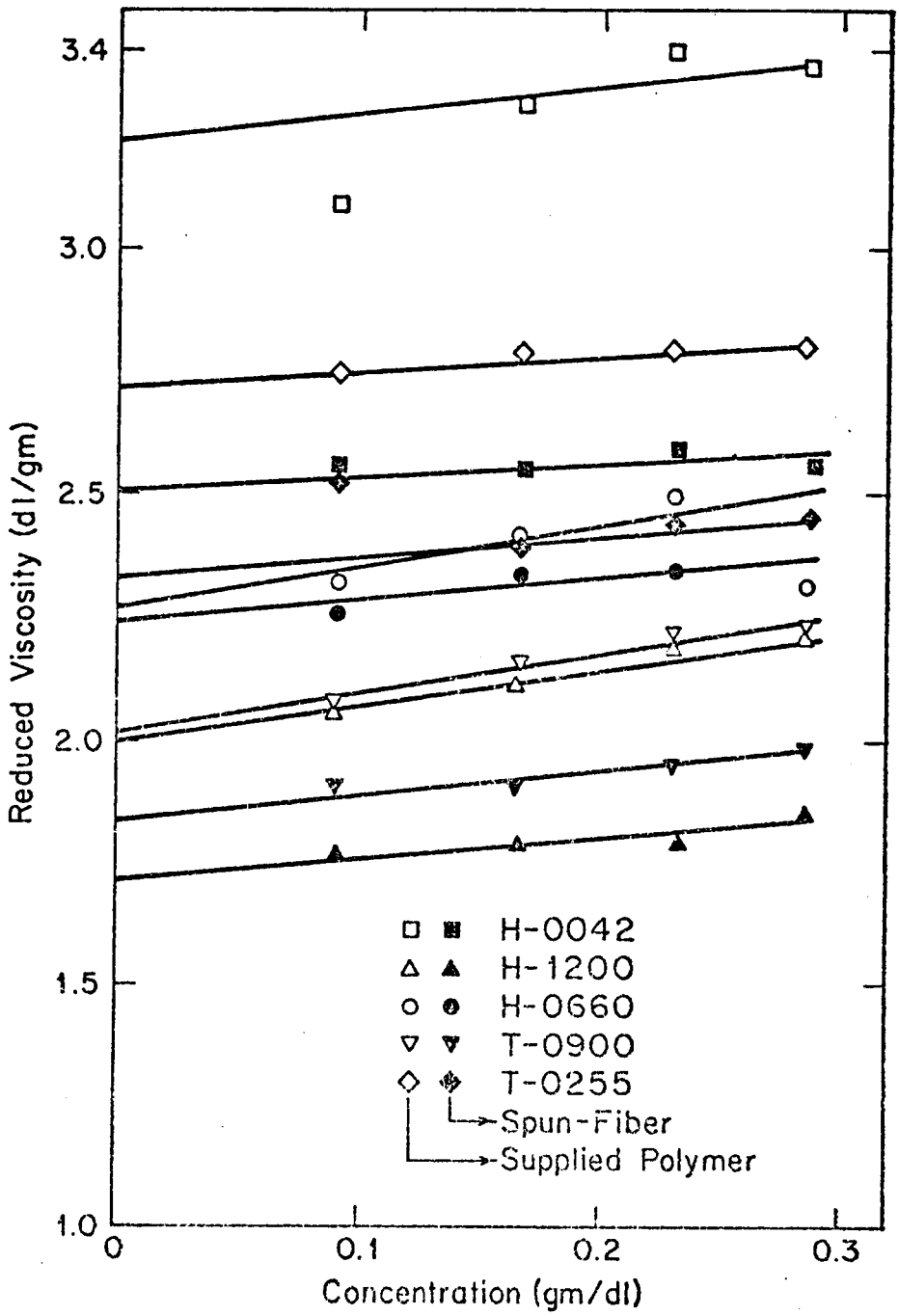


Figure 7. Plot of Reduced Viscosity Versus Concentration Yielding Intrinsic Viscosities for Melt Spun and As-Received Polypropylenes. Measurements Were Made at 137°C in Decalin

TABLE III

CHARACTERIZATION OF SPUN POLYPROPYLENE FIBERS

Sample Code	Intrinsic Viscosity dl/gm	Weight Average Molecular Weight	Percent Thermal Degradation
H-0042	2.50 (2.55*)	3.14×10^5	27
H-0660	2.24	2.74×10^5	1
H-1200	1.70	1.94×10^5	18
T-0900	1.83	2.13×10^5	11
T-0255	2.33	2.88×10^5	17

*Courtesy of Hercules, Inc.

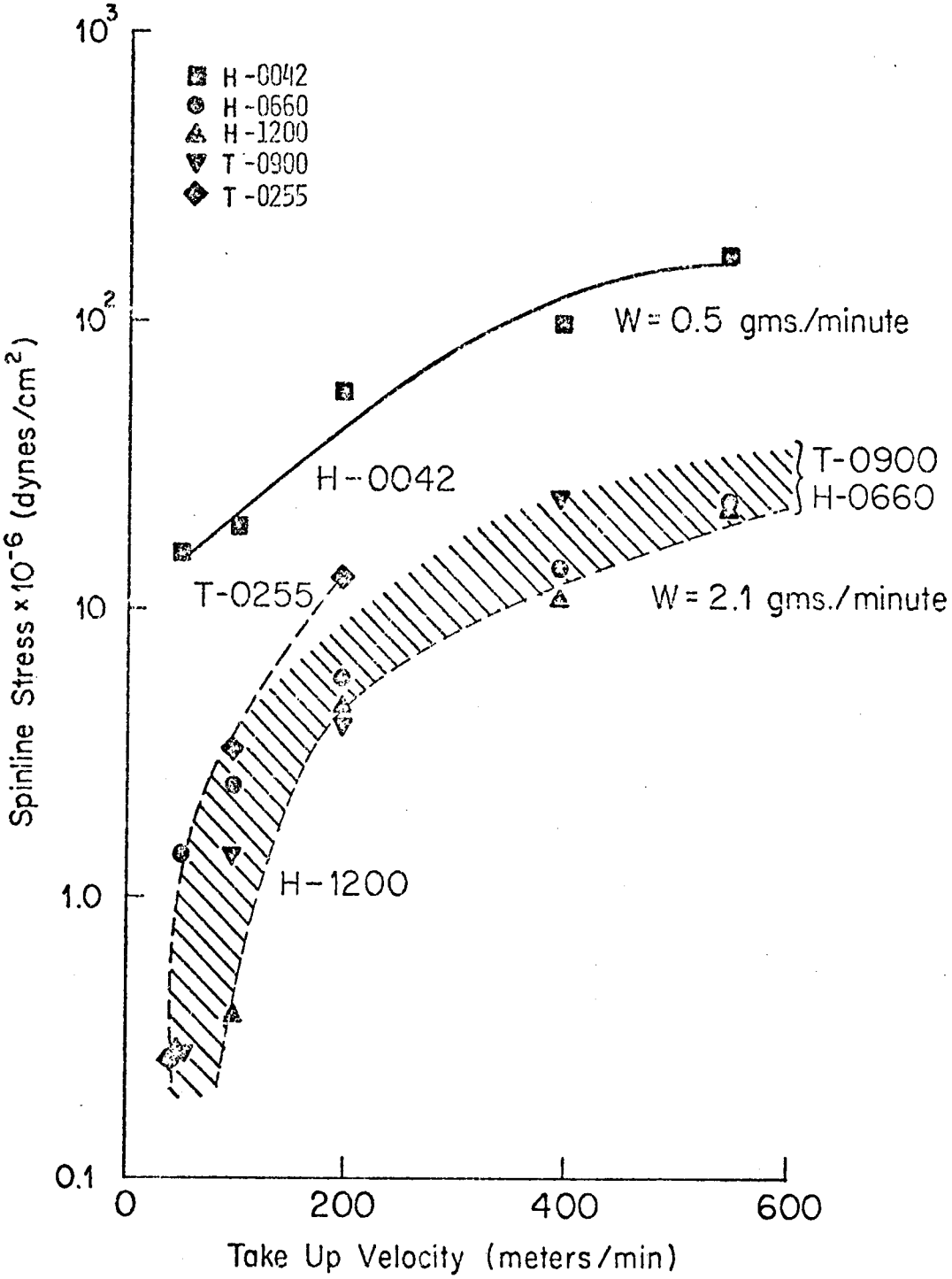


Figure 8. Effect of Take-Up Velocity and Mass Flow Rate on Spinline Stress for Polypropylene Monofilaments

and H-1200. Thus, in general, there was a trend toward increasing spinline stress levels with increasing molecular weight. The stress levels in the melt ranged from 0.3 x 10^6 dynes/cm^2 to 170.0 x 10^6 dynes/cm^2.

The spinline stress is a very important spinline variable through which the effects of take-up velocity, flow rate, extrusion temperature and molecular weight on morphology and mechanical properties of the spun fibers can be related. This will become evident as the remainder of this chapter is presented.

B. STRUCTURAL CHARACTERIZATION OF MELT SPUN FILAMENTS

Qualitative Characteristics

Depending on the threadline cooling rates, the spun filaments of polypropylene were either smectic (paracrystalline) or highly crystalline. The crystalline form is the monoclinic α-form. In the present study it is primarily the highly crystalline monoclinic filaments that were produced. The smectic form occurred only when rapid cooling rates were achieved by quenching the molten threadline into water.

Figure 9 shows WAXS patterns of filaments spun either into ambient air or into water at 9°C. The effect of increasing take-up velocity (and spinline stress) is also shown. It can be seen in Figure 9a, b, c that the samples H-0660 are highly crystalline and the c-axis orientation is increasing with take-up velocity. For the smectic form in Figure 9d, e, f it is evident that there is a transformation in crystal structure from an unoriented paracrystalline to highly oriented monoclinic type with increasing take-up velocity.

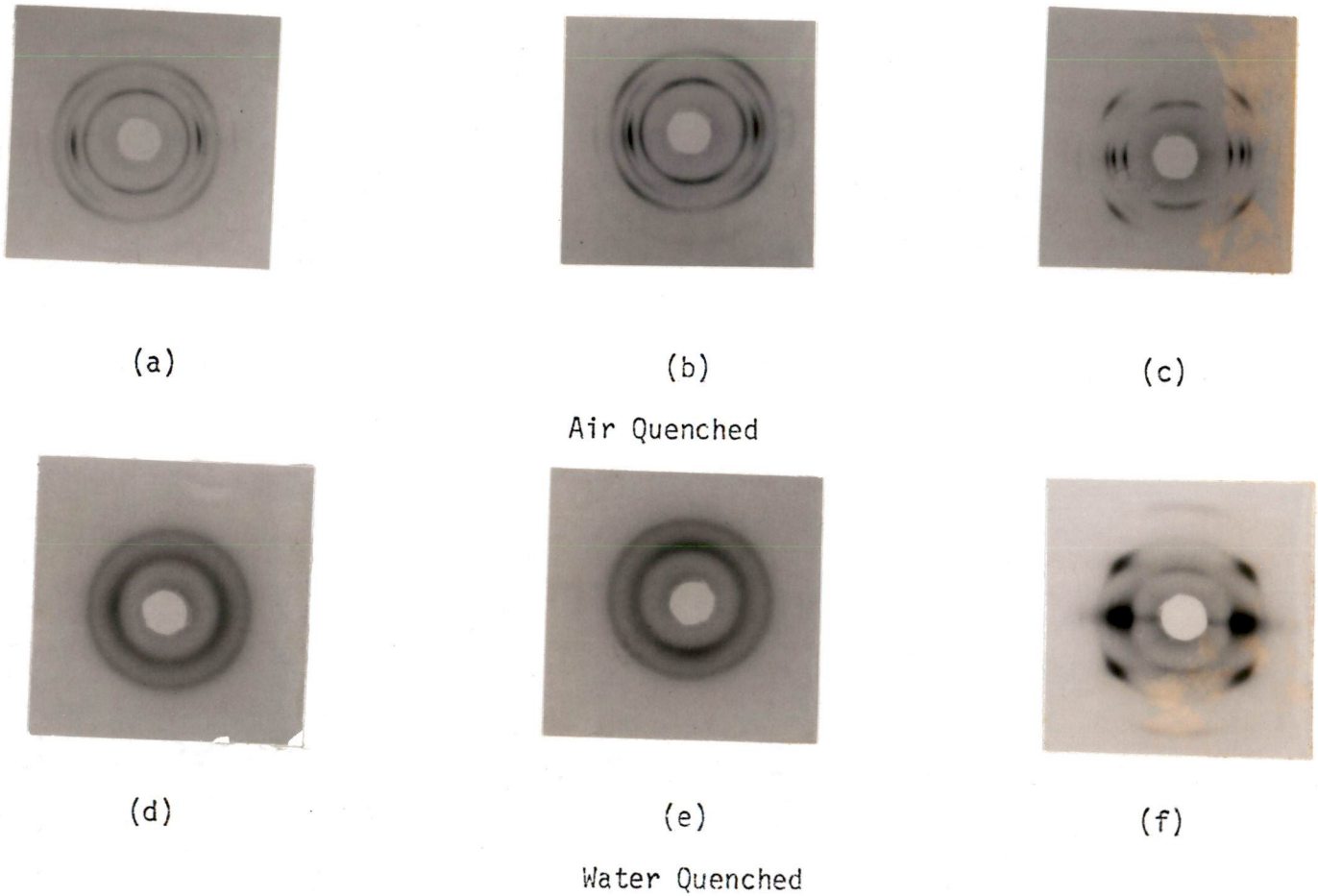


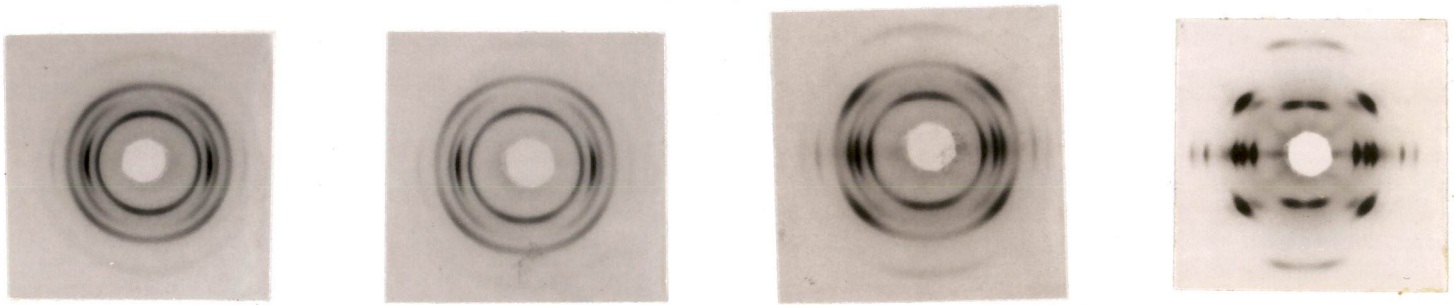
Figure 9. Effect of Take-Up Velocity and Cooling Medium on WAXS Patterns of Melt Spun H-0660 (a) 50 Meters/Min, (b) 200 Meters/Min, (c) 550 Meters/Min, (d) 25 Meters/Min, (e) 100 Meters/Min, (f) 300 Meters/Min

The effect of the molecular weight on orientation is shown qualitatively in Figure 10. Comparing the WAXS patterns in Figure 10a, b, and c for H-1200, T-900 and T-0255 at a melt flow rate of 2.1 grams/min, and take-up velocity 200 meters/min there seems to be a noticeable decrease in the 110 and 130 arc widths with increasing molecular weight indicating an increase of orientation.

Comparison of WAXS pattern for H-0042-200 (Figure 10d) with the other patterns in Figure 10 (spun at same take-up but higher melt flow rate) indicates that H-0042-200 has developed much higher levels of orientation than the other samples. This drastic difference in orientation is a result of a combination of two effects: (1) low flow rate and (2) higher molecular weight. Both effects give rise to higher levels of stress in the molten threadline and higher orientations in the spun filaments.

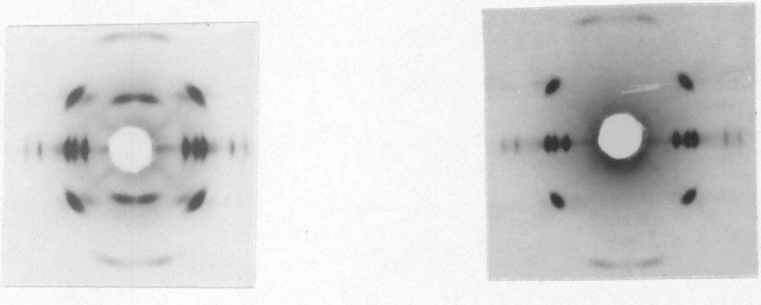
A careful observation of the highly oriented polypropylenes in Figure 10 indicate the presence of a bimodal distribution of the unit cells. This can best be seen by comparing the pattern for a highly oriented as-spun filament (with bimodal orientation) with the pattern of a highly oriented drawn sample without the bimodal orientation. Figure 11a shows highly oriented x-ray pattern for melt spun polypropylene showing bimodal orientation and Figure 11b shows the x-ray pattern of a cold drawn and annealed sample. This material is highly oriented with the c-axis parallel to the fiber axis and both a- and b-axes perpendicular to the fiber axis and randomly distributed about it.

Figure 12 shows the effect of spinline stress on the SAXS patterns. The SAXS patterns of fibers spun at low stresses exhibit a continuous



(a) (b) (c) (d)

Figure 10. Effect of Molecular Weight and Melt Flow Rate on Crystalline Orientation at 200 Meters/Min Take-up Velocity, (a) H-1200, (b) T-900, (c) T-0255, (d) H-0042 (0.5 gm/min)



(a) (b)

Figure 11. WAXS Pattern Showing Bimodal Orientation, (a) in Spun Fiber and the Lack of It (b) in Drawn Fiber

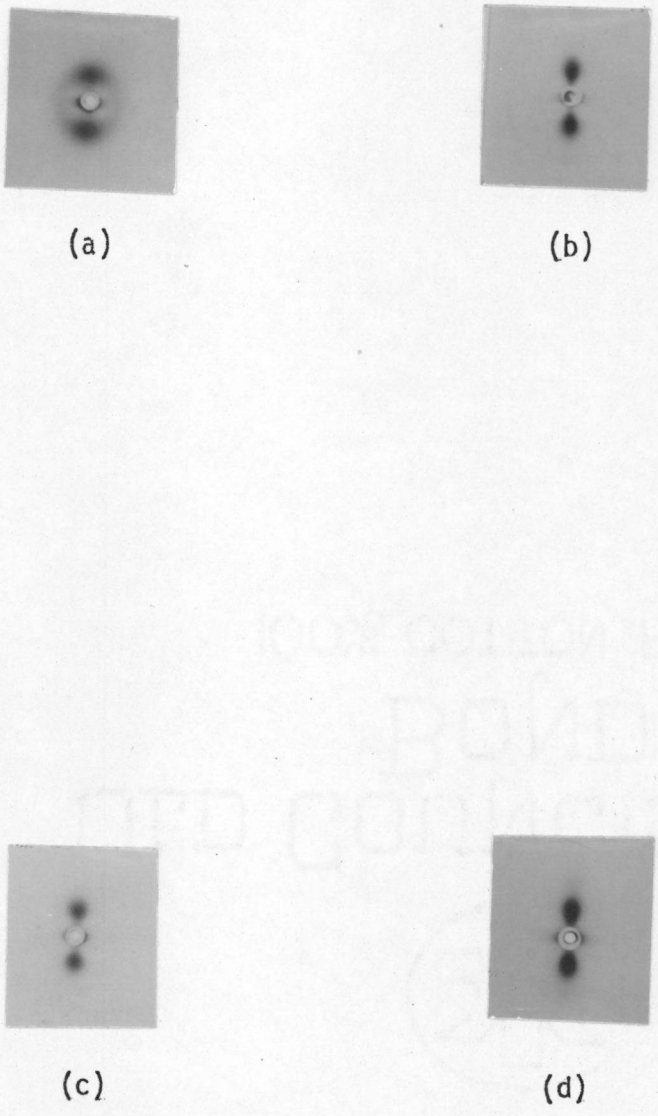


Figure 12. Effect of Spinline Stress on SAXS for Melt Spun Polypropylenes, (a) T-0255-50 (σ_L = 0.3 x 10^6 dynes/cm^2), (b) T-0255-200 (σ_L = 12.0 x 10^6 dynes/cm^2), (c) H-0042-50 (σ_L = 15.5 x 10^6 dynes/cm^2), (d) H-0042-200 (σ_L = 55.1 x 10^6 dynes/cm^2)

ring in Figure 12a which gradually changes to a two point pattern with increasing stress as shown in Figures 12b and 12c. At very high stress values, Figure 12d, the SAXS patterns show perfect two point patterns.

In the next three sections the results of quantitative measurements of crystallinity and orientation are presented.

Crystallinity

The percent crystallinity values in the spun fibers are given in Table IV as a function of the take-up velocity for each polymer. From the table it can be seen that the differences in the absolute values of the crystallinity levels in different specimens having different molecular weights at a given take-up velocity were small. However, an interesting trend in the crystallinity levels with take-up velocity was observed particularly for H-0042 specimens. Figure 13 shows the crystallinity data plotted as a function of spinline stress. The percent crystallinity starts at about 53.5 percent for low stress spun samples (0.3×10^6 dynes/cm^2) and increases with spinline stress to 57.5 percent (170×10^6 dynes/cm^2). There does not appear to be a significant trend outside the experimental error, with molecular weight. Generally, the fibers spun from Tenite^R polypropylene seem to have slightly lesser crystallinity levels than the Hercules Profax^R fibers.

Crystalline Orientation Factors

Figure 14 shows Hermans-Stein c-axis crystalline orientation factor (f_c) for isotactic polypropylene plotted against the take-up velocity. The orientation function increases steadily with the take-up velocity. The figure also shows the effect of the molecular weight on the

TABLE IV

PERCENT CRYSTALLINITY FOR POLYPROPYLENES AT VARIOUS TAKE-UP VELOCITIES

	Take-up Velocity (m/min)				
Sample	50	100	200	400	500
H-0042	55.8	55.9	57.2	57.4	57.4
H-0660	-	-	-	-	-
H-1200	53.1	54.1	54.1	54.1	55.5
T-0255	53.1	54.0	52.3	-	-
T-0900	53.8	53.0	53.8	55.5	-

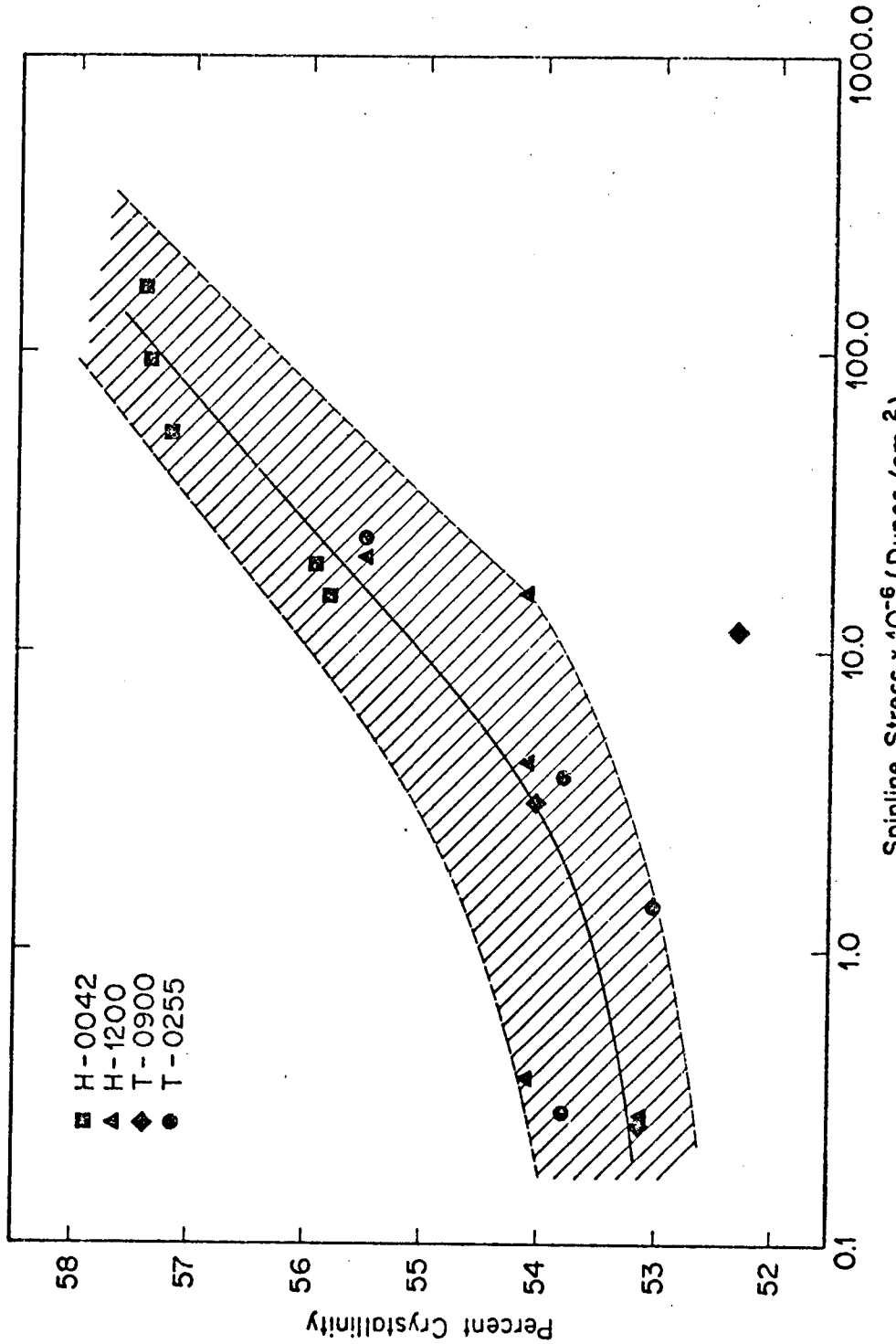


Figure 13. Changes in Percent Crystallinity with Spinline Stress for Polypropylene Fibers

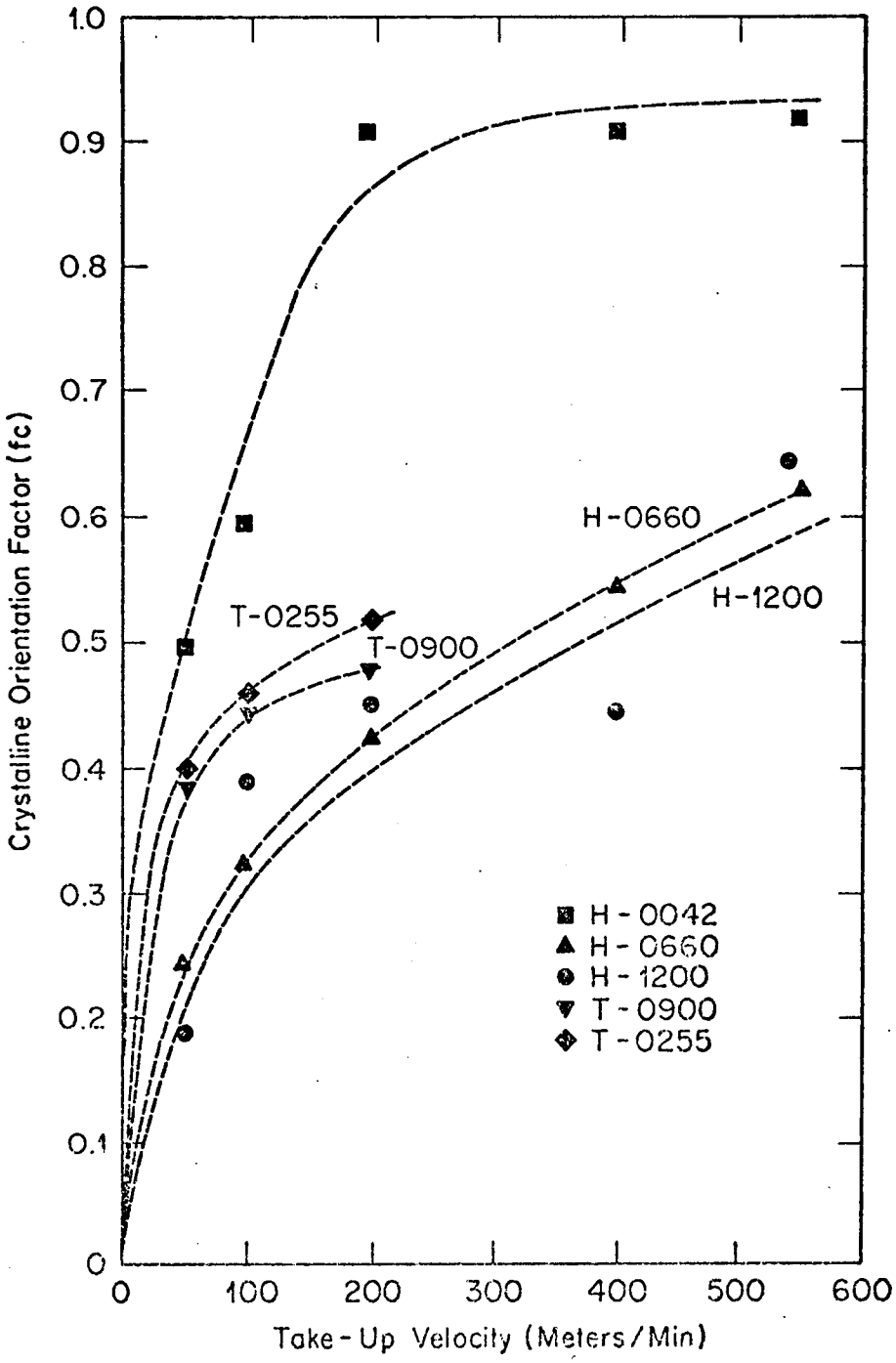


Figure 14. Crystalline Orientation Factor (f_c) as a Function of Take-Up Velocity in Polypropylene Fibers

orientation factors. At any given take-up velocity f_c was found to be higher for higher molecular weight samples. The effect of tacticity, if any, on f_c is not very clear from these results. The large effect of a combination of low flow rate and high molecular weight is exhibited by the H-0042 filaments. At take-up velocities of 200, 400 and 550 meters/min these filaments show very high values of f_c (~ 0.9).

Figure 15 shows crystalline orientation functions plotted versus the spinline stress for all the samples. Each of the orientation functions $f_{a'}$, f_b, and f_c falls on a single curve within the experimental accuracy. This shows the importance of the spinline stress on the development of morphology during melt spinning. The value of f_c increases with spinline stress, leveling off at 0.91, which indicates that the c-axes are tending to become more aligned with the fiber axis with increasing stress. The b-axis orientation function (f_b) decreases rapidly reaching a value of -0.48 indicating a near perpendicular alignment of the b-axis with the fiber axis. The value of $f_{a'}$ starts at about -0.06 and finally approaches -0.43. The high f_c values observed in the spinline are very interesting to note and were obtained at very high levels of spinline stresses. This appears to be a special spinning regime which has previously been given little attention although Kitao, et al. has also reported high f_c values (0.85) at high melt draw ratios (2000). This regime and its relation to the behavior at lower spinline stresses needs to be given additional study in the future.

Birefringence and Amorphous Orientation

The Hermans-Stein orientation factors discussed earlier refer to

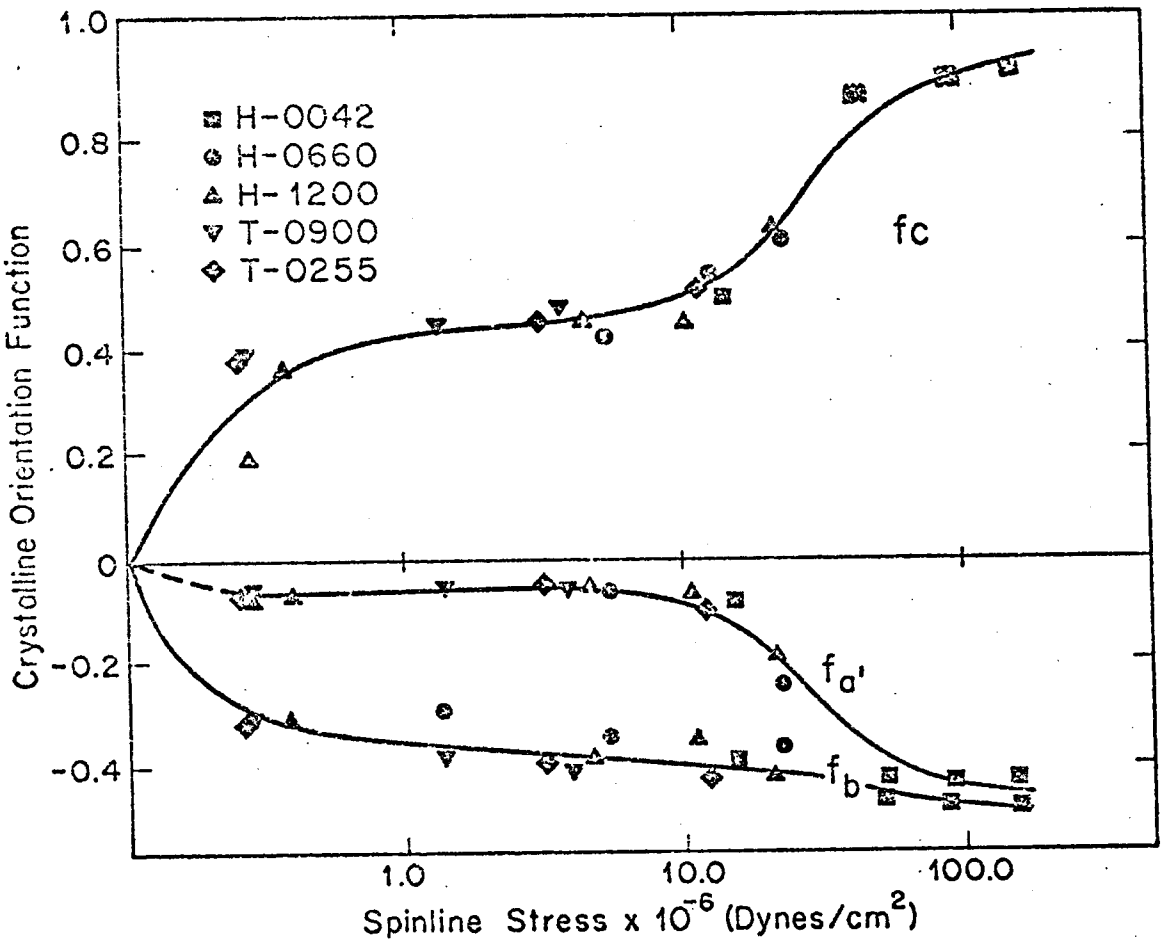


Figure 15. Orientation Functions ($f_{a'}$, f_b, and f_c) of Polypropylene Filaments as a Function of Spinline Stress

the crystalline phase of the samples. However, it was also noted that these polypropylene fibers are considerably less than 100 percent (about 55 percent) crystalline. This suggests that orientation in the amorphous regions may also be significant. The measured birefringence is a measure of average molecular orientation in the samples.

Figure 16 shows the variation of birefringence with increasing take-up velocity and increasing molecular weight. The birefringence increases with take-up velocity. Fibers with higher molecular weight have higher birefringence at any given take-up velocity. Samples T-0900 and T-0255 show a relatively faster rate of development of orientation in comparison with H-0660 and H-1200.

Figure 17 is a plot of measured total birefringence and also the amorphous phase contribution to birefringence versus spinline stress. The measured birefringence increases from 4.0×10^{-3} at low stress (0.3×10^{6} dynes/cm^2) to about 20×10^{-3} at a spinline stress of 170×10^{6} dynes/cm^2. The birefringence seems to level off at higher stresses. The amorphous birefringence shows considerable scatter in the data, but this appears to be due to the fact that it is determined as a relatively small difference between two larger numbers. The amorphous birefringence is negative at low spinline stresses and increases to a positive value as shown by the scatter band in Figure 17. The amorphous phase orientation amounts to about 25 percent of the total birefringence. Figure 17 shows no significant effect of molecular weight, flow rate and tacticity on birefringence, which is not reflected in the spinline stress. This emphasizes the importance of spinline stress as a useful processing parameter to correlate

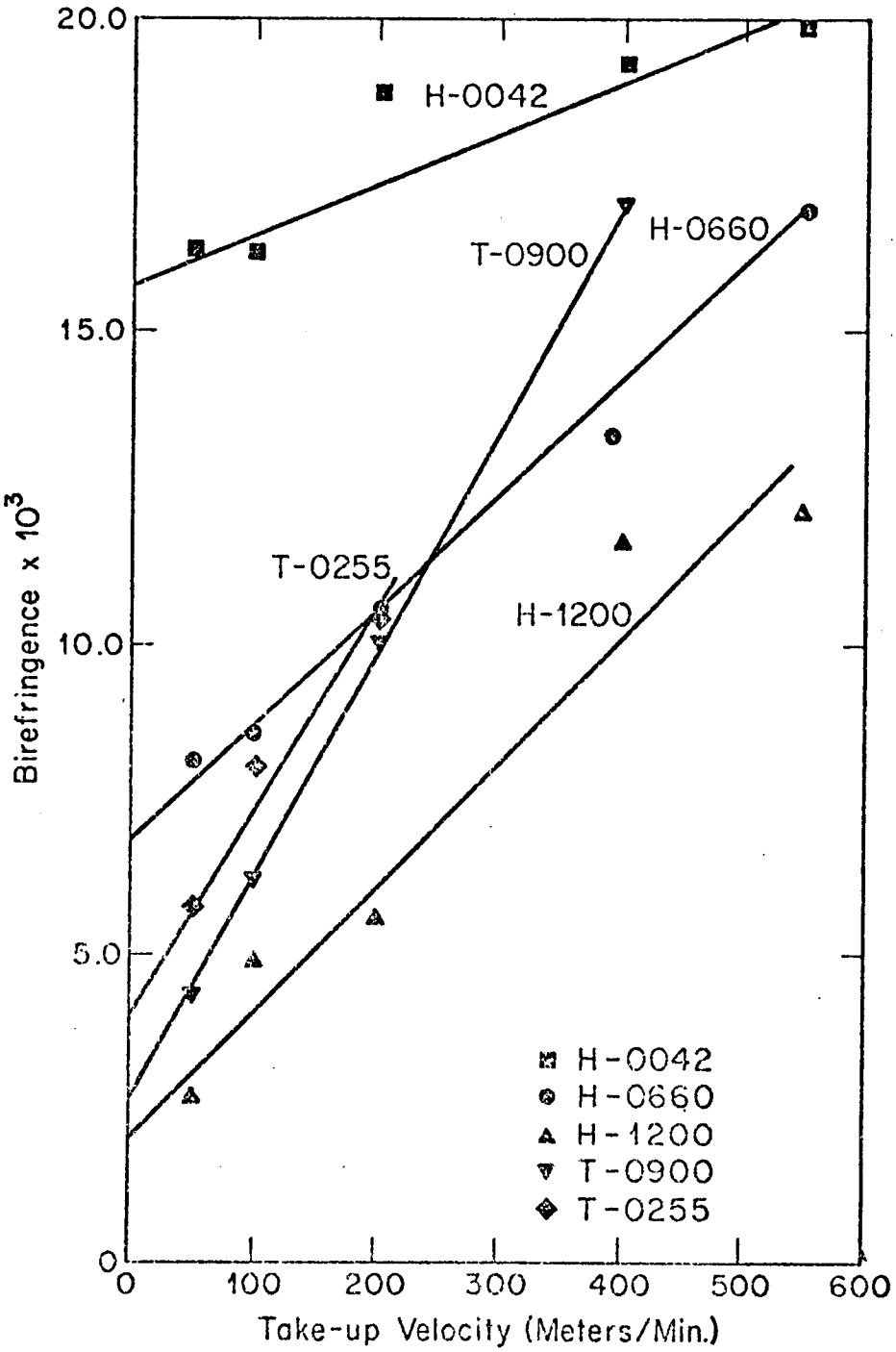


Figure 16. Birefringence in Polypropylene Filaments as a Function of Take-up Velocity

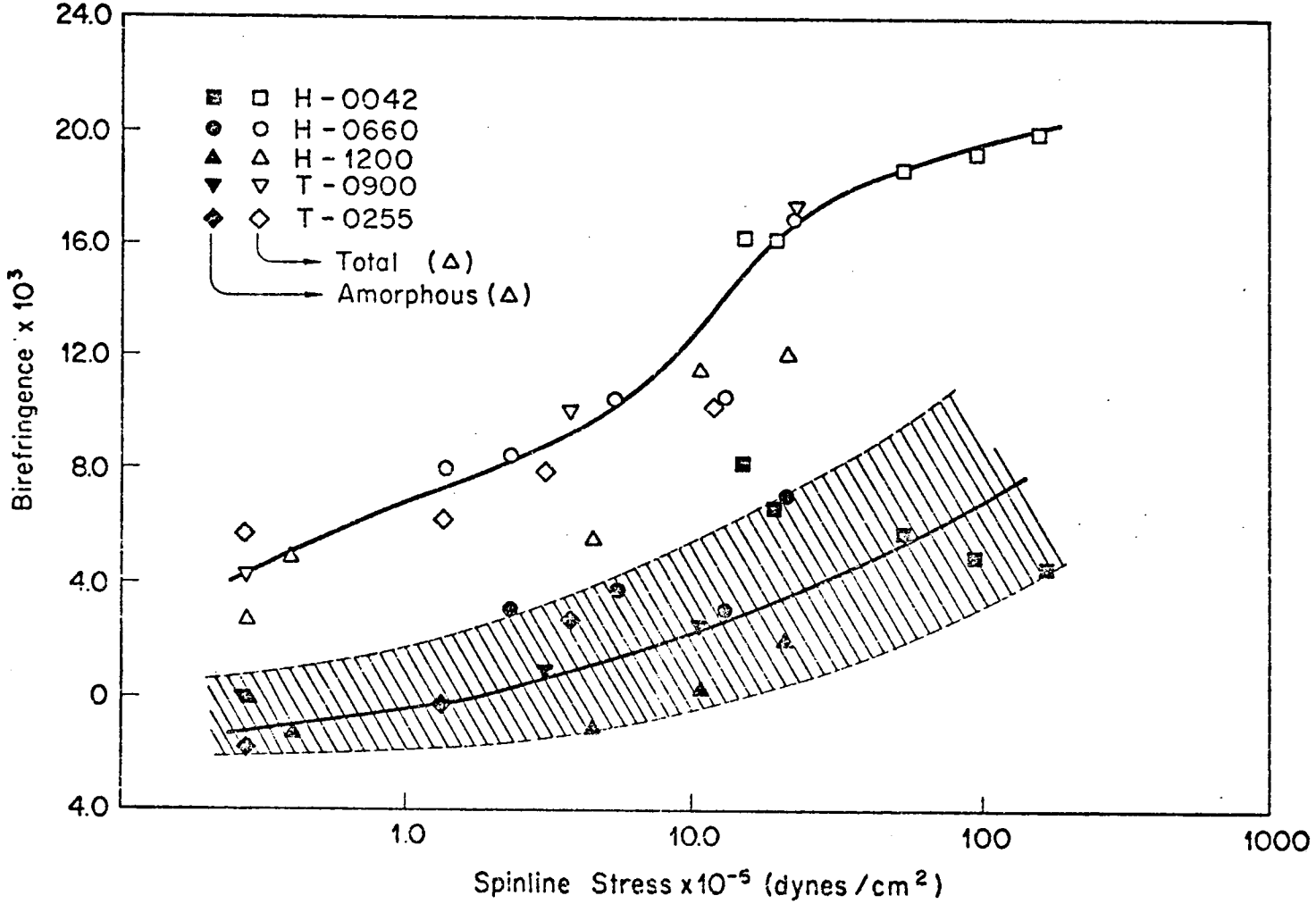


Figure 17. Total and Amorphous Birefringence of Polypropylene Filaments as a Function of Spinline Stress

average molecular orientation.

Figure 18 is a plot of amorphous and crystalline orientation function versus the spinline stress. Although both the crystalline and amorphous orientation factors increase with increasing spinline stress, the orientation developed in the amorphous chains is always less than the orientation in the crystalline regions.

C. DISCUSSION OF MELT SPUN FIBERS

Crystallinity

The fibers melt spun into ambient air were highly crystalline and the crystallinity values were similar to the values obtained by Sheehan and Cole (85), Samuels (83), and Henson and Spruiell (36). The increase in the crystallinity with the spinline stress in polypropylene is opposite to the trend observed in polyethylene. This behavior can be explained from the experimental results obtained by Henson and Spruiell (36). Henson and Spruiell showed that increase in spinline stress increases the crystallization start temperature, while increases in cooling rate decrease crystallization start temperature. In the spinline the crystallization rates increase with spinline stress, and increasing crystallization rates may lead to greater imperfection in the crystals. This latter effect would be expected to result in a decrease in crystallinity with increasing spinline stress as was observed in polyethylene. In the present polypropylene fibers it appears that this effect is offset by the increase in crystallization temperatures with increasing spinline stress, which would be expected to enhance crystalline perfection due to the greater molecular mobility.

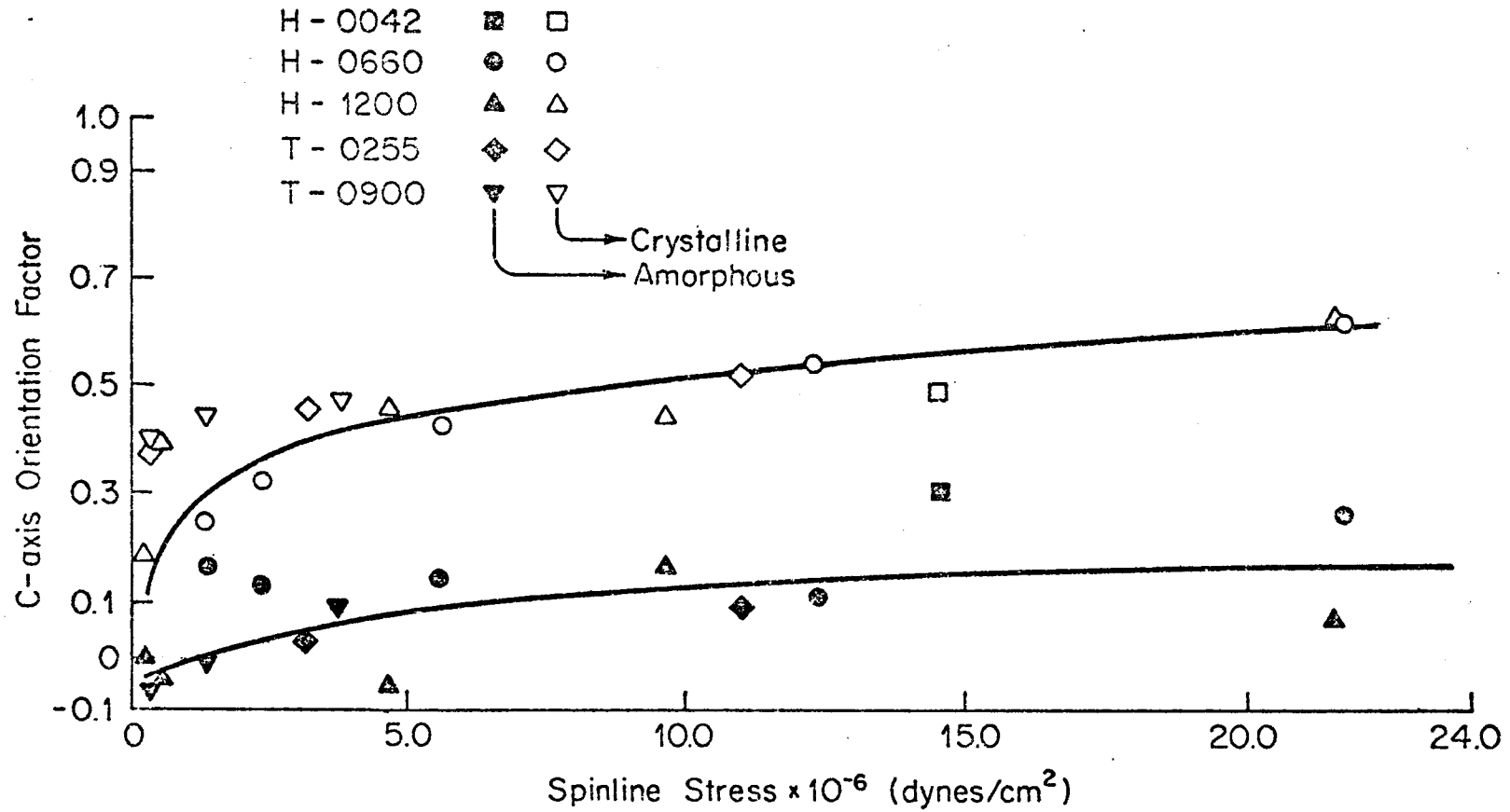


Figure 18. Crystalline and Amorphous Orientation Factors (f_c and f_{am}) of Polypropylene Filaments as a Function of Spinline Stress

Development of Structure (Morphology)

The development of morphology in the spinline of melt spun polypropylene is controlled by the stress levels in the spinline for any given cooling media. The effect of the other spinline variables like molecular weight, flow rate, melt temperature, and take-up velocity may effect the development of morphology independent of each other. But the combination of all these effects on morphology can be traced to their effect on spinline stress. Figures 15 (page 69), 17 (page 72), 18 and 19 support this argument. Figure 19 shows the crystalline orientation function of varying molecular weights, tacticity, melt flow rate and melt temperature (data from Henson and Spruiell (85)) plotted against the spinline stress. Within the experimental error all these data points seem to fall on a single curve, which shows the development of orientation in the molecular chains is only a function of the stress levels they were subjected to in the melt spinning process.

The development of morphology with increasing spinline stress can be partially followed through SAXS patterns (Figure 12, page 63). The ring SAXS pattern observed at low spinline stresses appears to be indicative of a nearly unoriented lamellar super structure probably a spherulitic structure. Samuels (83) observed spherulitic morphology in transmission electron microscope (TEM) replicas of spun polypropylene (83). The occurrence of two-point patterns at high stress appears to be due to the development of a slow nucleated morphology similar to the one discussed for polyethylene (1, 22, 88, 100). This interpretation in polypropylene is supported by the TEM observations of lamellae stacked parallel to the fiber axis by Fung, et al. (28). TEM photomicrographs which appear to show row

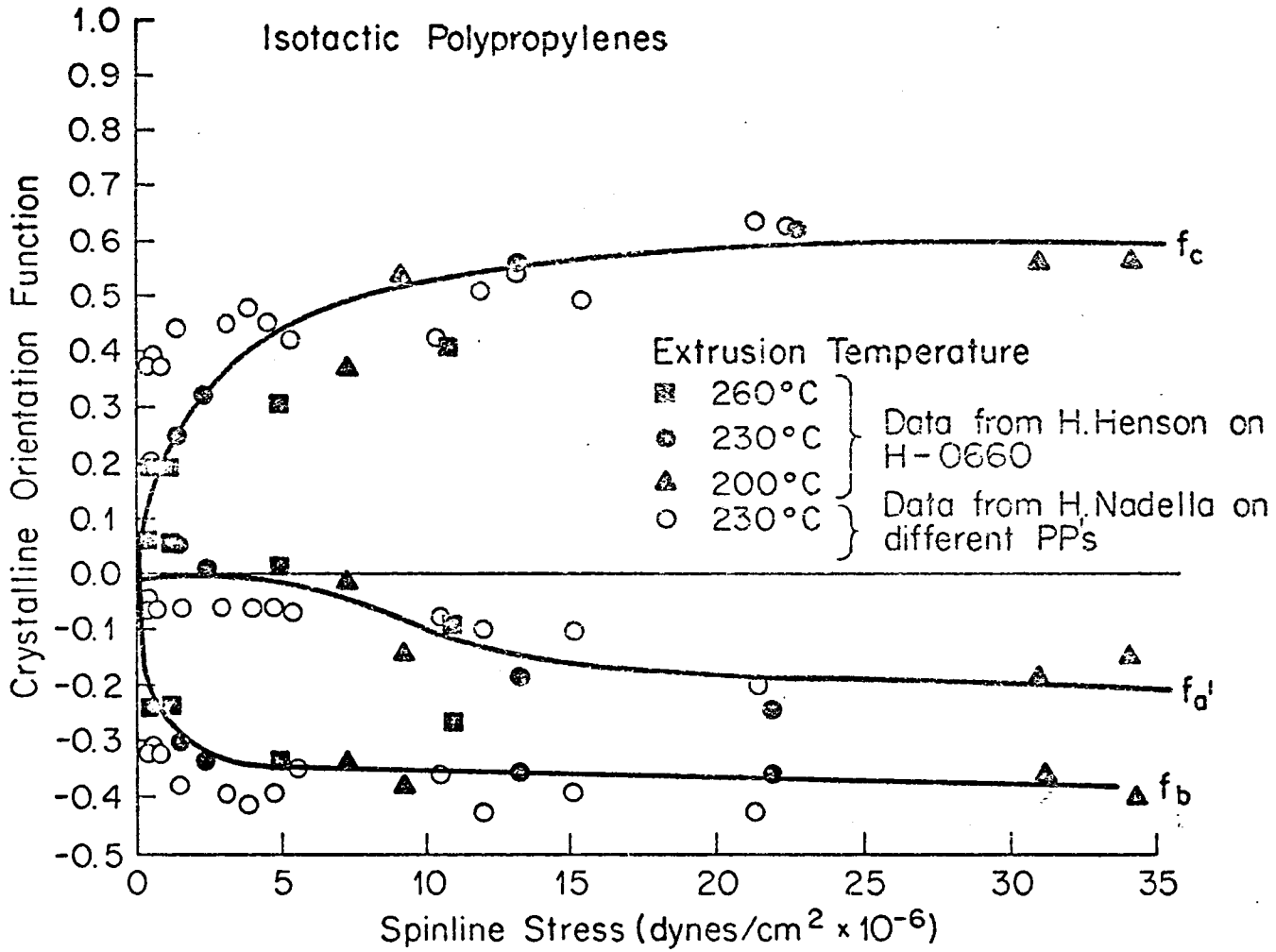


Figure 19. Comparison of Orientation Factors Obtained by Henson (36) for Three Different Spinning Temperatures on H-0660 to the Present Results for Different Polypropylenes

structures in polypropylene film extruded under high stress (and annealed) have been presented by Sprague (87).

Though there is general similarity in the development of crystalline orientation during spinning of polypropylene to that of polyethylene (see Figures 14 and 15, pages 67 and 69 respectively), the presence of bimodal distribution of unit cell orientations in polypropylene complicates the situation and makes polypropylene unique. The morphology in polypropylene, complicated by bimodal orientation, is not fully resolved. It has been considered by Clark (19), Clark and Spruiell (21), and Anderson and Carr (7). Clark and Spruiell's (21) morphological model for flow crystallized polypropylene is shown in Figure 20 which is applicable at high spinline stresses, where two point patterns of SAXS are obtained. In the development of the model shown in Figure 20, it was assumed that the crystallization proceeds in two stages. In the first stage, a row structure of planar lamellae develops from some sort of fibril nuclei. The lamellae grow with the growth axis of the lamellae parallel to the a'-axis of the unit cell. During this primary crystallization, some molecules are rejected from the growing lamellae into regions between them. These molecules crystallize a short time later in a secondary stage of crystallization. The orientation of the crystals in this secondary population is presumably controlled by an epitaxial matching between the fold surface of the primary crystals and the 13Å repeat of the polypropylene molecule. This matching requires that the chain axes of the secondary component be perpendicular to the chain axis of the primary component. The proposed interpretation of bimodal orientation thus consists of a row structure of planar lamellae interconnected by the tie molecules, which give rise to

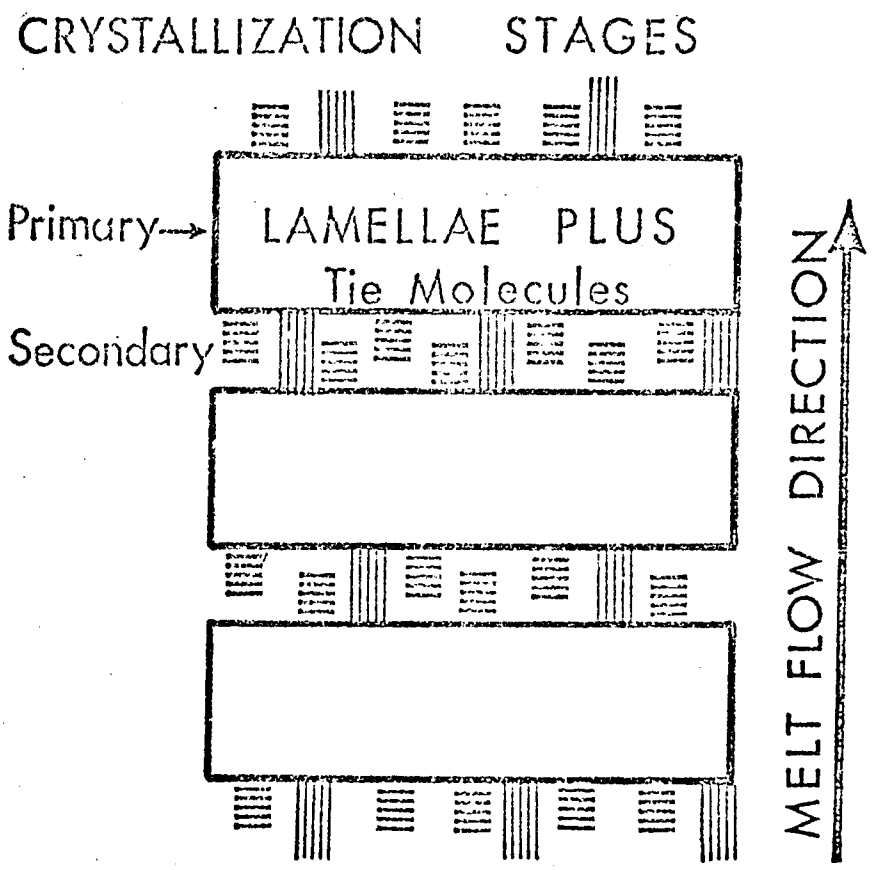


Figure 20. Morphological Model for Bimodal Orientation of Polypropylene

Source: E. S. Clark and J. E. Spruiell, American Chemical Society Polymer Preprints (2), 1975.

the c-axis oriented contribution, together with small interlamellar crystals in the a'-orientation as a result of their epitaxial relationship with the primary row structure (88).

CHAPTER V

TENSILE PROPERTIES OF MELT SPUN FIBERS

A. TYPICAL TENSILE CURVES

The tensile properties of the melt spun fibers were determined using an Instron Tensile Tester. The tests were carried out at room temperature and at an elongation rate of two inches per minute.

Figure 21 shows typical stress strain behavior for filaments of different molecular weights at take-up velocities of 50 and 550 meters per minute. For a given molecular weight the fibers taken up at a higher take-up velocity have higher modulus, yield strength and tensile strength (breaking stress). The elongation to break decreases with increasing take-up velocity. A distinct yield point is observed in H-1200-50 and H-0660-50. As take-up velocity is increased, the yield drop and the necking elongation becomes less prominent. Note that the yield drop is essentially absent in H-1200-550. The high molecular weight samples H-0042 did not exhibit a significant yield drop or necking behavior even when spun at the lowest take-up velocity, 50 meters per minute (Figure 21).

B. TENSILE PROPERTIES AND SPINLINE VARIABLES--RESULTS

Figures 22, 23, 24, and 25 show the elastic modulus, yield strength, tensile strength and percent elongation to break plotted against the spinline variable take-up velocity. Modulus is a difficult

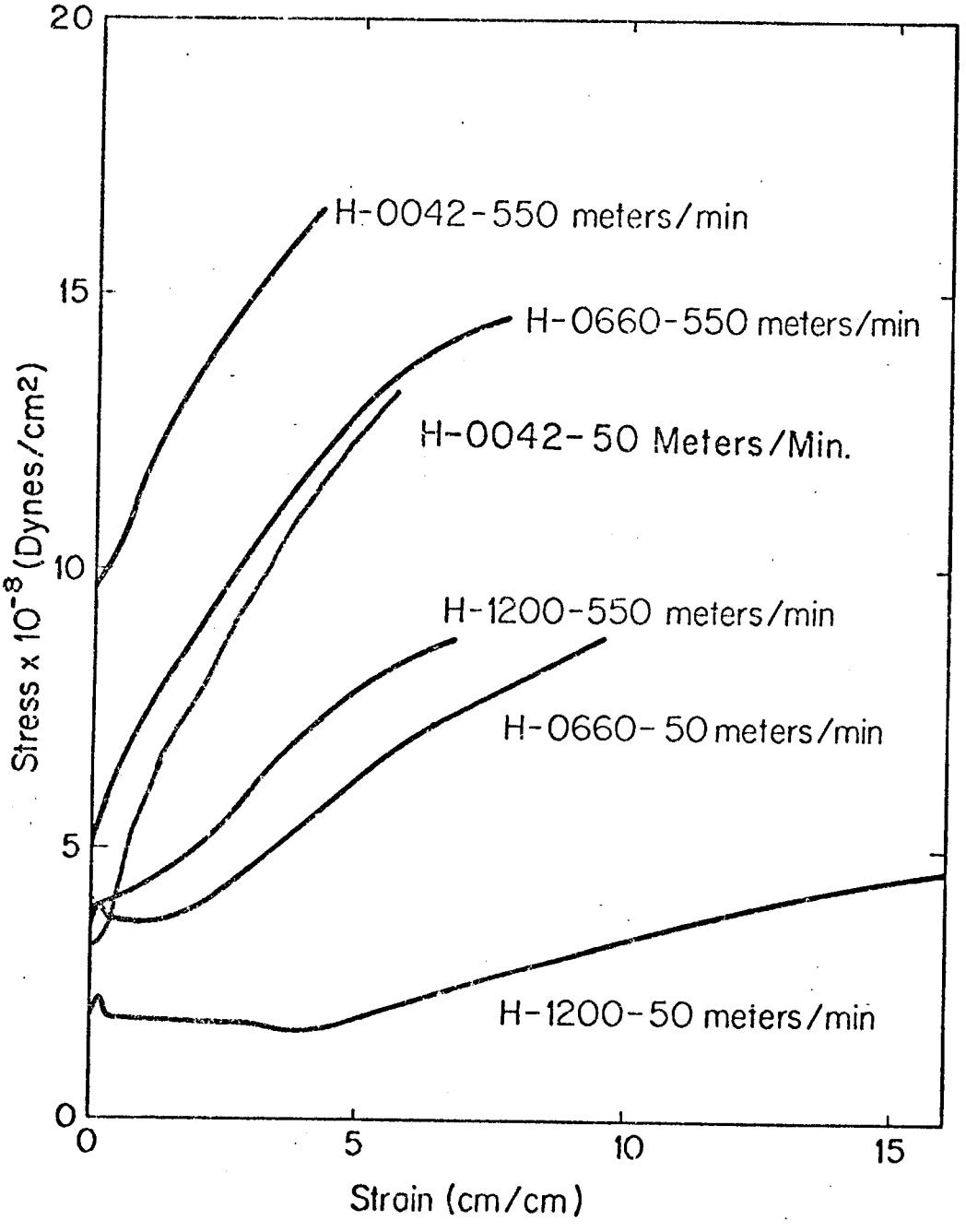


Figure 21. Typical Tensile Curves for Polypropylene Filaments

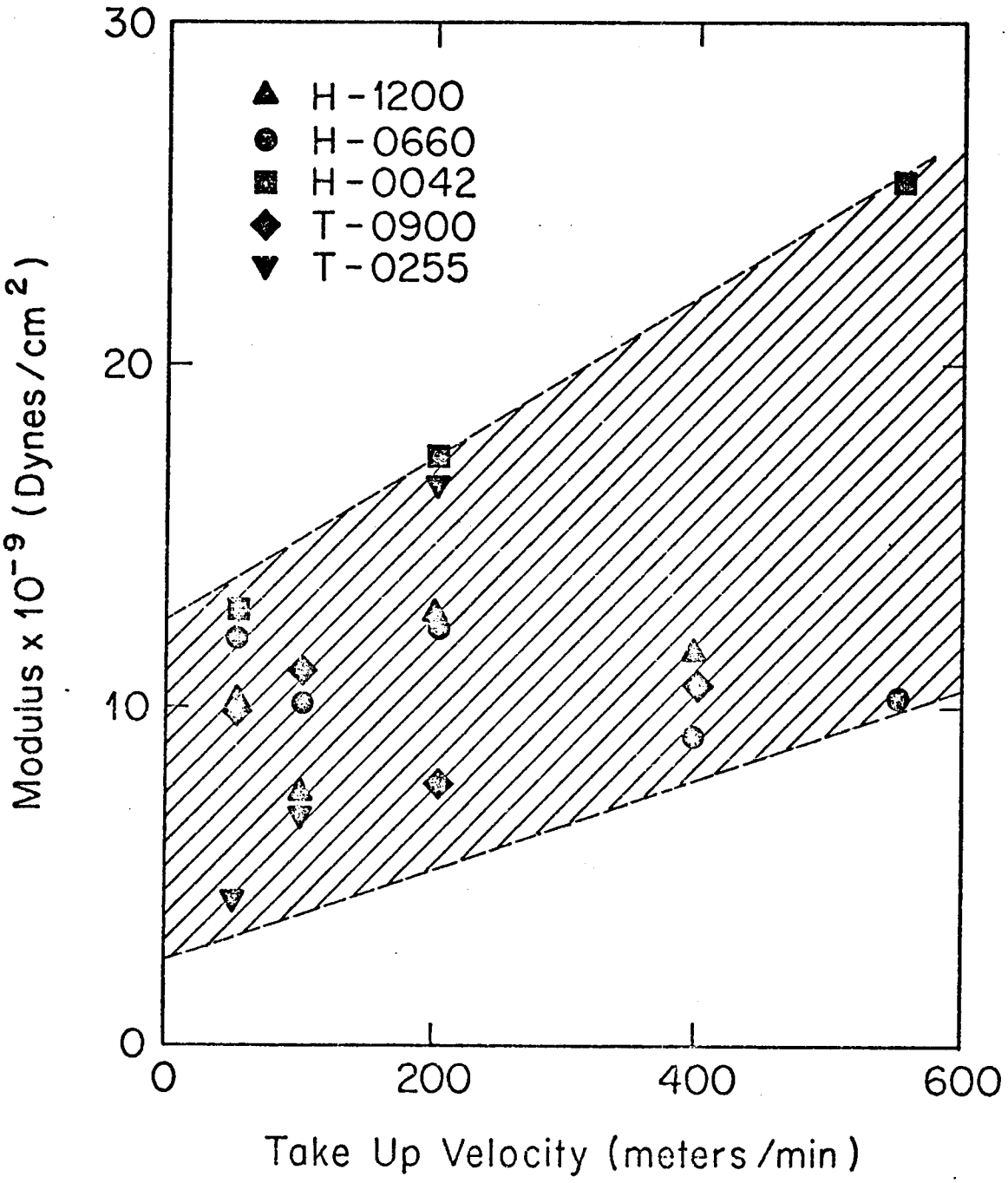


Figure 22. Modulus Versus Take-up Velocity of Polypropylene Filaments

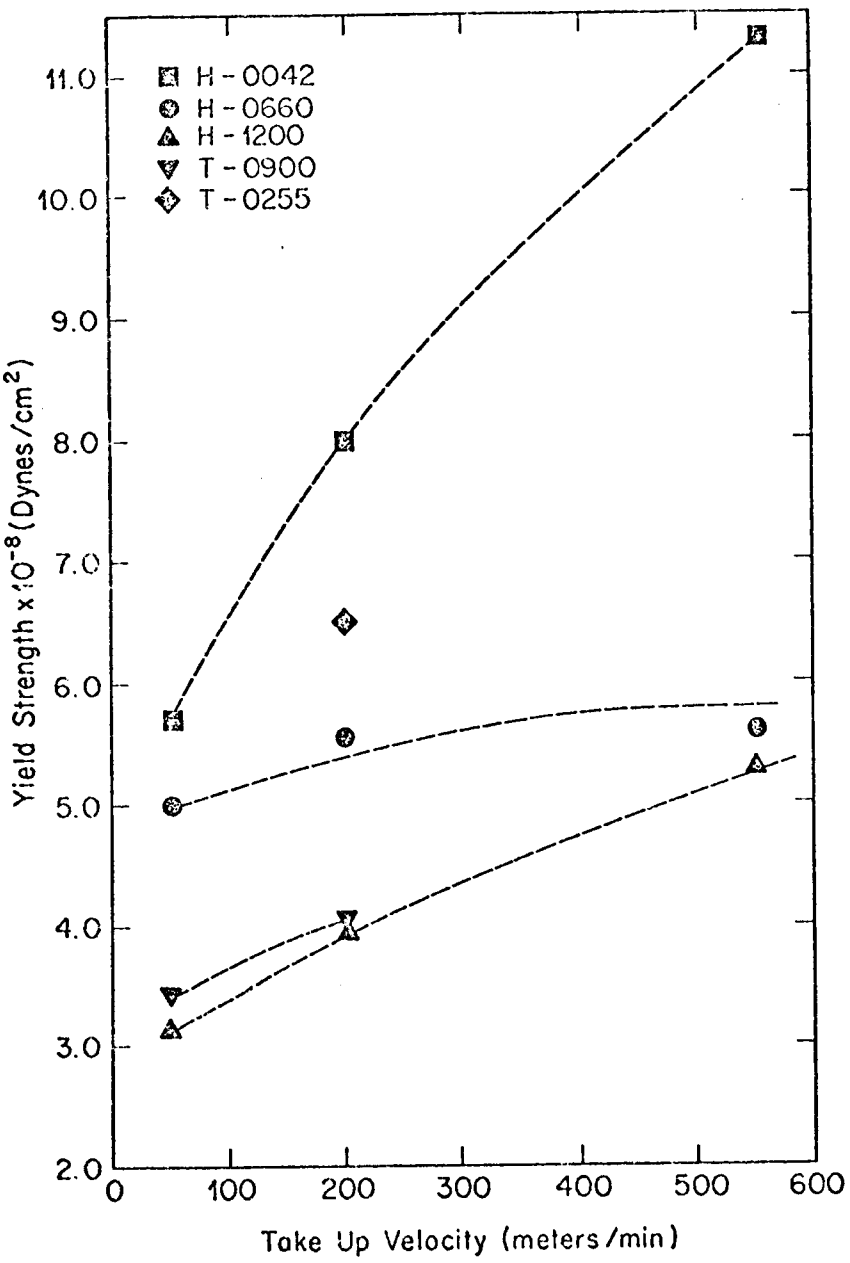


Figure 23. Yield Strength Versus Take-up Velocity of Polypropylene Filaments

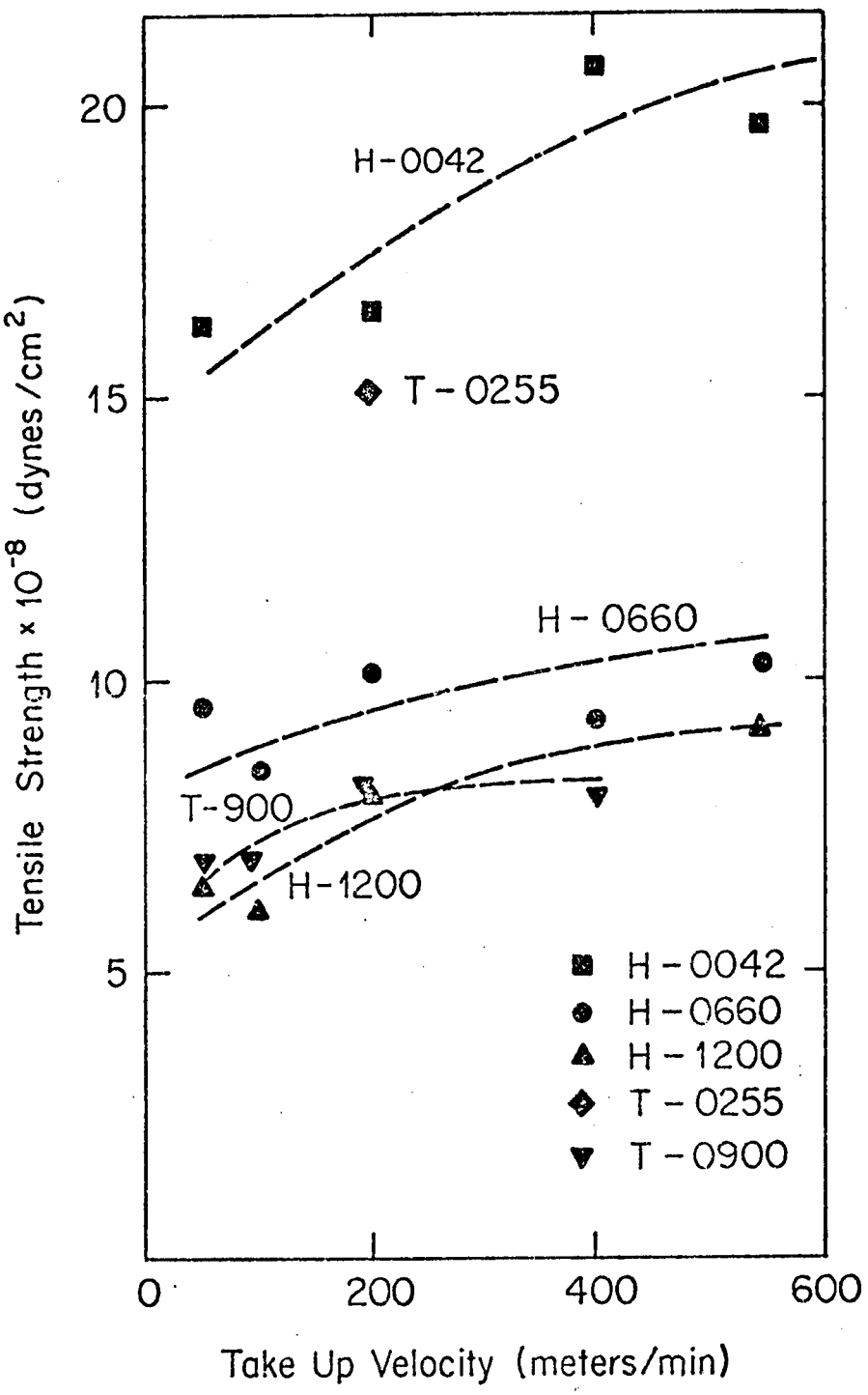


Figure 24. Tensile Strength Versus Take-up Velocity of Polypropylene Filaments

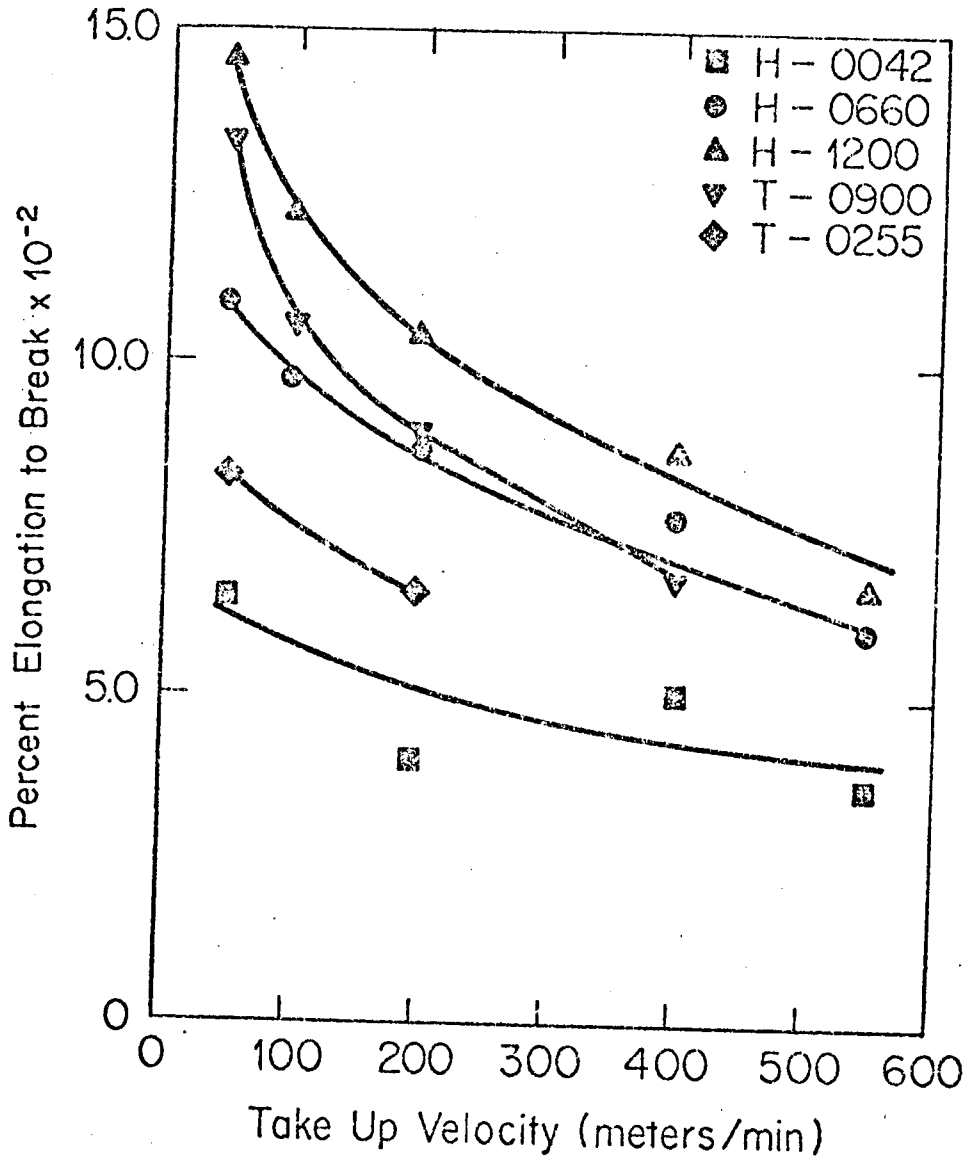


Figure 25. Percent Elongation to Break Versus Take-up Velocity of Polypropylene Filaments

property to measure accurately and the data in Figure 22 are scattered. However, a general trend toward increased tensile modulus can be observed with take-up velocity. The effect of molecular weight can be observed with take-up velocity. The effect of molecular weight on modulus is not clear from Figure 22. Figure 23 shows that the yield strength increases with take-up velocity for samples of each molecular weight. At a given set of spinning conditions the yield strength increases as the molecular weight increases. A similar trend is observed in the behavior of the tensile strength, Figure 24. Elongation to break (Figure 25) decreases with increasing take-up velocity for each type of polypropylene. The higher the molecular weight of the fiber, the less it can be elongated before it fractures.

Figures 26 through 29 show modulus, yield strength, tensile strength and percent elongation to break plotted against the spinline stress. For all the samples the modulus, yield strength and tensile strength increases while the percent elongation decreases with the spinline stress. It is of interest that the tensile property results from samples of different molecular weights appear to lie within a scatter band which is hardly broader than the expected scatter for the data from a given molecular weight sample. That is, the data appear to be correlated together by the spinline stress.

Figure 30 shows the elastic recovery at 100 percent elongation on the second cycle of the as-spun unannealed fibers. The elastic recovery also increases with the spinline stress. A maximum recovery of about 40 percent was observed at a spinline stress of 170×10^6 dynes/cm^2.

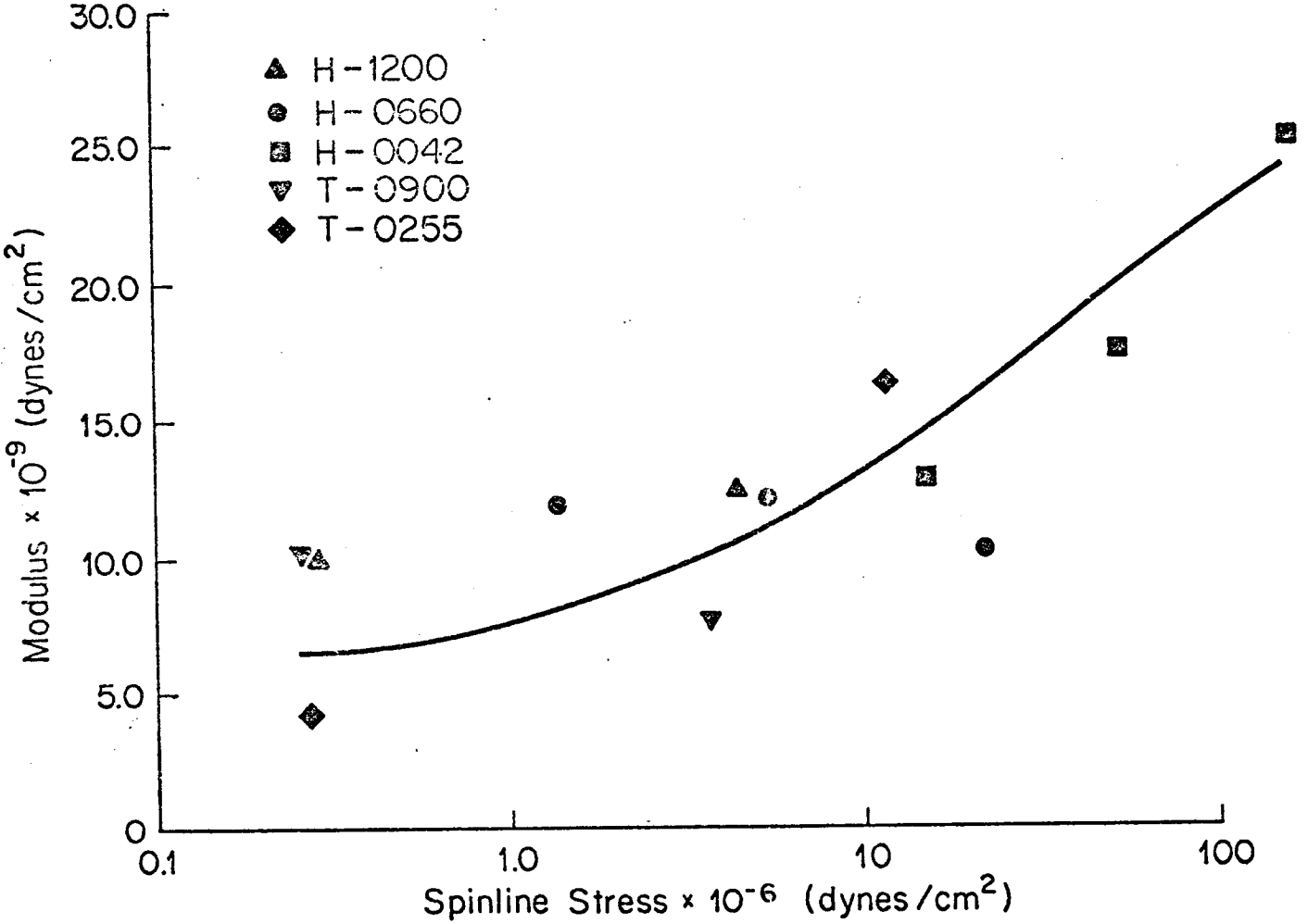


Figure 26. Elastic Modulus Versus Spinline Stress of Polypropylene Filaments

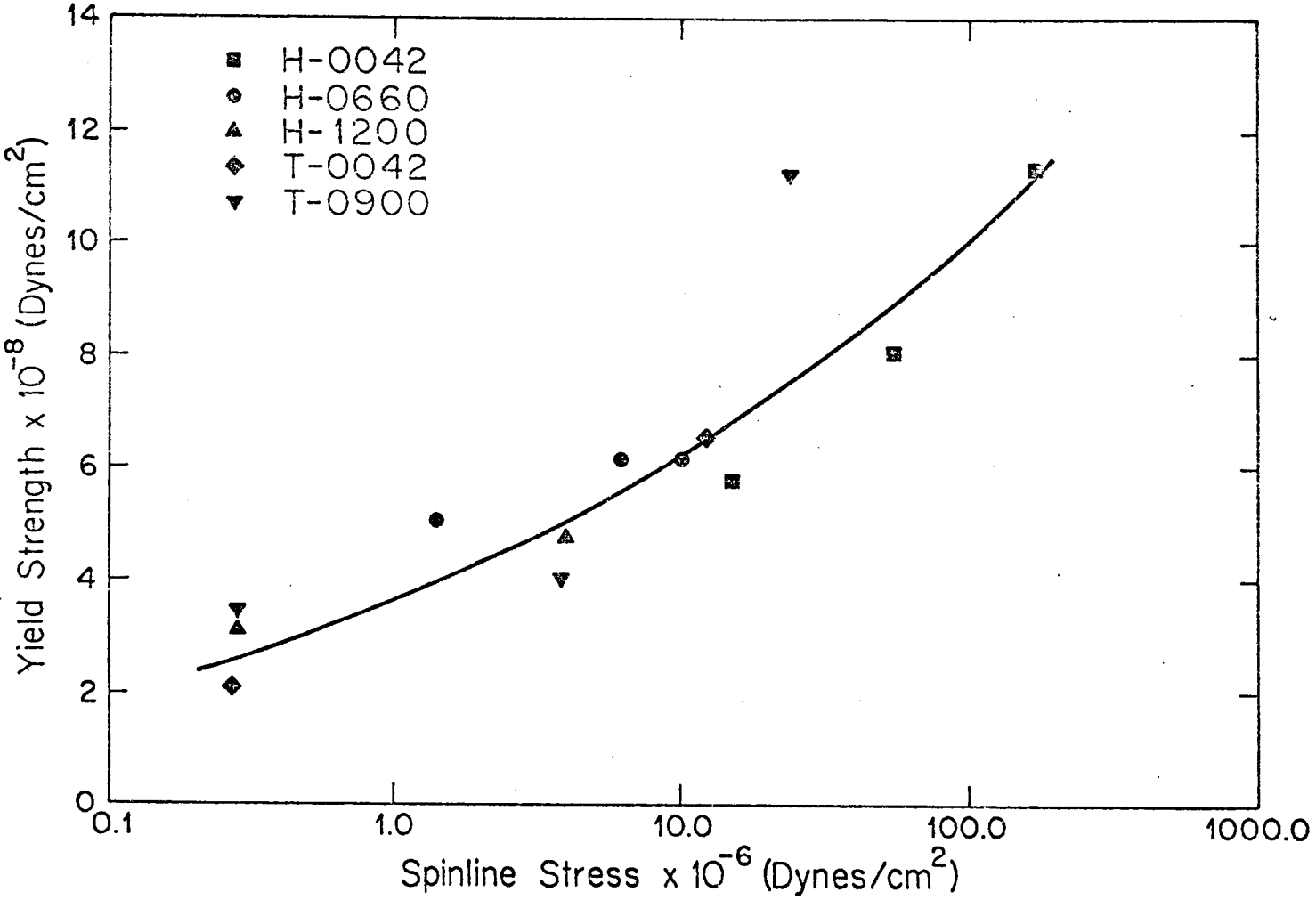


Figure 27. Yield Strength Versus Spinline Stress of Polypropylene Filaments

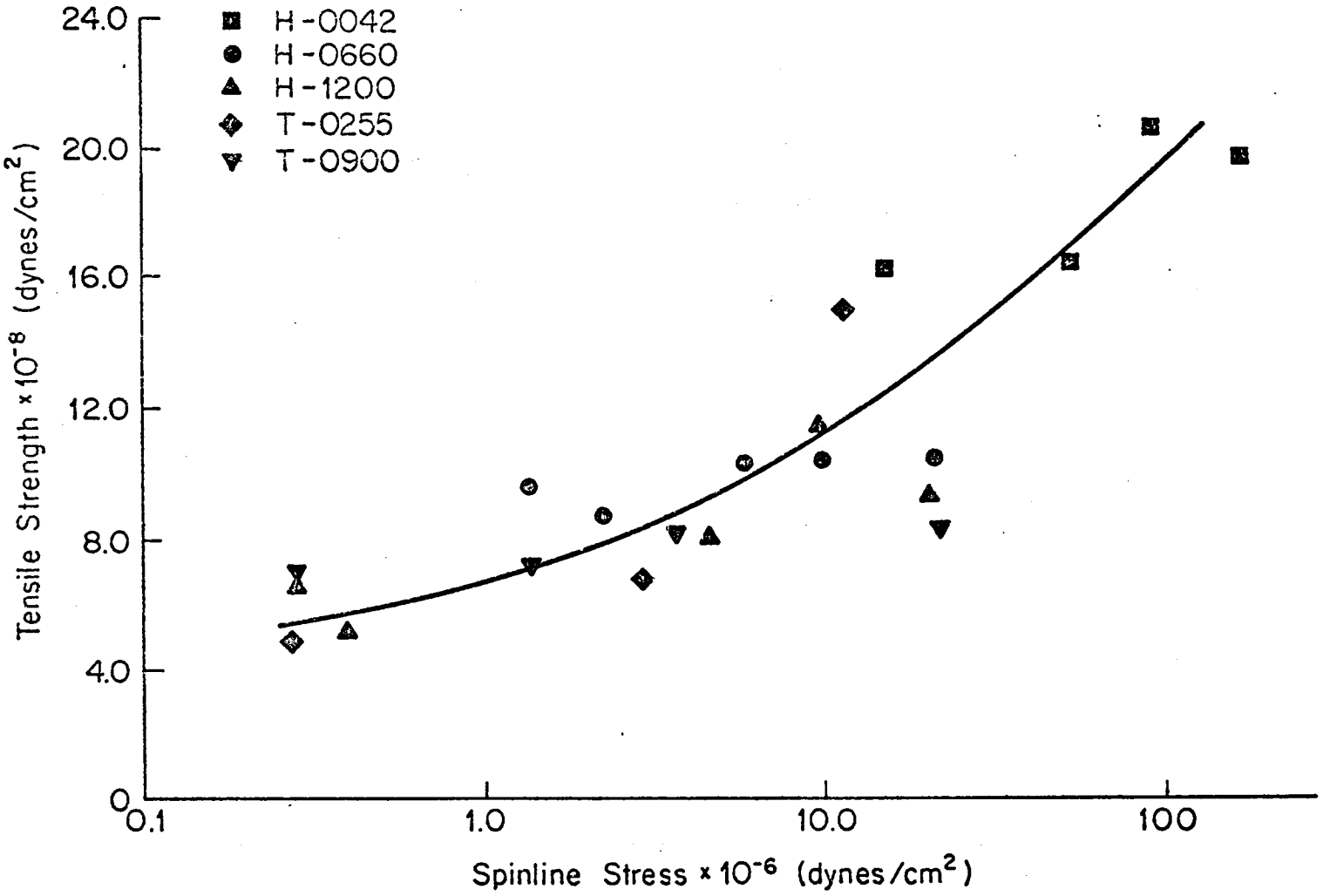


Figure 28. Tensile Strength Versus Spinline Stress of Polypropylene Filaments

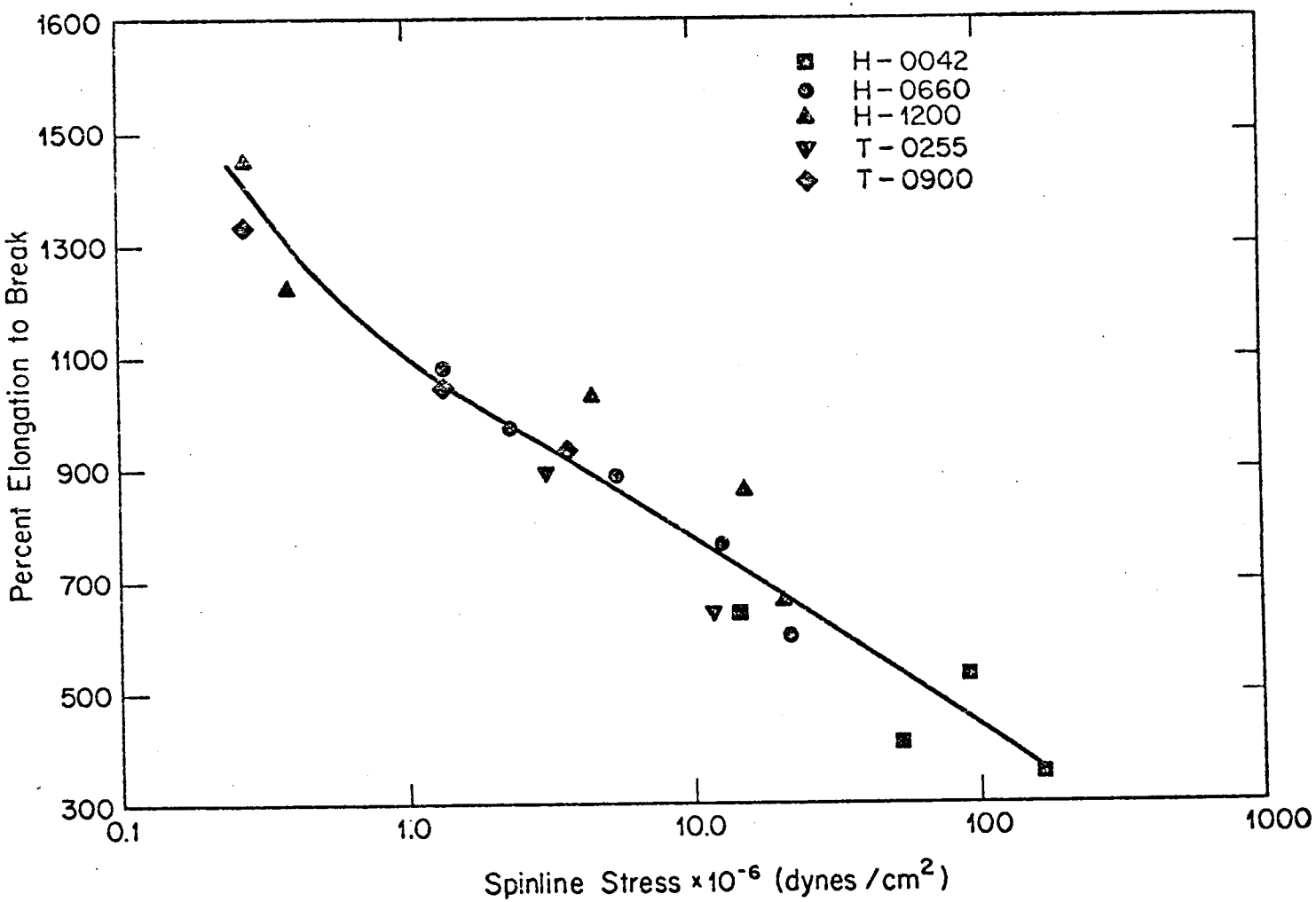


Figure 29. Percent Elongation to Break Versus Spinline Stress of Polypropylene Filaments

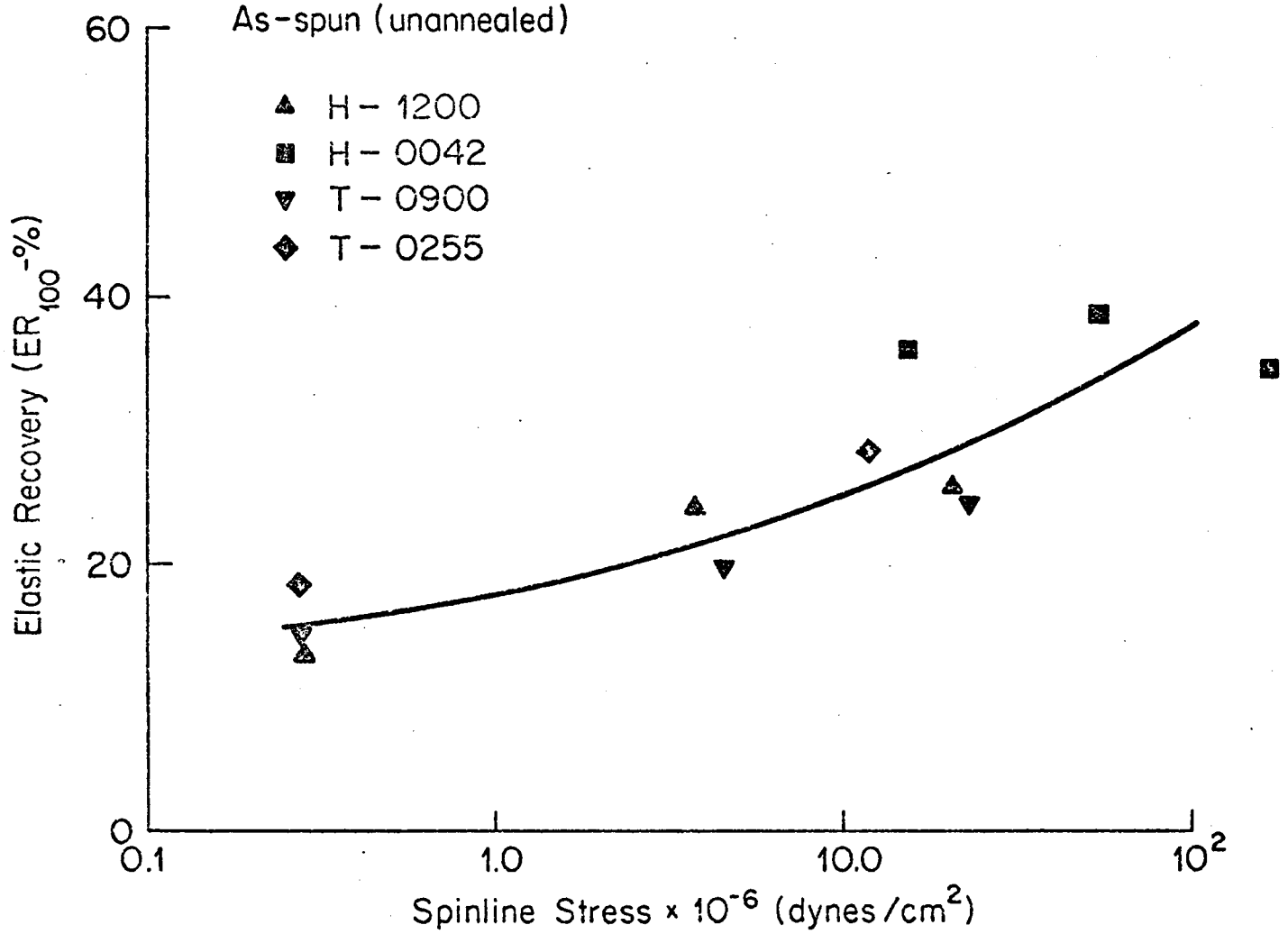


Figure 30. Percent Elastic Recovery on the Second Cycle at 100 Percent Extension Versus Spinline Stress of As-Spun Unannealed Polypropylene Filaments

C. TENSILE PROPERTIES AND STRUCTURAL VARIABLES--RESULTS

Figures 31, 32, and 33 show an increase in the modulus, yield strength and tensile strength with the measured birefringence. The scatter of the data seen in Figures 31, 32, and 33 appears to be a result of experimental error. In Figure 34, elongation to fracture is shown to decrease with the birefringence.

Figures 35 through 38 show the tensile properties plotted against the c-axis crystalline orientation factor. The modulus and tensile strength increases sharply with f_c whereas elongation to break decreases rapidly with f_c. Figure 36 shows a gradual increase in the yield strength with increasing f_c. The scatter in the tensile properties in Figures 35, 36, and 37 appears to be within the experimental limitations.

The mechanical properties were also plotted against the amorphous orientation factors. These plots for tensile strength and elongation to break are shown in Figures 39 and 40, respectively. As f_{am} increases the trends in mechanical properties are similar to those observed for the crystalline orientation factor, but there is even greater scatter in the relationship. This scatter is in part expected because f_{am} was calculated by subtracting two large numbers to obtain a small number (see Equation 10), and there is some uncertainty in f_{am} values.

D. DISCUSSION OF TENSILE PROPERTIES

The stress strain behavior of the polypropylene filaments is in agreement with the previous work on polyethylene (1, 22, 100) and polypropylene (36). The effect of molecular weight on stress versus strain

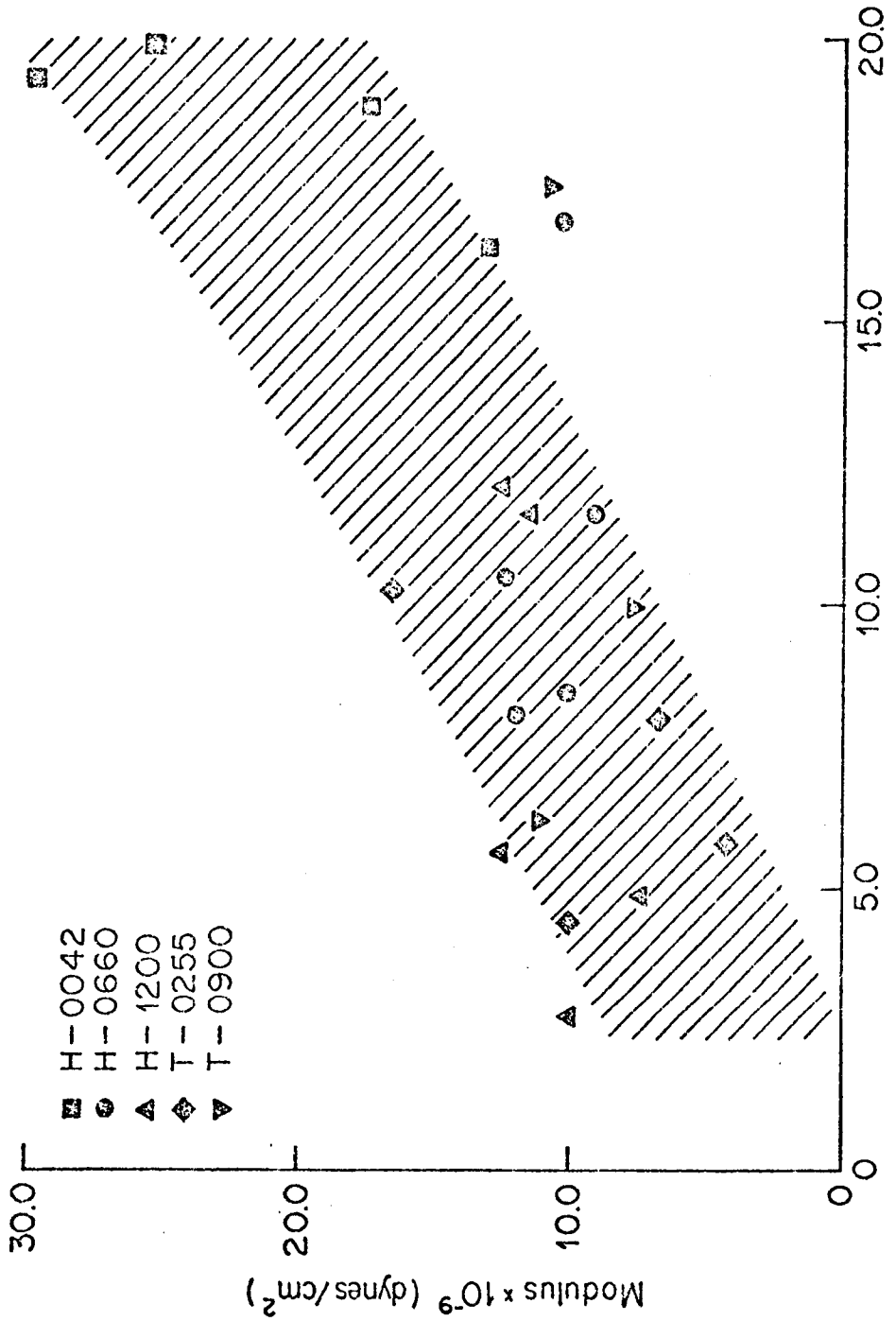


Figure 31. Modulus Versus Birefringence of Spun Polypropylene Filaments

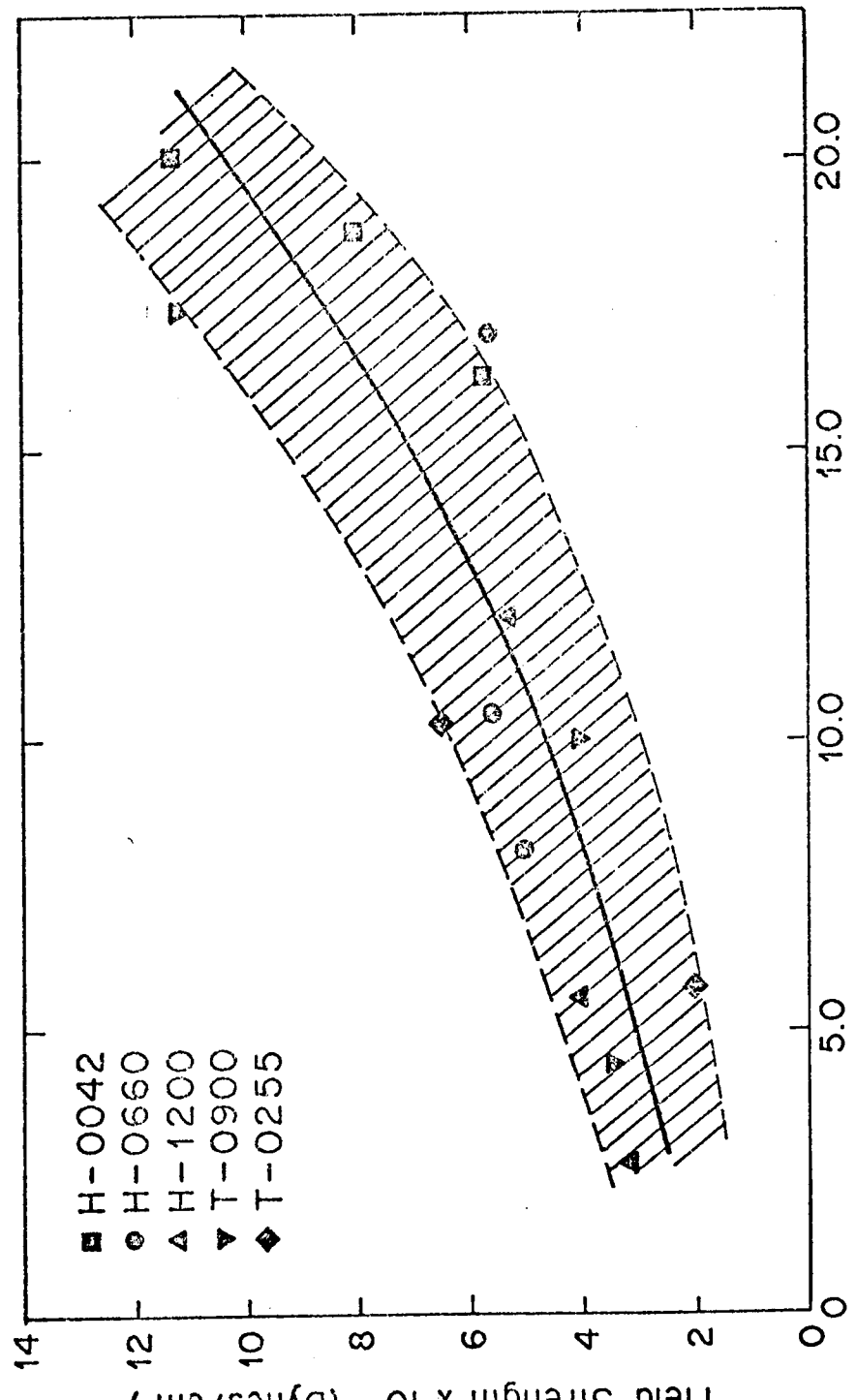


Figure 32. Yield Strength Versus Birefringence of Polypropylene Filaments

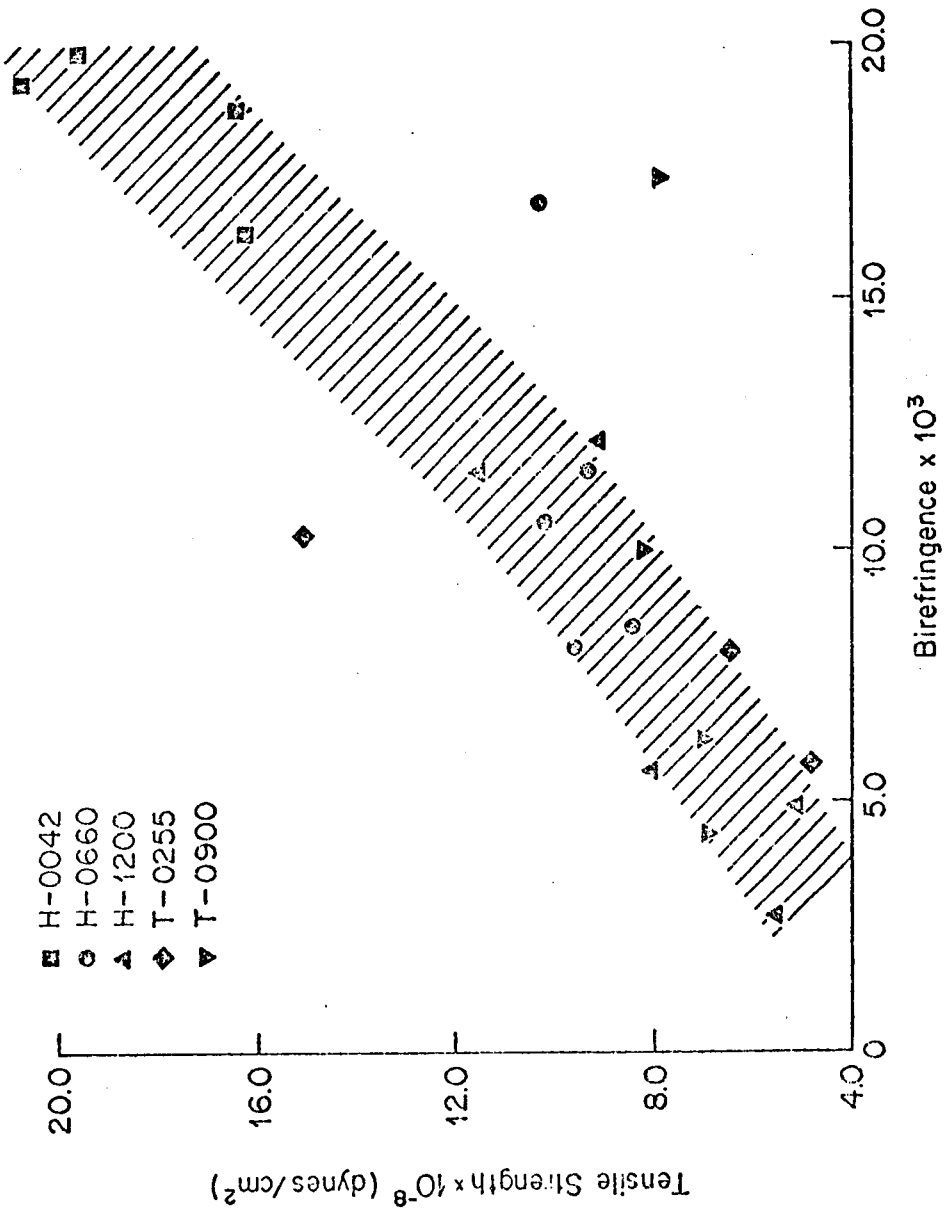


Figure 33. Tensile Strength Versus Birefringence of Polypropylene Filaments

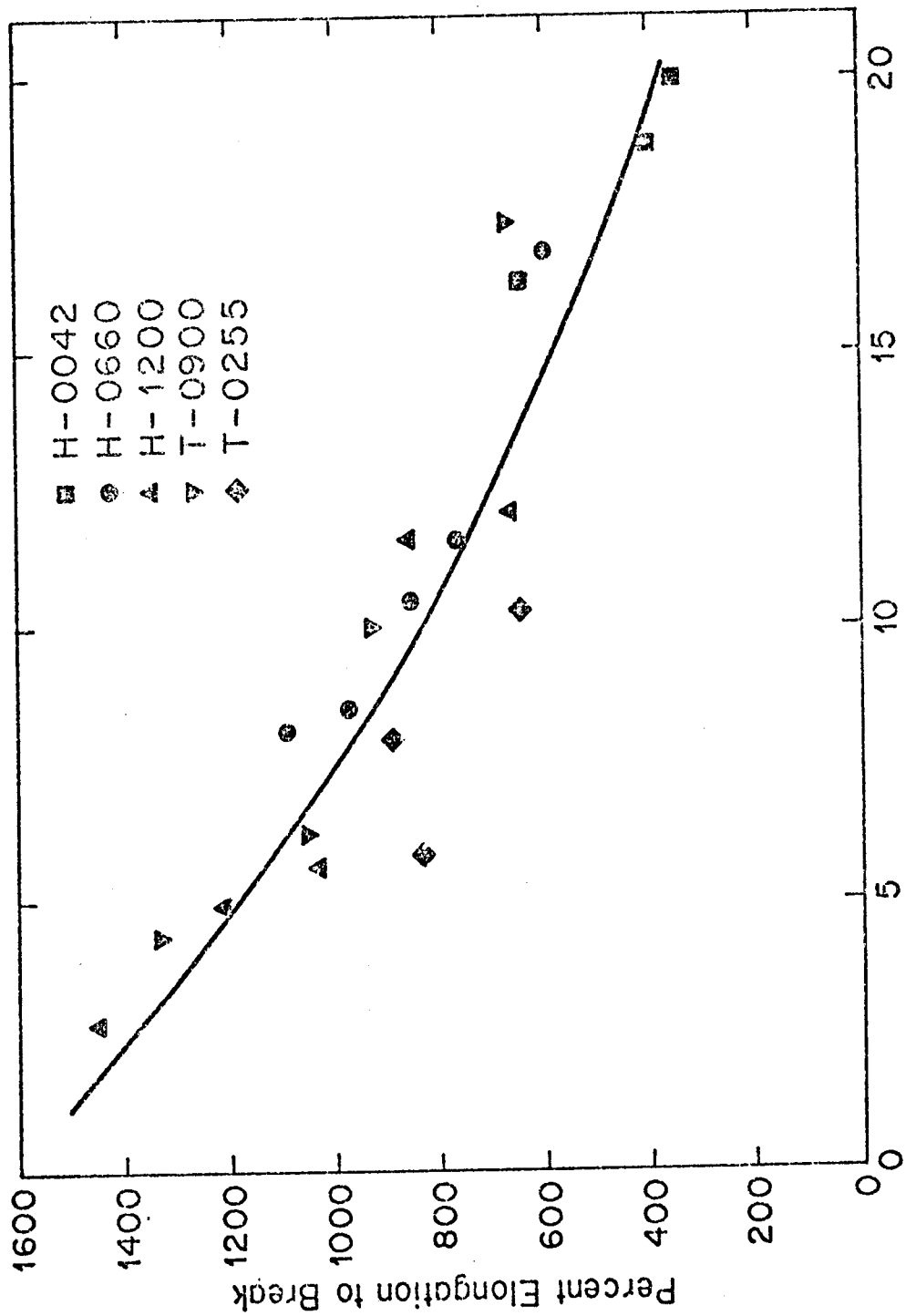


Figure 34. Percent Elongation to Break Versus Birefringence of Polypropylene Filaments

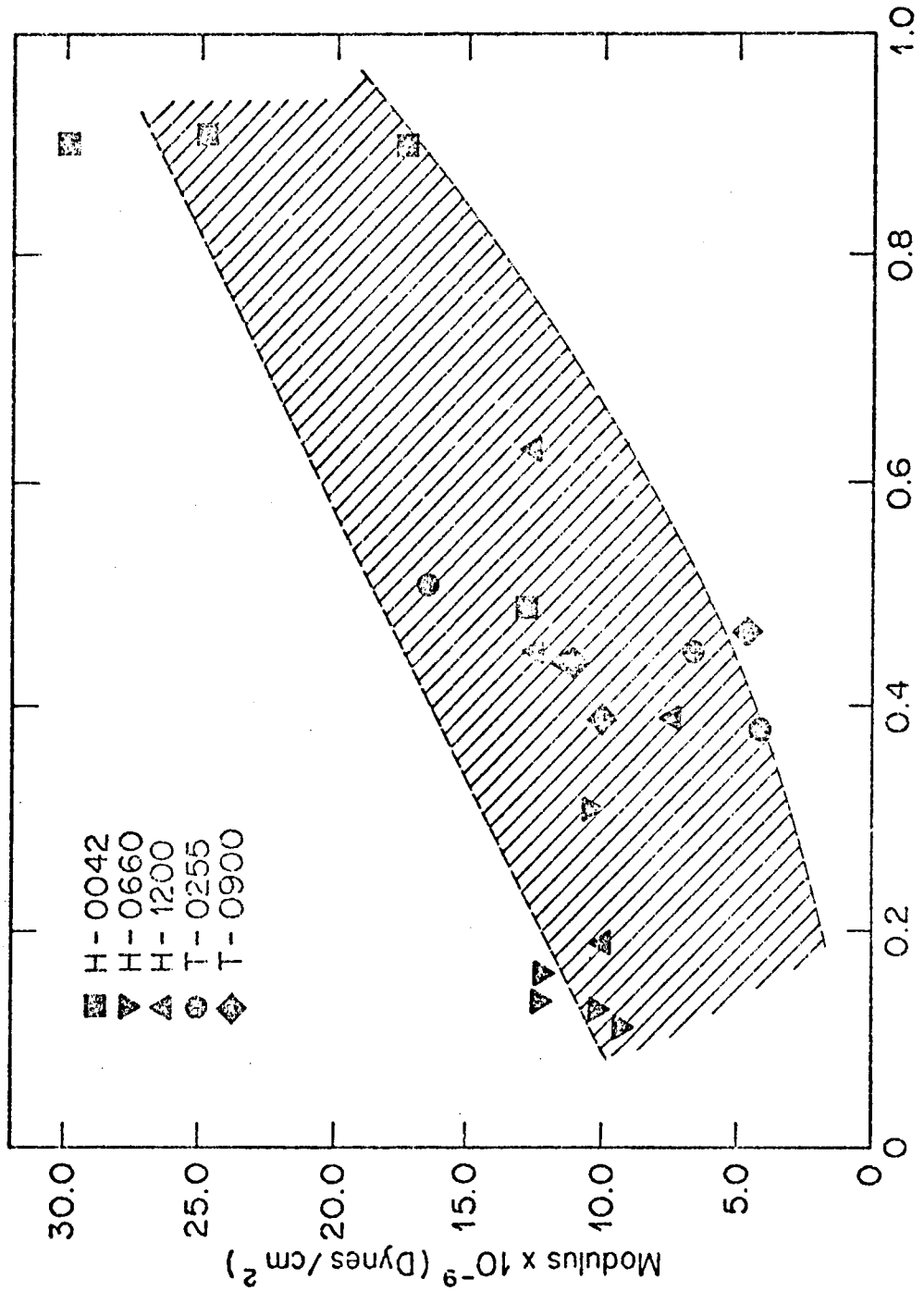


Figure 35. Modulus Versus Crystalline Orientation Factor, f_c, of Melt Spun Polypropylene Filaments

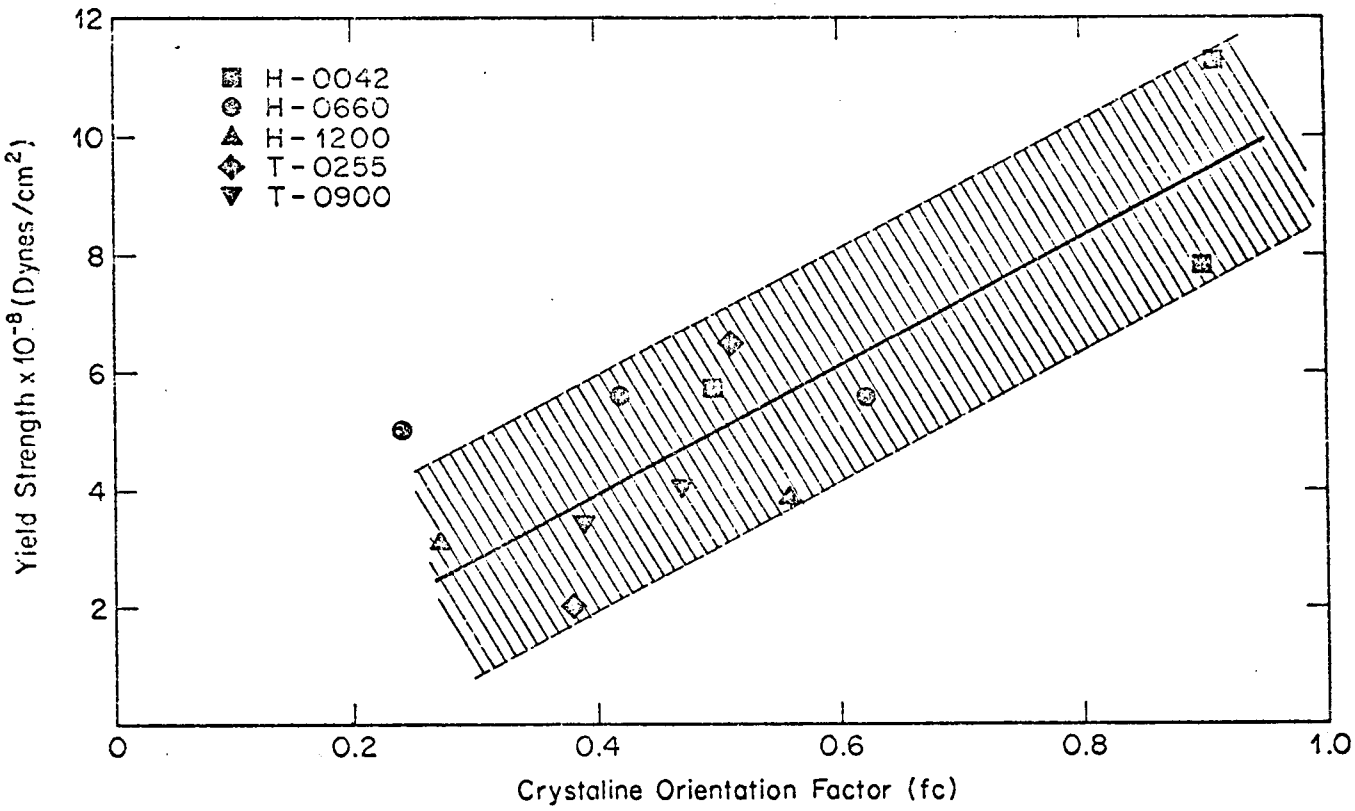


Figure 36. Yield Strength Versus Crystalline Orientation Factor, f_c, of Melt Spun Polypropylene Filaments

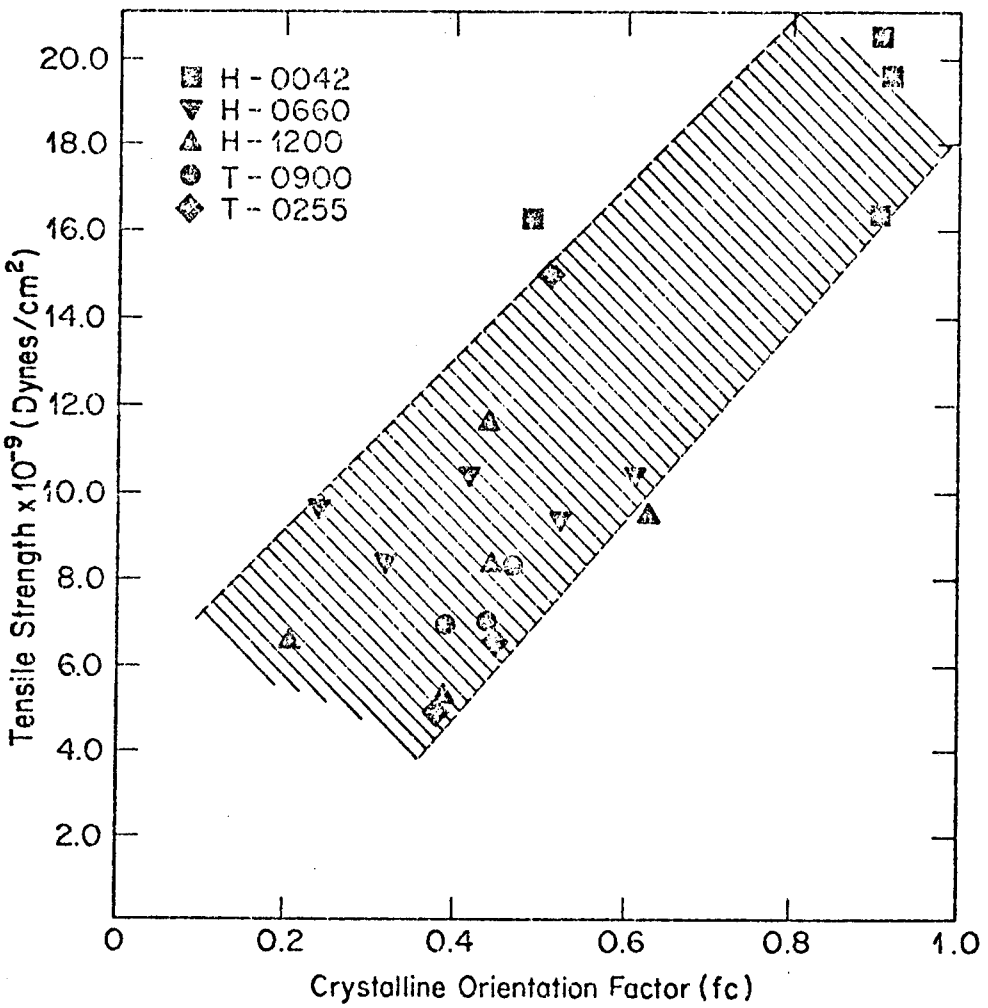


Figure 37. Tensile Strength Versus Crystalline Orientation Factor, f_c, of Melt Spun Polypropylene Filaments

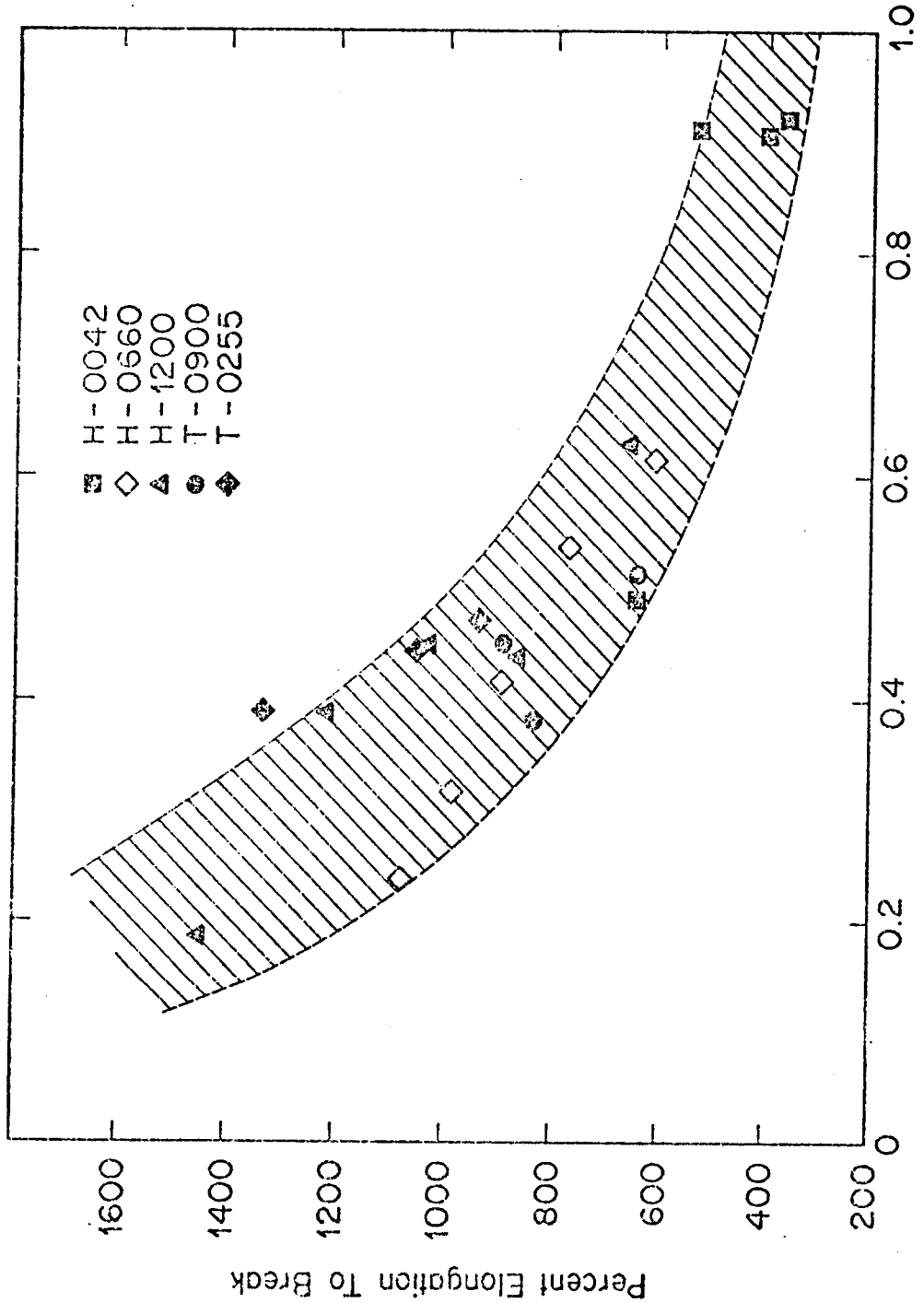


Figure 38. Percent Elongation to Break Versus Crystalline Orientation Factor, f_c, for Melt Spun Polypropylene Filaments

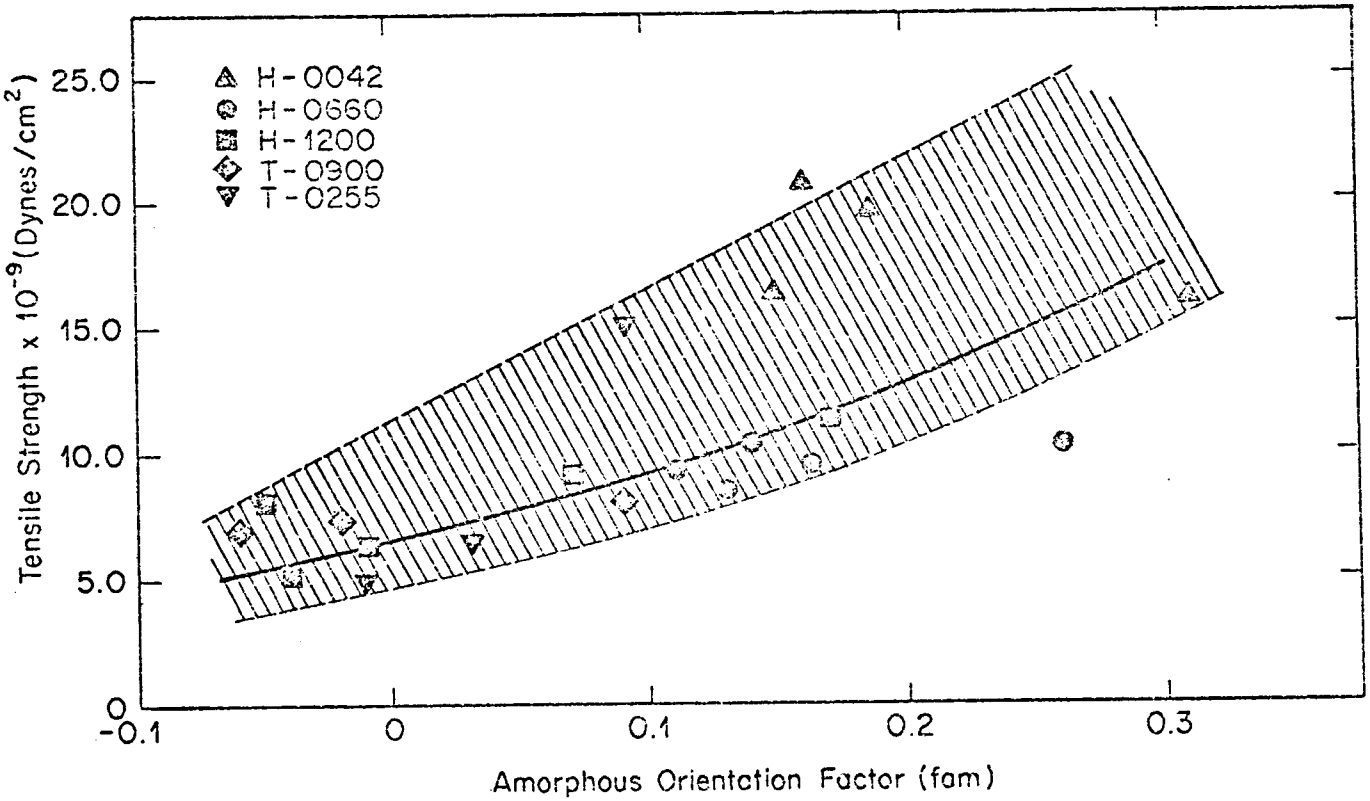


Figure 39. Tensile Strength Versus Amorphous Orientation Factor, f_{am}, of Melt Spun Polypropylene Filaments

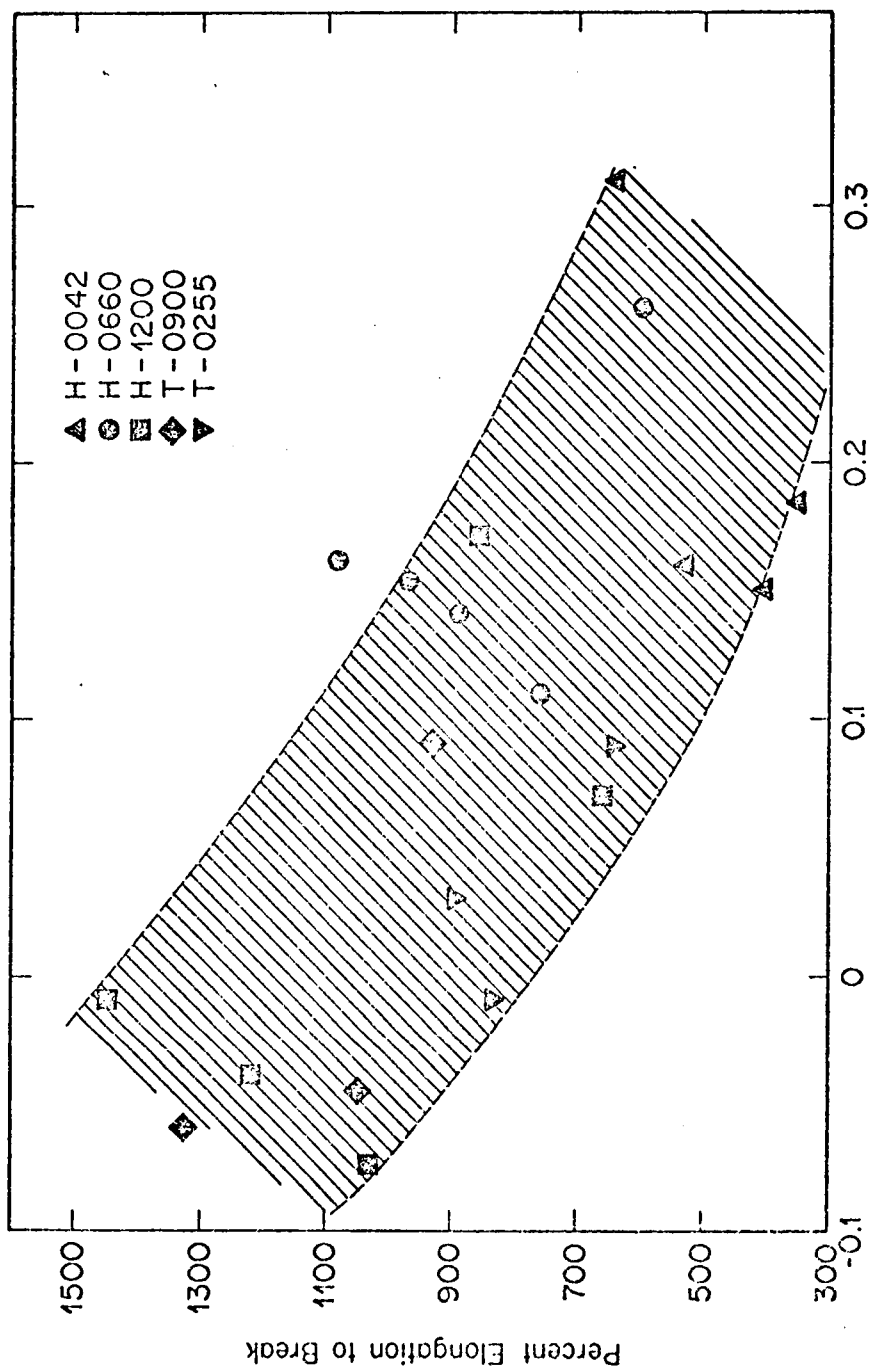


Figure 40. Percent Elongation to Break Versus Amorphous Orientation Factor, f_{am}, of Melt Spun Polypropylene Filaments

and tensile properties versus take-up velocity plots is in general agreement with the trends observed in polyethylene (100). The general trends observed in the tensile properties and the elastic recovery are similar to those of polyethylene (100).

Correlation with Spinline Variables

In general it appears that plotting properties as a function of the take-up velocity results in separation of the curves according to molecular weight as seen in Figures 24 and 25, pages 84 and 85. Figures 26 through 29, pages 86 through 90, can be interpreted to mean that the observed effects on tensile properties of the filaments of several spinning variables like take-up velocity, flow rate and molecular weight of the polymer results because changes in these parameters cause a change in the spinline stress. These figures show excellent correlation of the tensile properties of the melt spun filaments with the spinline stress. This result is not surprising because it was shown in Chapter IV that the development of orientation (and probably morphology as well) in the spun fibers depends primarily on the spinline stress.

Correlation of Properties with Structural Variables

Several investigators (1, 22, 100) have correlated the tensile properties of spun fibers with the c-axis orientation function, f_c. Samuels (83), studying drawn polypropylenes, used average and amorphous orientation factors. Dees and Spruiell (22) reported that in spun polyethylene filaments the amorphous contribution to the birefringence is small over the entire range of spinning conditions they investigated. This may be the reason for the good correlation of the tensile properties

with the c-axis crystalline orientation in polyethylene.

In the present work a correlation of tensile properties was attempted in a broader perspective.

The uniform variation of the tensile properties with birefringence shown in Figures 31 through 34, pages 93-96, for all the polypropylene filaments indicates that the tensile properties correlate well with the average molecular orientation in the melt spun fibers. Figures 31, 32, 33, and 34, pages 93-96, respectively, show strong tendency in the modulus, yield strength, elongation to break and tensile strength with c-axis crystalline orientation factor. The correlation of the tensile properties with amorphous orientation seems to be all right except for the broad scattering in the experimental results.

In conclusion, the tensile properties of melt spun polypropylene fibers seem to correlate best with spinline stress. This appears to result from the fact that the morphology developed in the filaments is controlled by the spinline stress present during the solidification process.

Individual structural parameters such as birefringence, c-axis crystalline orientation factor and amorphous orientation factor, all provide some degree of correlation of the data. For spun polypropylene filaments there is little difference between the correlations provided by these various parameters.

CHAPTER VI

DRAWING AND HEAT TREATMENT OF MELT SPUN FIBERS

Fibers spun with a broad range of spinline stresses having high (H-0042) and low molecular weights (H-1200) were selected for studying the effects of drawing and heat treatment on the structure and mechanical properties.

Table V gives a list of the samples, stress levels in the spinline and the draw ratios used in the study. The choice of draw ratios were discussed in Chapter III. Each filament was drawn just beyond the natural draw ratio (Stage I), nearly to fracture (Stage III) and intermediate to these two values (Stage II). Table V also shows a code system that will be used in the discussion of results.

A. STRUCTURAL CHANGES IN THE FILAMENTS SUBJECTED TO MECHANICAL AND THERMAL TREATMENT

Wide Angle X-Ray Diffraction--Results

Figure 41 shows WAXS patterns of melt spun and cold drawn filaments. It can be seen that the crystal structure has been transformed from monoclinic type to smectic form. Since the x-ray data are richer in the oriented monoclinic crystalline state than in the disordered (smectic) state, the drawn filaments were subjected to an annealing process. This process transforms the smectic structure into highly oriented monoclinic structure, as will be seen in Figure 42. Spot

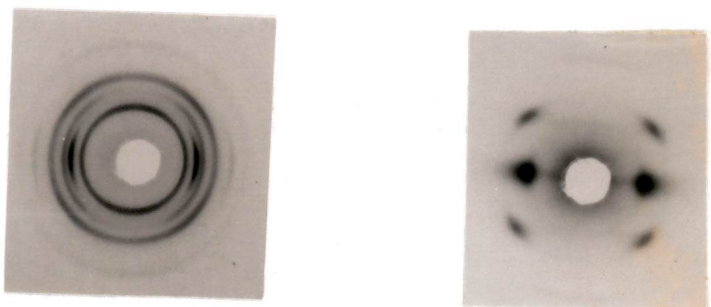
TABLE V

CHARACTERISTICS OF SPUN FIBERS SELECTED FOR DRAWING STUDIES AND DRAW RATIOS

Code Names	Specimen	Take-up Velocity meters/min	Spinline Stress dynes/cm^2	Draw Ratios		
				I	II	III
H-1200-200 D and T Series	H-1200	200	4.6×10^6	4.0	6.8	9.5
H-1200-550 D and T Series	H-1200	550	21.5×10^6	2.5	4.9	6.2
H-0042-50 D and T Series	H-0042	50	15.5×10^6	2.0	4.1	6.2
H-0042-550 D and T Series	H-0042	550	170×10^6	2.0	2.9	3.8

D series = drawn at 140°C (TI, TII, and TIII).

T series = cold drawn and annealed at 140°C for 15 minutes (DI, DII and DIII).



(a) (b)

H-1200-200

Figure 41. Effect of Cold Drawing on Melt Spun Fiber, (a) Melt Spun and (b) Cold Drawn Fiber (Before Annealing)

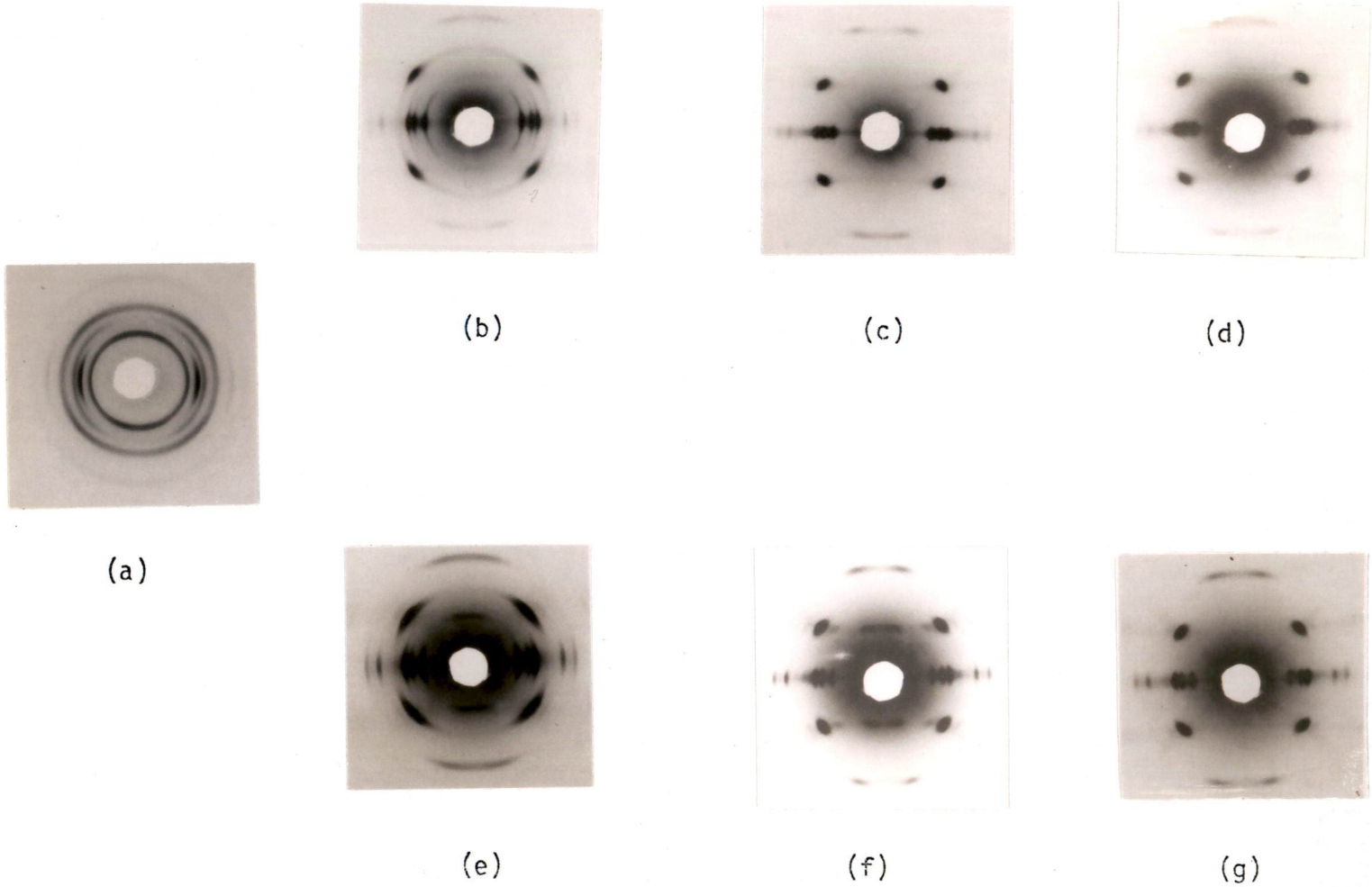


Figure 42. WAXS Patterns for Low Molecular Weight Polypropylene Filaments (H-1200) Spun at 200 Meters/Min Showing the Effects of Either Cold Drawing at 140°C, (a) As-Melt Spun, (b) DI, Draw Ratio = 4.0, (c) DII, Draw Ratio = 6.8, (d) DIII, Draw Ratio = 9.5, (e) TI, Draw Ratio = 6.4, (f) TII, Draw Ratio = 6.8, (g) TIII, Draw Ratio = 9.5

checks on the crystallinity of cold drawn and annealed filaments indicated that their crystallinity is slightly higher than that of the as-spun filaments. Values of about 61 percent were observed by density gradient column.

Figure 42 shows WAXS patterns for the low stress spun (H-1200-200) D (drawn and annealed, 140°C) and T (drawn at 140°C) series. Qualitatively there is not much difference in the development of orientation between the D and T series (compare (c) with (f) and (g) in Figure 42) in the higher draw region. In both of the series high orientations were observed at Stage II of drawing compared to Stage I and there seems to be a decrease in the crystallite size as indicated by the broadening of x-ray spots in the equatorial direction. This feature is more pronounced in the cold drawn and annealed samples. Additional annealing could probably result in patterns even more similar to the patterns of hot drawn samples. Little, if any, bimodal orientation was observed in the drawn H-1200-200 samples.

Figures 43 and 44 show WAXS patterns for the H-0042-50 and H-0042-550 series. Figures 43 and 44 seem to indicate a slightly lower degree of orientation development after drawing to Stage III than in Figure 42. Traces of a'-oriented reflections were also observed at low draw ratios. Figure 44, showing pattern spun under very high stress is highly oriented ($f_c \sim 0.91$) in the as-spun condition and shows little increase in orientation upon drawing.

The crystalline orientation factors for some of the drawn fibers were estimated from selected micro densitometer scans of the WAXS patterns. These results are presented in Appendix A. At higher draw

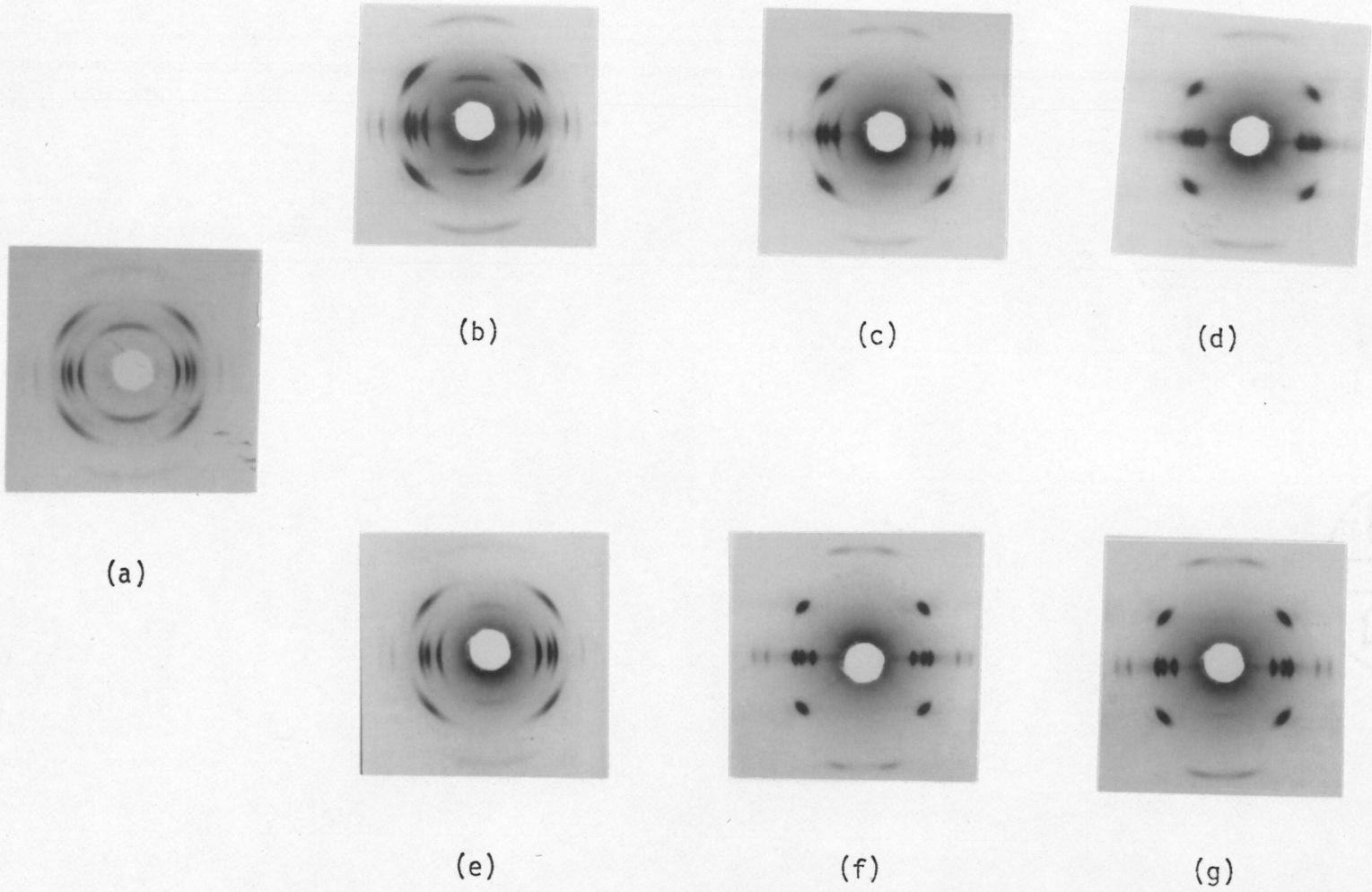


Figure 43. WAXS Patterns for High Molecular Weight Polypropylene Filaments (H-0042) Spun at 50 Meters/Min Showing the Effects of Either Cold Drawing and Annealing at 140°C (b through d) or Hot Drawing at 140°C (e through g), (a) As-Melt Spun, (b) DI, Draw Ratio = 2.0, (c) DII, Draw Ratio = 4.1, (d) DIII, Draw Ratio = 6.2, (e) TI, Draw Ratio = 2.0, (f) TII, Draw Ratio = 4.1, (g) DIII, Draw Ratio = 6.2

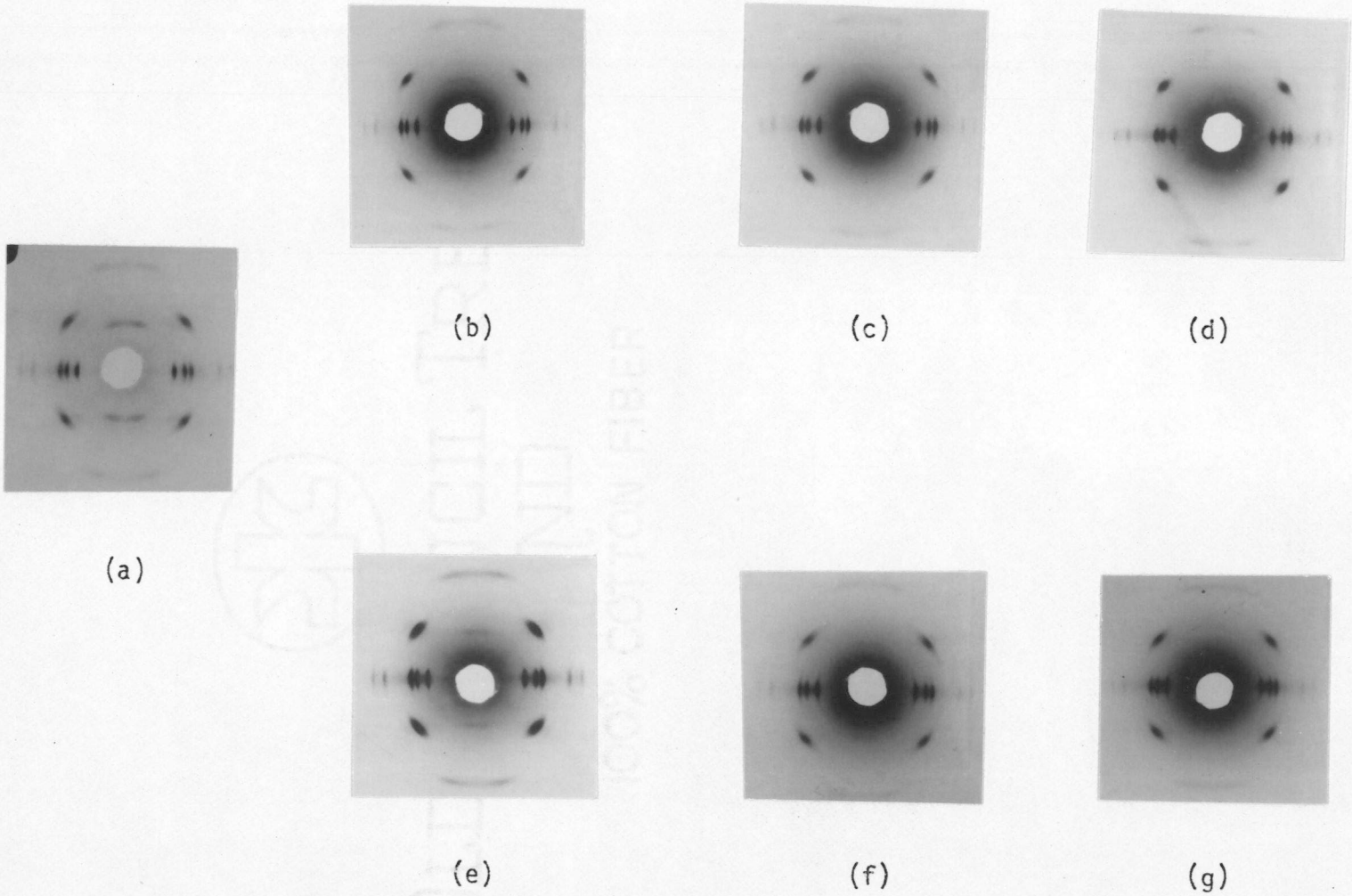


Figure 44. WAXS Patterns for High Molecular Weight Polypropylene Filaments (H-0042) Spun at 550 Meters/Min Showing the Effects of Either Cold Drawing and Annealing at 140°C (b through d) or Hot Drawing at 140°C (e through g), (a) As-Melt Spun, (b) DI, Draw Ratio = 2.0, (c) DII, Draw Ratio = 2.9, (d) DIII, Draw Ratio = 3.8, (e) TI, Draw Ratio = 2.0, (f) TII, Draw Ratio = 2.9, (g) TIII, Draw Ratio = 3.8

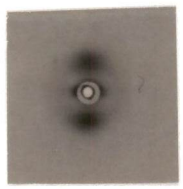
ratios, all the samples seem to have f_c values of 0.78 to 0.94

Small Angle X-Ray Scattering--Results

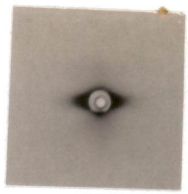
Figure 45 shows SAXS patterns for the as-spun, hot drawn at 140°C, cold drawn and annealed at 140°C for H-1200-200 specimens. The extent of drawing was to Stage II. Figure 45 shows a ring pattern for the spun fiber, equatorial streaks with traces of meridinal spots cold drawn fiber and meridinal and equatorial spots for the annealed and hot drawn specimens.

Birefringence--Results

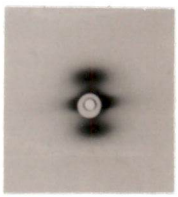
Samuels (83) has carried out detailed study of structure development in drawn polypropylene films and fibers. In the present work birefringence was used for quantitative orientation studies on drawn filaments. It is interpreted as the average molecular orientation developed in the specimen. Figure 46 presents a plot of birefringence of spun and drawn fibers plotted versus the draw ratios. The birefringence increases with the draw ratio. The increase in the birefringence is rapid in the low draw ratio regions. In general, beyond a certain draw ratio, characteristic of the starting sample, the birefringence appears to level off. In the low draw ratio regions the birefringence is higher for the T-series compared with D-series. But at high draw ratios, the D-series reach higher birefringence values than do the T-series samples drawn to equal extension. As suggested by Samuels (83), this may be due to higher crystallinity in annealed samples. For a given extension, samples with higher spinline stress values show higher levels of molecular orientations.



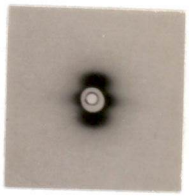
(a)



(b)



(c)



(d)

Figure 45. SAXS Patterns for As-Spun and Drawn (Draw Ratio = 6.8) H-1200-200 Fibers, (a) As-Spun, (b) Cold Drawn, (c) Cold Drawn, Annealed at 140°C for 15 Minutes, (d) Hot Drawn at 140°C (Time Taken for Drawing ∿ Seven Minutes)

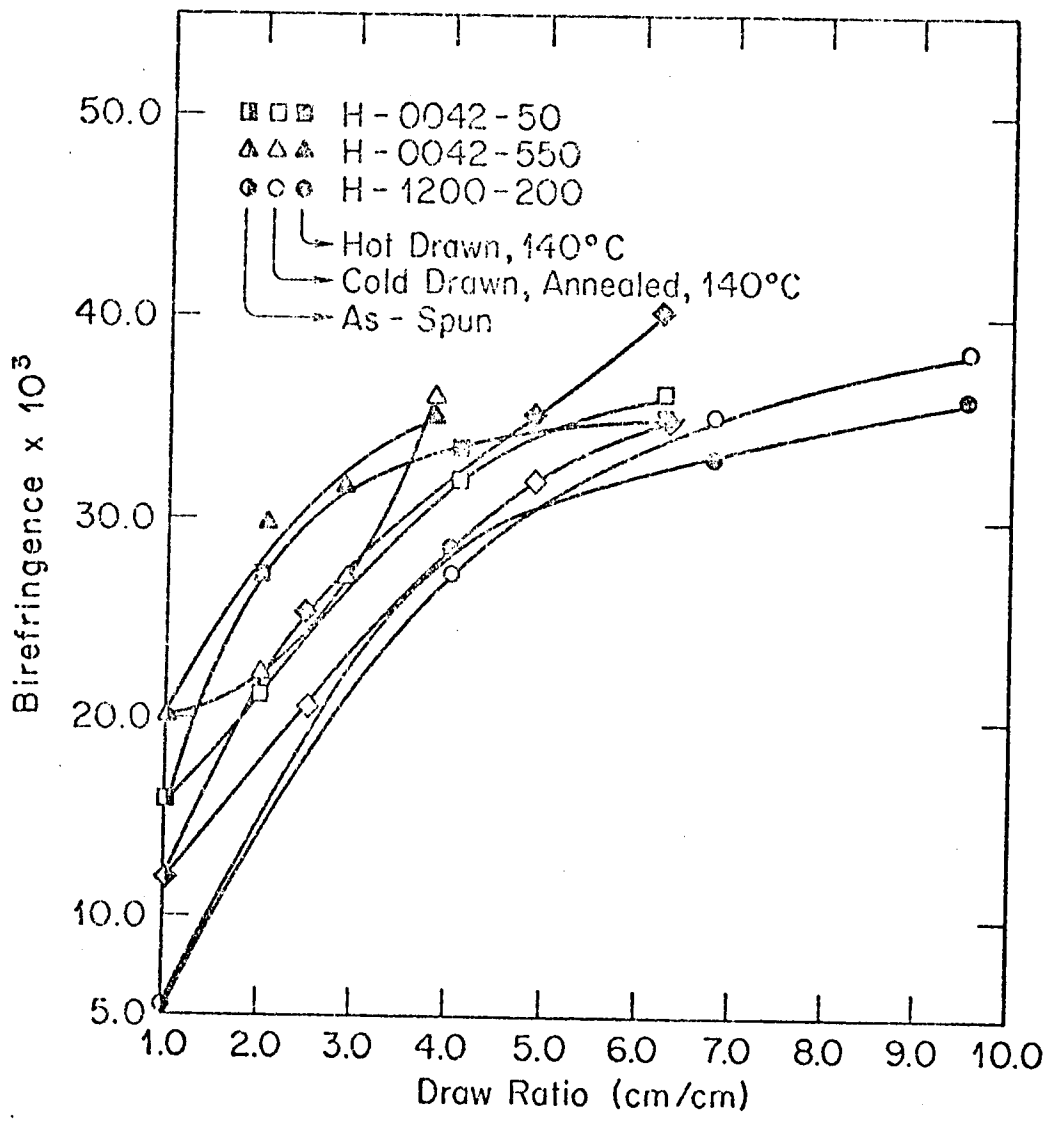


Figure 46. Birefringence Versus Draw Ratio of As-Spun, Cold Drawn and Annealed and Hot Drawn Polypropylene Fibers

Discussion of Structural Changes During Drawing and Annealing

The cold drawing process destroyed the ideal molecular packing and produced a transition to paracrystalline, smectic structure. However, annealing restored the monoclinic structure. Thus the net result of cold drawing and annealing was an increase in the crystallinity and orientation and a decrease in the crystallite size compared to the as-spun filaments. The measured value of crystallinity is comparable to the numbers noted by Samuels (83) for the drawn filaments. However, it is important to note that the SAXS pattern exhibited equatorial scattering which has often been interpreted as due to the presence of voids (91). Such voids would decrease the density of the sample and its apparent crystallinity. This would seem to further substantiate any increase in crystallinity due to the annealing treatment.

The development of orientation as was observed in Figures 42, 43 and 44 show little variation with the increasing draw ratio beyond the natural draw ratio.

From the SAXS patterns in Figure 45 it is clear that the drawing and annealing processes are causing substantial changes at the spherulite and lamellar level of the fiber. The structure of the spun H-1200-200 sample can be interpreted as a spherulitic morphology with a nearly random orientation of lamellar crystals. The pattern for the cold drawn specimen shows the absence of periodic structure; only equatorial scattering from voids parallel to fiber axis (exposure time 12 hours) is noticeable. This would seem to indicate that the lamellae are largely destroyed by the cold drawing. A model similar to that proposed by Peterlin (76) would seem to apply if the lamellae

are assumed to be almost destroyed. Annealing the cold drawn sample results in stacks of lamellar crystals with their faces perpendicular to the fiber axis. These lamellae are separated by interlamellar amorphous regions and tie molecules. These stacks of lamellae produce the two strong meridinal spots observed in the SAXS pattern. The width of these spots indicate that either the lamellar width is small or that the lamellae are slightly tilted to give broad meridinal spots as in drawn polyethylene. The annealed fibers also show the presence of voids parallel to the fiber axis, but these appear to be fewer in number than in the as-cold drawn samples. The long spacing for this specimen was found to be 147Å, which is close to the average value of 151Å reported by Samuels (83) for heat set samples. The SAXS pattern of the hot-drawn fibers show characteristics similar to those of the annealed sample. The long spacing in the hot drawn sample is greater ($L \sim 200Å$). There are fewer voids as is indicated by less equatorial diffuse scattering. The width of the meridinal reflection is smaller than for the cold drawn and annealed sample. This would seem to indicate that the lamellae have greater width in the direction perpendicular to the fiber axis than in the cold draw and annealed sample. The meridinal spots appear to be more intense in the hot drawn fibers for the same time of film exposure. This indicates that the drawing at higher temperature results in a more perfect lamellar structure. The annealing process adapted here (140°C, 15 minutes) partially restores the destroyed lamellar structure. It is also worthwhile to note that the hot drawing process at 140°C was completed in about half the time that was used in annealing process.

White, Dharod and Clark (100) and Sze, Spruiell and White (91) studied in detail the structural changes during cold drawing and annealing of polyethylene fibers. The present observations appear similar to those supported by these authors. Samuels (83) discussed different deformation behaviors in the low and high draw regions (see Chapter II) in which the spherulitic character of the fiber sub-structure is lost and the structure becomes micro-fibrillar. This region was not studied in detail in the present experiments.

B. MECHANICAL PROPERTIES OF DRAWN FIBERS

Results

The D- and T-series fibers were subjected to mechanical testing at a strain rate of 0.5 inches/min on an Instron Tensile Tester. Modulus, tensile strength and elongation to break were calculated for all the specimens.

Figure 47 shows typical stress-strain plot of drawn and as-spun specimens. From the figure it is clear that the drawn fibers show a remarkable increase in tensile strength and drastic decrease in elongation to break in comparison with the spun fibers. Though it is not clear from Figure 47, the modulus was also found to be high for the drawn samples.

Figure 48 shows the effect of draw ratio on the tensile strength. The tensile strength is increasing with increasing draw ratio. For a given specimen and draw ratio, the tensile strength is higher for series T in comparison with the series D. Also at given draw ratios the tensile strength is higher for the higher molecular weight samples

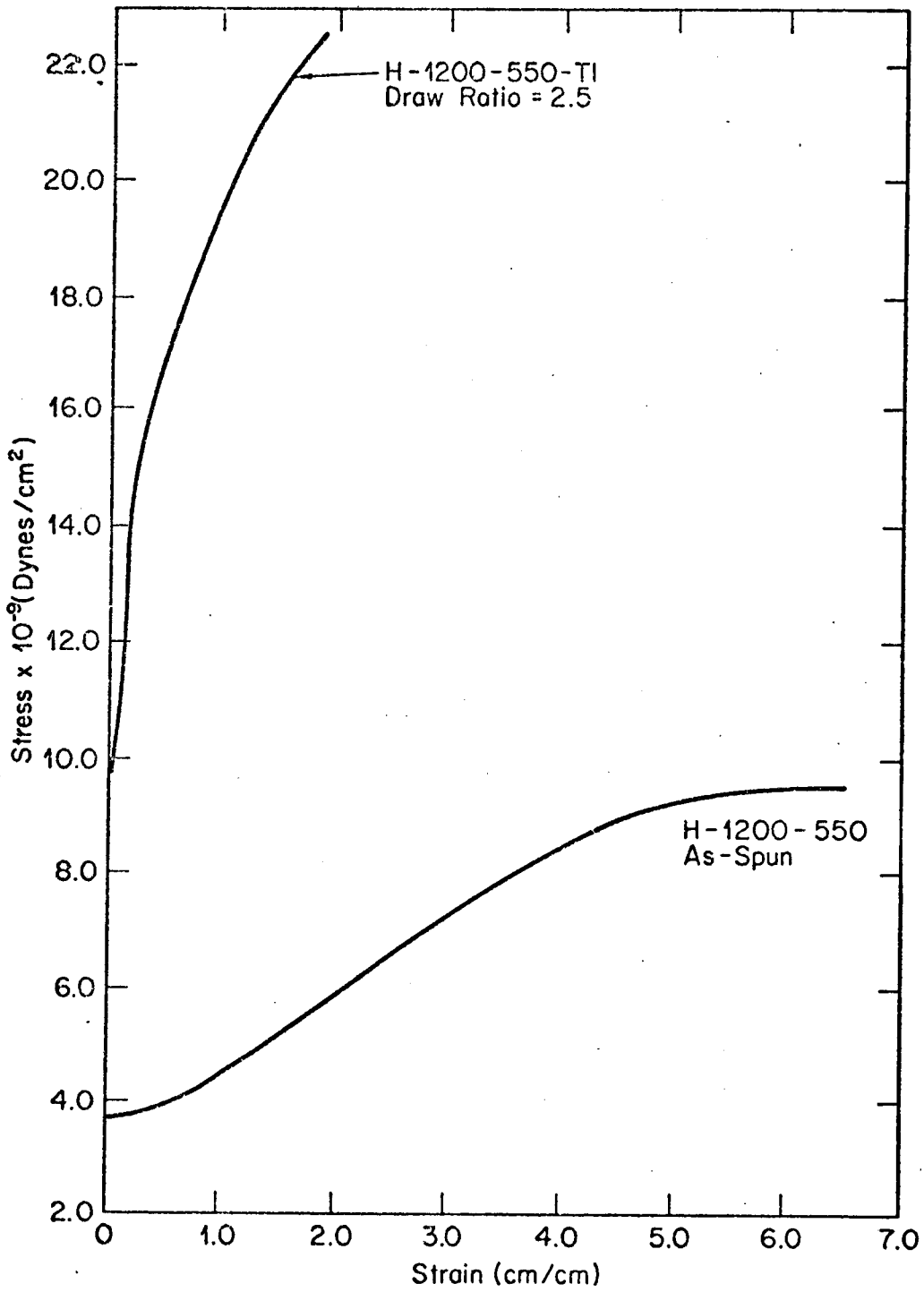


Figure 47. Typical Stress-Strain Curves for Drawn and As-Spun Polypropylene Fibers

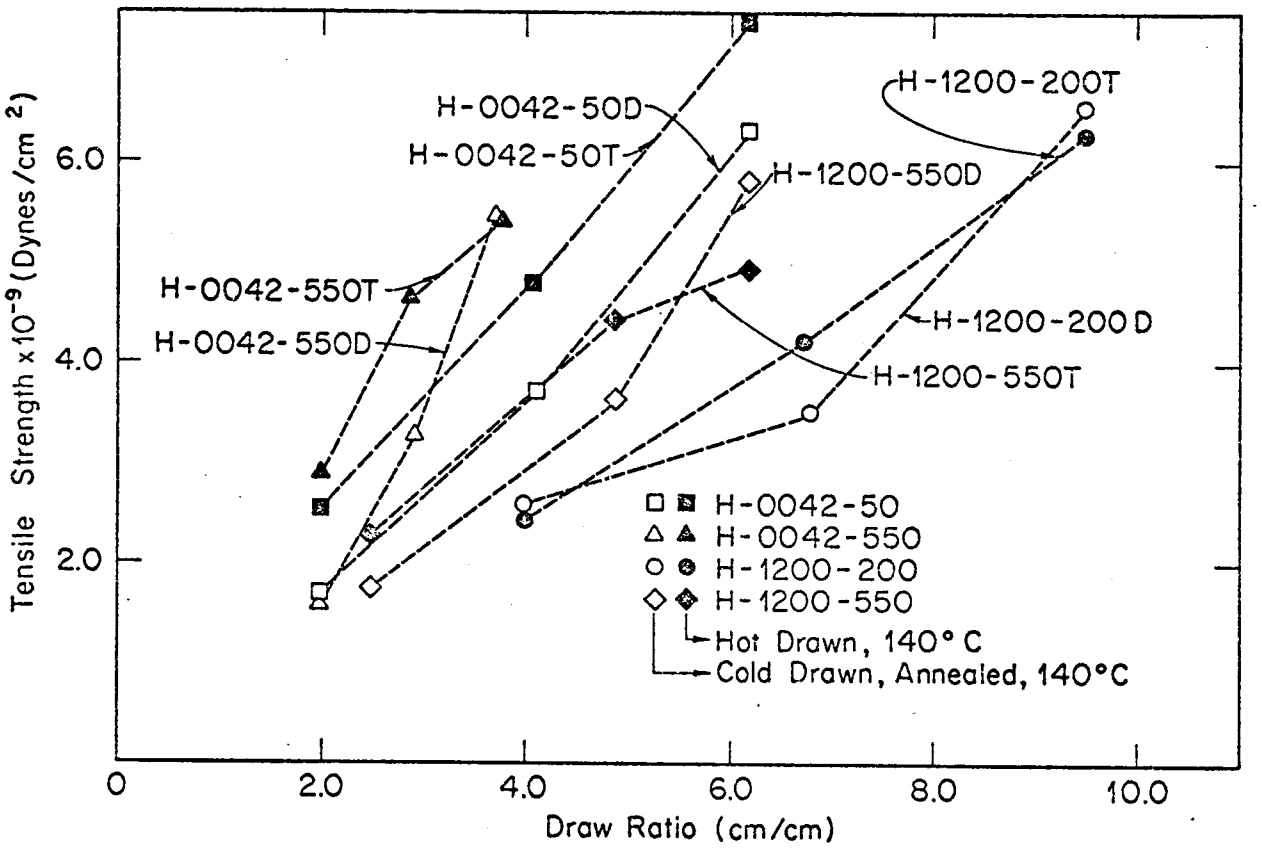


Figure 48. Tensile Strength Versus Draw Ratio of Cold Drawn and Annealed and Hot Drawn Polypropylene Fibers

and for filaments spun under high stress.

Figures 49, 50, and 51 show modulus, tensile strength and percent elongation to break plotted against the birefringence. The modulus and tensile strength are increasing for both series T and D, whereas the elongation to break decreases with birefringence.

Discussion of Mechanical Property Measurement

Though the mechanical properties show a regular behavior with draw ratio, a general correlation of the properties with draw ratio is not possible because of the dependence of the mechanical properties on the structure of the starting spun filament and the processing path (see Figure 48). Samuels (83) suggested that the state of orientation and not the fabrication draw ratio should be used to characterize mechanical properties of fibers and film. In the present work birefringence was used to correlate the mechanical properties of drawn samples. Figures 49, 50 and 51 show excellent correlation of mechanical properties with birefringence. Though the mechanical properties of the filaments greatly depend on the starting structure and the mechanical and thermal processes it was subjected to; knolwedge of the birefringence alone can lead to the determination of these properties. This is very important from the technological point of view because birefringence can be measured very easily. From the WAXS and the f_c values in Table VI (Appendix A), we can predict that the mechanical properties would not correlate with f_c. This is because the fibers are highly oriented and there is little change in the orientation from State I to Stage III of drawing during which the mechanical properties are increasing

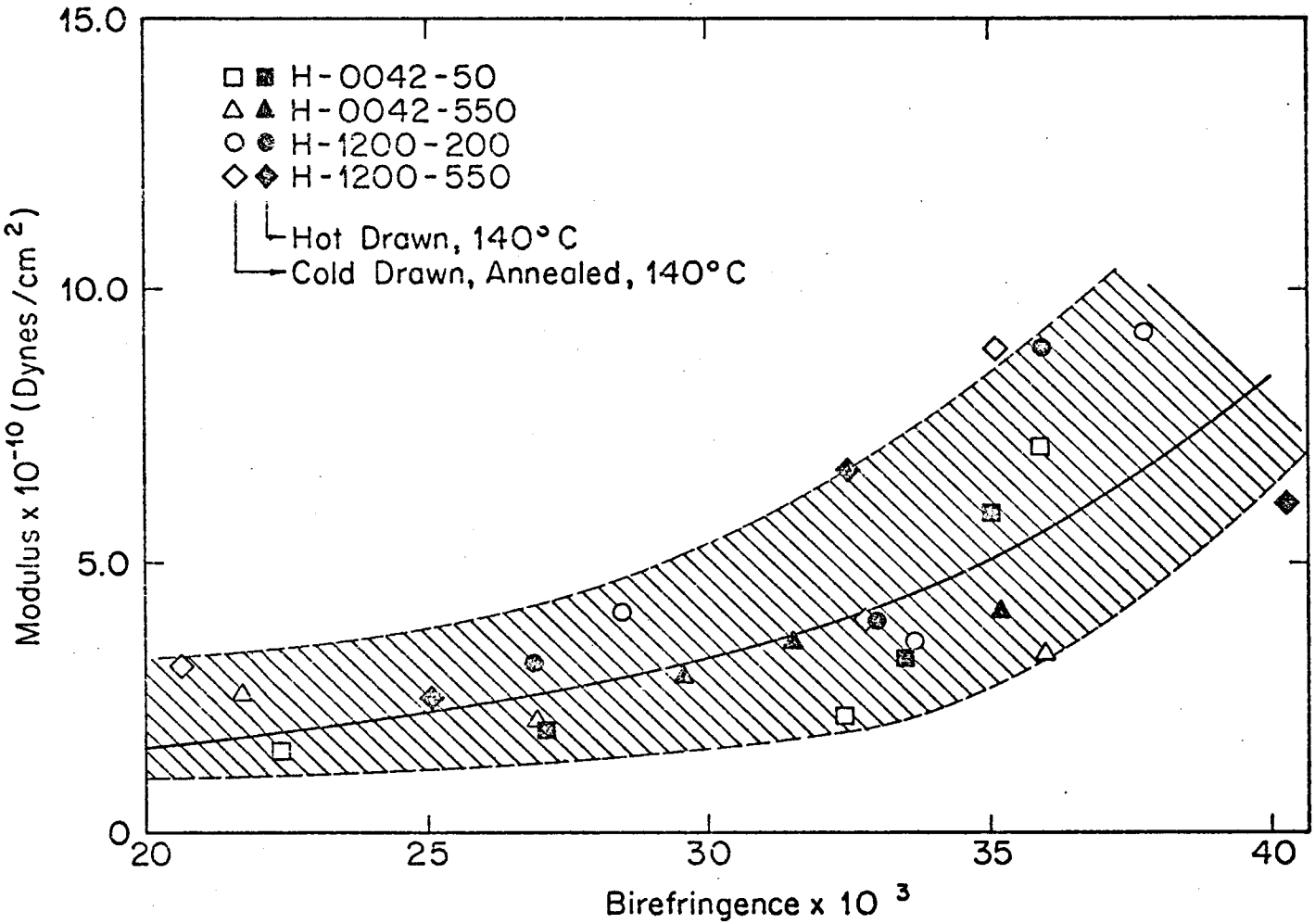


Figure 49. Modulus Versus Birefringence of Cold Drawn and Annealed and Hot Drawn Polypropylene Fibers

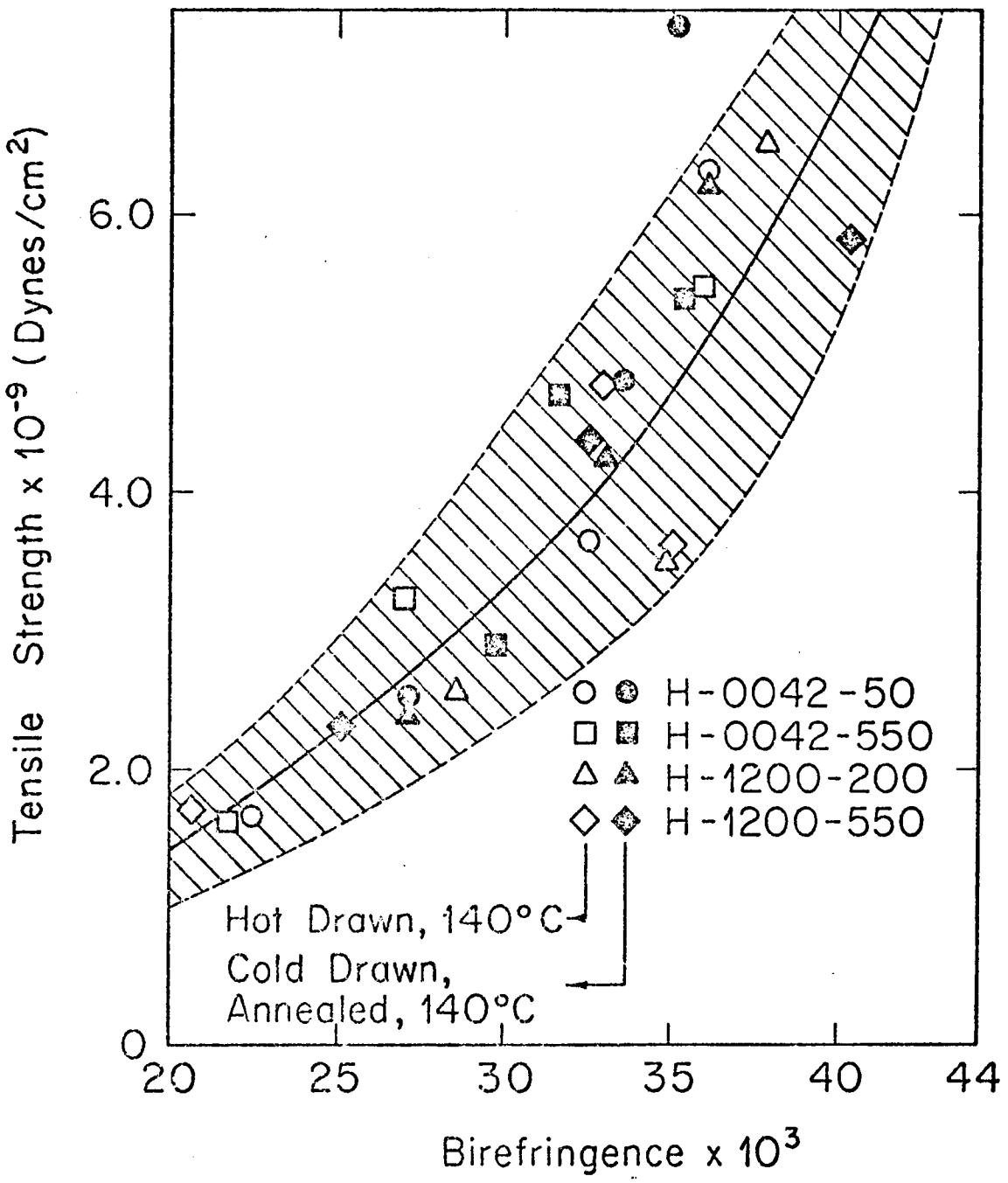


Figure 50. Tensile Strength Versus Birefringence of Cold Drawn and Annealed and Hot Drawn Polypropylene Fibers

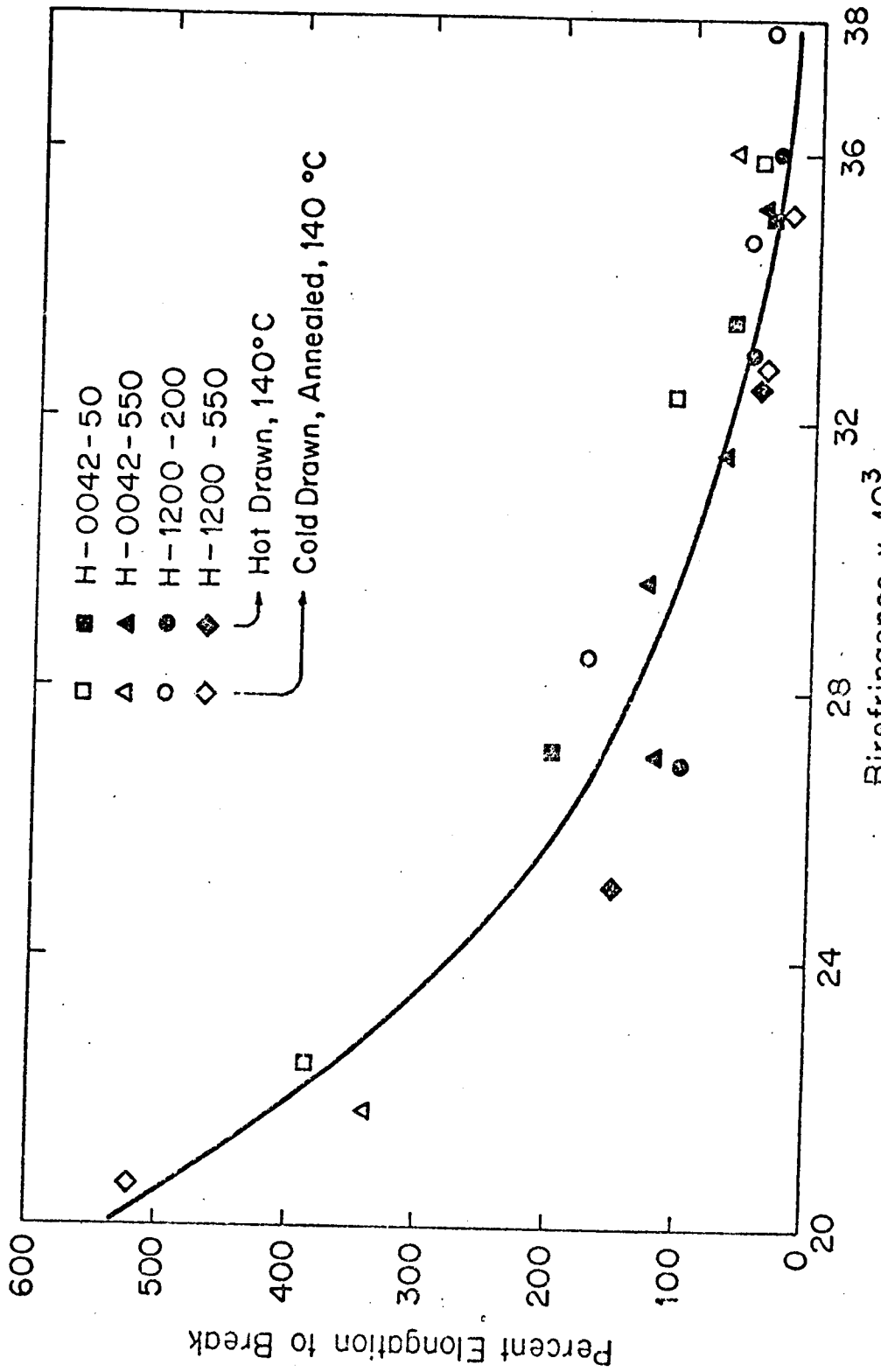


Figure 51. Percent Elongation Versus Birefringence of Cold Drawn and Hot Drawn Polypropylene Fibers

greatly.

Samuels (83) correlated the mechanical properties of the drawn filaments with either average orientation or amorphous orientation in the fiber. The amorphous orientation factor (f_{am}) showed essentially a linear relationship with tenacity. The average orientation is a weighed sum of crystalline and amorphous orientations. Clearly the present results correlate well with this quantity, since it is proportional to birefringence.

Samuels (83) uses the f_{av} value extensively in correlating the mechanical properties. He quotes a value of 0.76 for f_{av}, which is the transition region between a spherulitic and microfibrillar texture. With the results obtained, we cannot verify or deny this particular value. However, a comment is appropriate with regard to the draw regions characterized by Samuels (83). It appears that his results are generally valid for spherulitic starting materials. As the as-spun orientation increases and the morphology changes the drawing behavior is quite different as is evidenced by the present results for the H-0042 series samples.

CHAPTER VII

PROPERTIES OF SPUN AND DRAWN FIBERS

Chapter V discusses the correlation of tensile properties of spun fibers with spinline variables and structure. Chapter VI discusses correlation of mechanical properties with drawing variables and structure. In this chapter we will attempt to tie together the properties of spun and drawn fibers.

In Chapters V and VI the properties of spun and drawn fibers correlate reasonably well with birefringence. Figures 52, 53, and 54 show the mechanical properties of both as-spun and drawn fibers plotted versus birefringence. The spun samples include a range of molecular weights and fibers spun at different flow rates and spinline stresses. The results on drawn fibers include samples which were subjected to different mechanical and thermal processing. Figures 51 through 53 show excellent correlation of the properties of polypropylene fibers with birefringence. These figures show that for polypropylene fibers with the variables and the range of variables we have considered, a simple knowledge of birefringence at any stage during processing irrespective of the mechanical and thermal treatments, leads to the prediction of its mechanical properties. This remarkable behavior appears to be due to the fact that the average molecular orientation in the sample is a major factor which controls the mechanical properties in the range of samples and variables studied. There may be conditions under which this correlation is not valid and hence it should not be

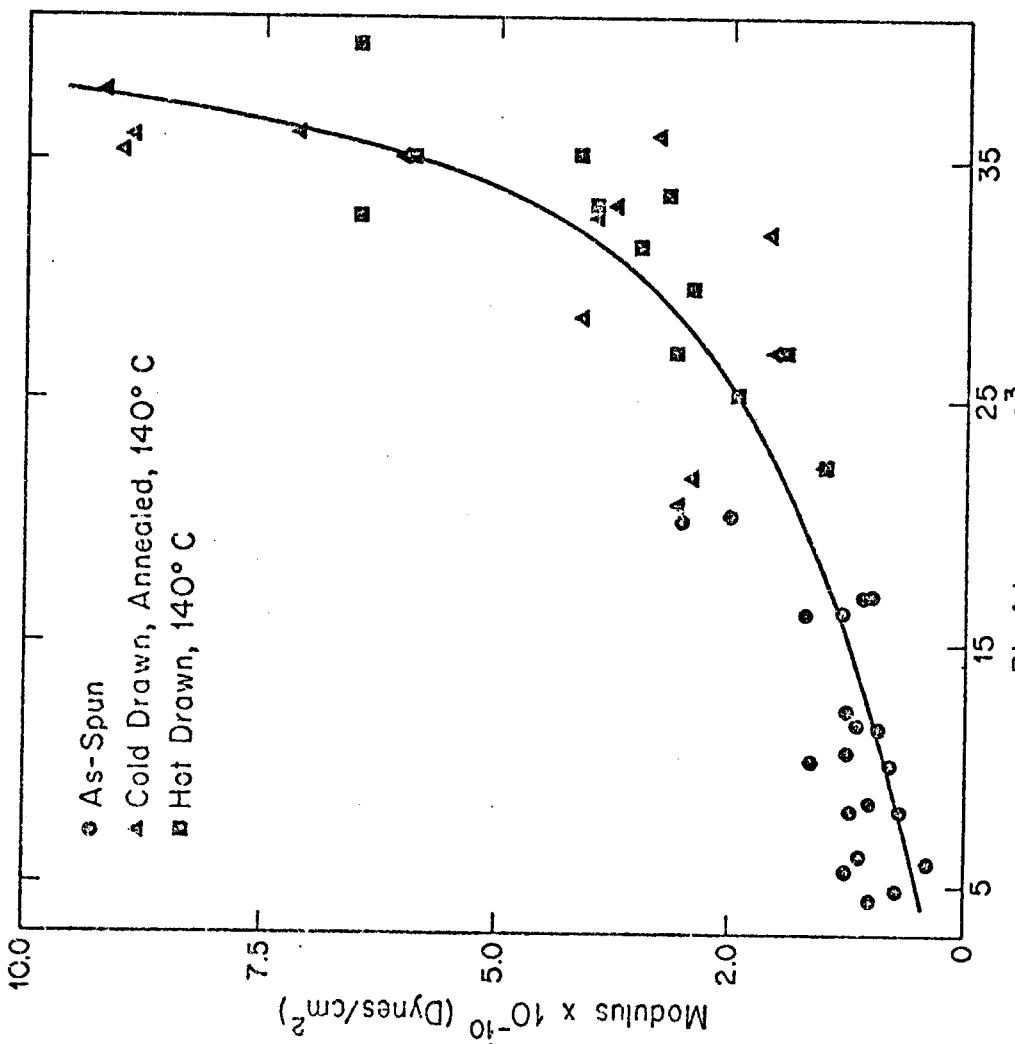


Figure 52. Elastic Modulus Versus Birefringence for Polypropylene Fibers. Variables Include Polymer Molecular Weight, Spinning Conditions (Flow Rate, Take-Up Velocity) and Drawing Procedures

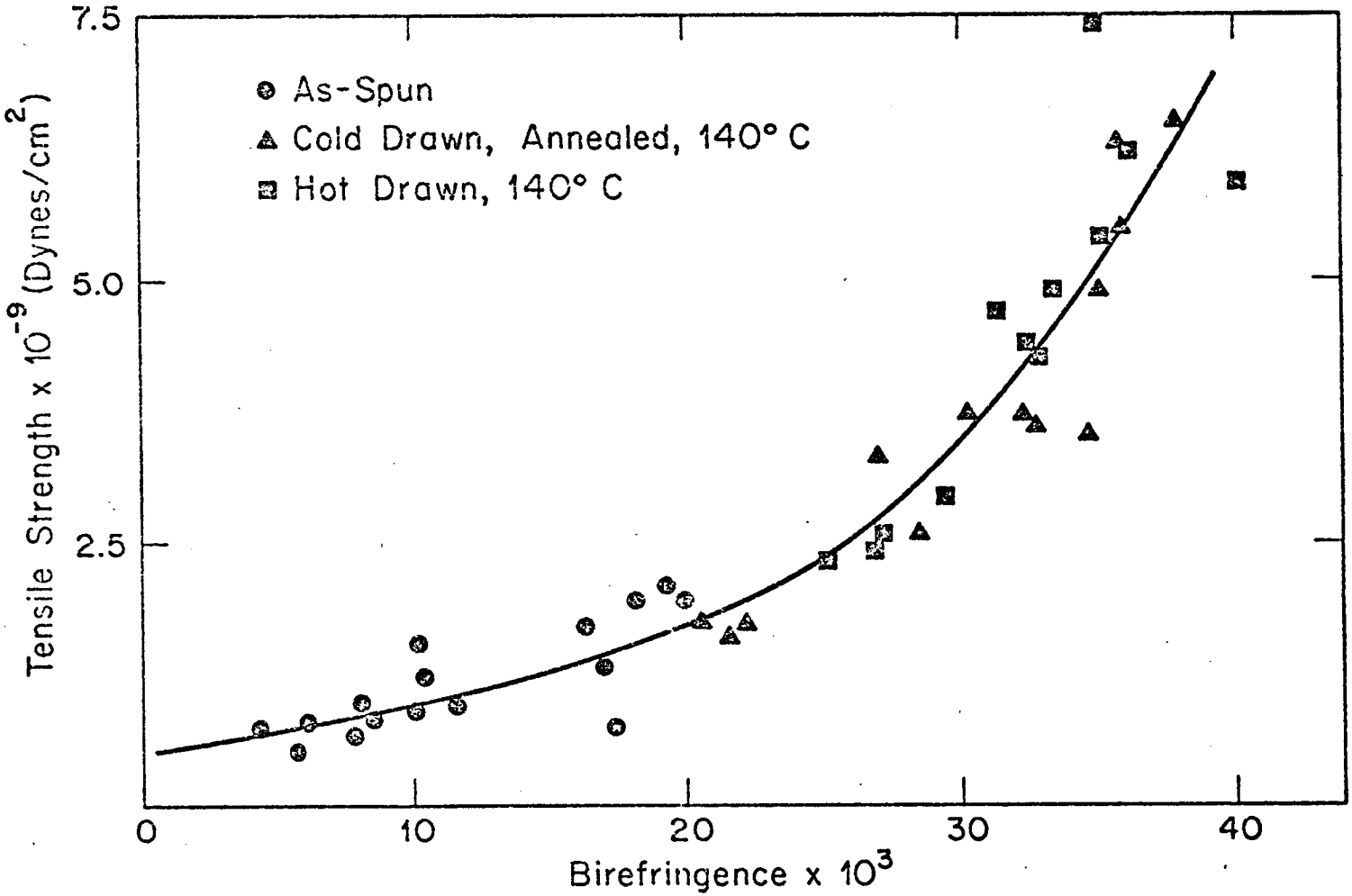


Figure 53. Tensile Strength Versus Birefringence for Polypropylene Fibers. Variables Include Polymer Molecular Weight, Spinning Conditions (Flow Rate, Take-Up Velocity) and Drawing Procedures

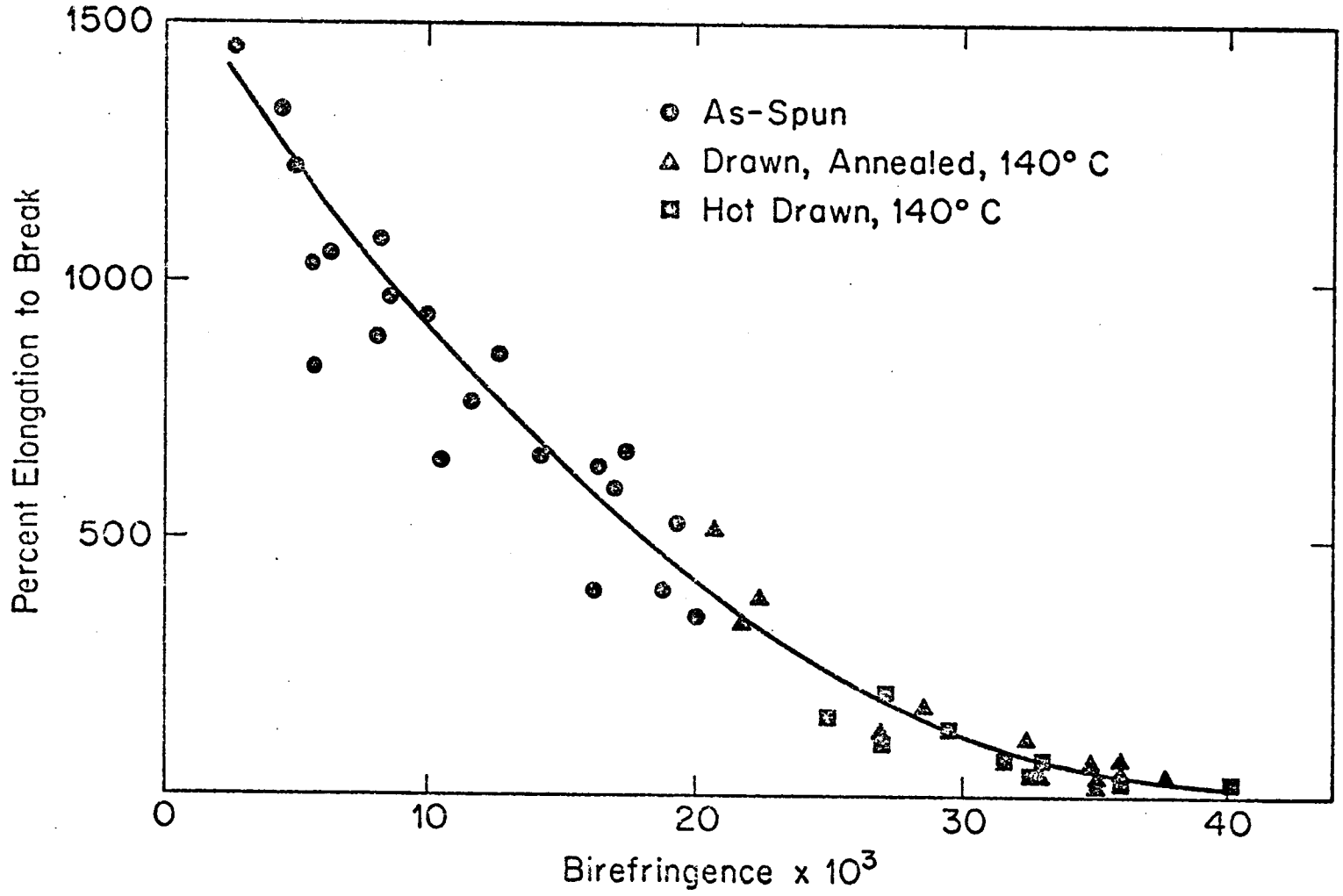


Figure 54. Percent Elongation to Break Versus Birefringence for Polypropylene Fibers. Variables Include Polymer Molecular Weight, Spinning Conditions (Flow Rate, Take-Up Velocity) and Drawing Procedures

considered universal for polypropylene. In particular, the curves show that estimates of properties become more unreliable as the birefringence (and orientation) increases. In this high orientation regime the properties depend on morphological features which are not necessarily reflected in birefringence or orientation measurements. Thus the region of very high strength filaments is a special topic and must be considered separately.

CHAPTER VIII

CONCLUSIONS AND RECOMMENDATIONS

In this chapter the major conclusions resulting from the experimental study are summarized. These are followed by recommendations for further study.

(1) The spinnability of the polypropylenes decreased with increased molecular weight. Melt fracture was observed for high molecular weight Profax® at 2.1 grams/min flow rate and 230°C extrusion temperature. Reducing the flow rate to 0.5 grams/min enabled us to spin this polymer. However, a greater degree (27 percent) of thermal degradation was observed in this high molecular weight material. The Tenite® polymers fractured in the spinline at lower take-up velocities than the Profax®, type 6823 [M.I. = 0.42] polymers. The precise reason for this behavior was not established, but it was suggested that differences in molecular weight distribution may be responsible.

(2) Spinline stress increased with increases in take-up velocity and molecular weight and decreased with increased flow rate.

(3) The crystallinity and orientation correlated with the spinline stress. It was concluded that the morphology of the spun filaments was largely determined by the spinline stress under which crystallization occurred. Variables such as molecular weight and spinning conditions (take-up velocity, mass flow rate, spinning temperature) effect the resulting morphology of the spun filaments, but the effects of the variables appear to be associated with their effect on

the spinline stress.

(4) The tensile properties of the spun fibers also correlated with the spinline stress. It was concluded that this was a result of the fact that the morphologies of the filaments were controlled by the spinline stress.

(5) Structural variables, f_c, f_{am} and birefringence, also gave useful correlations of tensile properties of the spun filaments. For as-spun filaments, correlations with birefringence and c-axis crystalline orientation factor appeared to have less scatter than the amorphous orientation factor, but there was little to recommend one of these correlations over the other.

(6) Modulus and tensile strength are generally higher in the drawn fibers than in the spun fibers. Percent elongation to break is generally lower in drawn fibers. However, at high spinline stresses the mechanical properties of the spun filaments approach those of some drawn fibers (see also conclusions (8) and (9) below). Increasing draw ratio improved modulus and tensile strength and decreased the elongation to break. There was also an indication that the hot drawn fibers showed better properties than the cold drawn and annealed fibers under the conditions investigated.

(7) Under the present drawing conditions the hot drawn fibers usually yielded somewhat better molecular orientation and more perfect (and larger) crystalline domains than the cold drawn and annealed samples. Based on the correlation of mechanical properties with birefringence discussed below, it is likely that these differences were largely responsible for the observed differences in mechanical properties.

(8) The mechanical properties of both the cold drawn and annealed and the hot drawn fibers correlated well with the birefringence, which is a measure of average molecular orientation in the filament.

(9) This correlation with birefringence could be extended to include spun fibers as well as drawn filaments. It is significant that the correlation seemed valid independent of the molecular weight of the polymer and the spinning and/or drawing conditions. At this stage it is appropriate to note that the correlation with birefringence should not be extrapolated into higher draw ratio ranges as it appears that mechanical properties continue to increase in this range while birefringence (orientation) saturates. Also the correlation probably should be restricted to filaments produced by methods similar to those used in the present investigation.

Recommendations for further study include the following:

(1) The effects of the extrusion rate, spinneret dimensions and molecular weight distribution need further study.

(2) In the present experiments, there seems to be a transition in the spinline stress from moderate values to high which resulted in a jump (from about 0.6 to 0.91) in the crystalline orientation factors. This transition region needs further study.

(3) More complete characterization of both spun and drawn fibers through small angle light scattering and transmission electron microscopy would be useful.

(4) A careful study of the deformation mechanism at low draw ratios is needed which emphasizes the differences in behavior of

samples which exhibit necking and those which do not exhibit definite yield and necking behavior is needed.

BIBLIOGRAPHY

BIBLIOGRAPHY

1. Abbott, L. E. and J. L. White, Appl. Poly. Symposium, No. 20, 247 (1973).

2. Abbott, L. E., M.S. Thesis in Chemical Engineering, University of Tennessee, Knoxville (1973).

3. Acierno, D., J. N. Dalton, J. M. Rodriguez and J. L. White, J. Appl. Poly. Sci., 15, 2395 (1971).

4. Addink, E. J. and J. Bientema, Polymer, 2, 185 (1961).

5. Aggarwal, S. L., G. P. Tilley and O. J. Sweeting, J. Poly. Sci., 51, 551 (1961).

6. Alexander, L. E., X-Ray Diffraction Methods in Polymer Science, John Wiley and Sons, Inc., New York (1969).

7. Anderson, P. G. and S. H. Carr, J. Material Sci., 10, 870 (1975).

8. Ashby, G. E. and D. F. Hoeg, J. Poly. Sci., 39, 535 (1959).

9. Avrami, M., J. Chem. Phys., 7, 1103 (1939), 8, 212 (40), 9, 177 (1941).

10. Balta, F. J. and A. Peterlin, J. Material Sci., 4, 722 (1969).

11. Bergerzoni, A. and A. J. Diecresce, Poly. Eng. Sci., 6, 45 (1966).

12. Bettleheim, F. A. and R. S. Stein, J. Poly. Sci., 31, 523 (1958).

13. Billmeyer, F. W., Textbook of Polymer Science, Interscience Publishers, New York (1962).

14. Boye, C. A., M. T. Watson and H. W. Patton, J. Poly. Sci., 47, 139 (1960).

15. British Patent Specification, 935,809 (1962).

16. Carothers, W. H. and J. W. Hill, J. Am. Chemical Soc., 54, 1579 (1932).

17. Chen, I. J., G. E. Hagler, L. E. Abbott, D. C. Bogue and J. L. White, Trans. Soc. Rheol., 16, 473 (1972).

18. Chiang, R., J. Poly. Sci., 28 (1958).

19. Clark, E. S., Bulletin of American Physical Soc., (March 1970).

20. Clark, E. S., Poly. Sci. and Technology, Vol. 1, R. W. Lenz and R. S. Stein, Editors, Plenum Press, New York (1972).

21. Clark, E. S. and J. E. Spruiell, Poly. Eng. Sci., 16(3), 176 (1976).

22. Dees, J. R. and J. E. Spruiell, J. Appl. Poly. Sci., 18, 1055 (1974).

23. Dharod, K. C., M.S. Thesis in Chemical Engineering, The University of Tennessee, Knoxville (1973).

24. Danusso, F., G. Moraglio, W. Ghiglia, L. Molta and G. Talamini, Chim. & Ind., 41, 748 (1959).

25. Fankuchen, I. and M. Mark, J. Appl. Phys., 15, 364 (1944).

26. Frank, H. P., Polypropylene, Gordon and Breach Publishers, New York (1968).

27. Freeman, H. I. and M. J. Coplan, J. Appl. Poly. Sci., 8, 2389 (1964).

28. Fung, P. Y. F., E. Orlando and S. H. Carr, Poly. Eng. Sci., 13, 295 (1973).

29. Garby, J. A. and R. H. Ralston, SPE Trans., (January 1964).

30. Geil, P. H., Polymer Single Crystals, Krieger, New York (1973).

31. Gezovich, D. M. and P. H. Geil, Poly. Eng. Sci., 8(3), 202 (1968).

32. Glenz, W., A. Peterlin and W. Wilkes, J. Poly. Sci., Pt. A-2, 9, 1243 (1971).

33. Griffith, H. J. and G. Ranby, J. Poly. Sci., 38, 107 (1959).

34. Han, C. D. and R. R. Lamonte, Trans. Soc. Rheol., 16, 447 (1972).

35. Han, C. D., R. R. Lamonte and J. Shah, J. Appl. Poly. Sci., 16, 3307 (1972).

36. Henson, H., M.S. Thesis, University of Tennessee, Knoxville (in progress) and H. Henson and J. E. Spruiell, private contact.

37. Hermans, P. H., J. J. Hermans, D. Vermeer and A. Weidinger, Red. Chim. Trav., 65, 427 (1946).

38. Higgins, T. D. and G. M. Bryant, J. Appl. Poly. Sci., 8, 2399 (1964).

39. Hosemann, R., J. Appl. Phys., 34, 25 (1963).

40. Hoshino, S., E. Meinecke, J. Powers and R. S. Stein, J. Poly. Sci., Pt-A, 3, 3041 (1968).

41. Hoshino, S., J. Powers, D. G. Legrand, H. Kawai and R. S. Stein, J. Poly. Sci., 58, 185 (1962).

42. Ishibashi, T., K. Aoki, and Y. Ishii, J. Appl. Poly. Sci., 14, 1597 (1970).

43. Kapur, S. and C. E. Rogers, J. Poly. Sci., 10, 2107 (1972).

44. Kasai, N. and M. Kakudo, J. Poly. Sci., Pt. A2, 1955 (1961).

45. Kase, S. and T. Matsuo, J. Poly. Sci., Pt. A-3, 2541 (1965).

46. Katayama, K., T. Amano and K. Nakamura, Kalloid Z, 226, Heft-2, 125 (1967).

47. Katz, J. R., Kolloid Z, 36, 300 (25).

48. Keith, H. D. and F. J. Padden, J. Appl. Phys., 30, 1485 (1959).

49. Keith, H. D. and F. J. Padden, J. Appl. Phys., 30, 1479 (1959).

50. Keller, A. J. Poly. Sci., 15, 31 (55); 17, 291 (55); 21, 363 (58).

51. Keller, A. J. Poly. Sci., 17, 35 (1955).

52. Keller, A. and M. J. Machin, J. Macromol. Sci. Phys., B1(1), 41, (1967).

53. Khokhani, M. J. and J. E. Spruiell (manuscript in progress).

54. Khoury, F., J. Research of the N.B.S. A., 70A, No. 1 (1966).

55. Kim, H. C. and L. Mandelkern, J. Poly. Sci., Pt. A2, 6, 181 (1968).

56. Kitao, T., S. Ohya, J. Furukawa and Yamashita, J. Poly. Sci.-Phys., 11, 1091 (1973).

57. Krassig, J. and J. W. Ketchren, J. Poly. Sci., 51, 123 (1961).

58. Kresser, T. O. J., Polypropylene, Reinhold Publishing Company, New York (1960).

59. Lamonte, R. R. and C. D. Han, J. Appl. Poly. Sci., 16, 3285 (1972).

60. Mandelkern, L., F. A. Quinn and P. J. Flory, J. Appl. Phys., 25, 830 (1954).

61. Meares, P., Polymers: Structure and Bulk Properties, D. Van Nostrand Company, London (1965).

62. Marrow, D. R., J. Macromol Sci. Phys., 133(1), 53 (1969).

63. Marrow, D. R. and B. A. Newman, J. Macromol Sci. Phys., 53 (1969).

64. Miklowlitz, I., J. Colloid Sci., 2, 193 (1947).

65. Millbert, E. M., J. Appl. Phys., 33, 1766 (1962).

66. Miller, R. L., Polymer, 1, 135 (1960).

67. Nakamura, J., T. Watanabe and K. Katayama, J. Appl. Poly. Sci., 16, 1077 (1972).

68. Natta, G. P., J. Am. Chem. Soc., 77, 1708 (1955).

69. Natta, G., P. Corradini, M. Cesari, Atti. Accad. Naz. Lincei, Rend. Classe Sci. fis-mat-e Nat., [8], 21, 365 (1956).

70. Natta, G., M. Peraldo, and P. Corradini, Atti. Accad. Maze. Lincei, Rend., 26, 14 (1959).

71. Natta, G. and P. Corradini, Nuovo Cimento, 15, 40 (1960).

72. Natta, G. Makromol Chem, 35, 193 (1960).

73. Natta, G., I. Pesquon, A. Zambelli, and G. Gatti, Makromol Chem., 70, 191 (1964).

74. Padden, F. J. and H. D. Keith, J. Appl. Phys., 37, 4013 (1966).

75. Pearson, J. R. A. and M. A. Matovich, Ind. Eng. Chem. Fundamentals, 8, 605 (1969).

76. Peterlin, A., J. Material Sci., 6, 490 (1971).

77. Sakaokusk and A. Peterlin, J. Appl. Phys., 38, 4152 (1967).

78. Samuels, R. J., J. Poly. Sci., Pt. A, 3, 1741 (1965).

79. Samuels, R. J., J. Poly. Sci., Pt. E, 20, 253 (1967).

80. Samuels, R. J., J. Poly. Sci., Pt. A, 3, 1741 (1968).

81. Samuels, R. J., J. Poly. Sci., Pt. A-2, 6, 2021 (1968).

82. Samuels, R. J., J. Poly. Sci., Pt. A-2, 10, 385 (1972).

83. Samuels, R. J., Structured Polymer Properties, John Wiley & Sons, Inc., New York (1974).

84. Sheehan, W. C. and Cole, J. Appl. Poly. Sci., 8, 2359 (1964).

85. Sobue, H. and Y. Tabata, J. Poly. Sci., 39, 427 (1959).

86. Spearot, J. A. and Metzene, Trans. of the Soc. of Rheology, 16:3, 495 (1972).

87. Sprague, B. S., J. Macromol Sci.-Phys., 157 (1973).

88. Spruiell, J. E. and J. L. White, Appl. Poly. Symposia, 27, 121 (1976).

89. Stein, R. S., J. Poly. Sci., 31, 327(58); 27, 381 (1956).

90. Stein, R. S. and F. H. Norris, J. Poly. Sci., 24, 1383 (1957).

91. Sze, G. M., J. E. Spruiell and J. L. White, J. Appl. Poly. Sci. (in progress); W. O. Statton, J. Poly. Sci., 58, 205 (1962).

92. Takahara, H. and H. Kawai, Reports on Progress in Poly. Phys. in Japan, 9 (1966).

93. Takyanagi, M. and T. Kusumoto, Koyo, Kagren Zasshi, 62, 587 (1959).

94. Tung, L. H. and W. C. Taylor, J. Poly. Sci., 21, 144 (1956).

95. Turnby, S. G. and H. Keskkula, J. Appl. Poly. Sci., 9, 2693 (1965).

96. Turnbull, D. and J. E. Fisher, J. Chem. Phys., 17, 71 (1949).

97. Turner Jones, A., J. M. Aizlewood and D. R. Becket, Makromol Chem., 75, 134 (1964).

98. Turner Jones, A. and A. J. Cobbold, Polymer Letters, 6, 539 (1968).

99. Von Hans, J. L., Makromol Chem., 109, 204 (1967).

100. White, J. L., K. C. Dharod and E. S. Clark, J. Appl. Poly. Sci., 18, 2539 (1974).

101. Wilchinsky, Z. W., J. Appl. Phys., 30, 792 (1959).

102. Wilchinsky, Z. W., J. Appl. Phys., 31, 1969 (1960).

103. Wyckoff, J. Poly. Sci., 62, 83 (1962).

104. Ziabicki, A. and K. Kedzierska, J. Appl. Poly. Sci., 2, 14 (1959).

105. Ziabicki, A. and K. Kedzierska, Kolloid Zeitschrift, 171, 52 (1960).

106. Ziabicki, A. and K. Kedzierska, Kolloid Zeitschrift, 175, 14 (1961).

107. Ziabicki, A. and K. Kedzierska, J. Poly. Sci., 6, 361 (1962).

108. Ziabicki, A. and K. Kedzierska, J. Poly. Sci., 6, 111 (1962).

109. Ziabicki, A., Appl. Poly. Symposium, No. 6, 1 (1967).

110. Ziabicki, A., Man Made Fibers, edited by H. Mark, S. Atlas and E. Cernia, New York (1967).

APPENDICES

APPENDIX A

TABLE VI

ESTIMATED VALUES OF CRYSTALLINE ORIENTATION FACTORS OF THE DRAWN FIBERS

Sample	Draw Ratio	Crystalline Orientation Factor, f_c	
		Cold Drawn Annealed	Hot Drawn
H-0042-50	2.0	0.82	0.78
	4.1	0.88	0.93
	6.2	0.92	0.92
H-0042-550	2.0	0.93	0.93
	2.9	0.94	0.94
	3.8	0.94	0.94
H-1200-200	4.0	0.86	0.80
	6.8	0.93	0.90
	9.5	0.93	0.93

APPENDIX B

TABLE VII

EXPERIMENTAL DATA OF POLYPROPYLENE FIBERS SPUN AT 230°C EXTRUSION TEMPERATURE

Polymer	Flow Rate gm/min	Take-up Velocity m/min	Diameter Microns	Spinline Stress x 10^{-8} dynes/cm^2	Modulus x 10^{-9} dynes/cm^2	Yield Strength x 10^{-8} dynes/cm^2	Tensile Strength x 10^{-8} dynes/cm^2	Percent Elongation to Break x 10^{-2}	Percent Elastic Recovery	Percent Crystallinity	Total Birefringence x 10^3	Amorphous Birefringence x 10^3	Crystalline Orientation Factors f_e	f_b	f_a	Amorphous Orientation Factor
H-1200	2.1	50	255	0.3	10.0	3.1	6.5	14.5	12.8	53.1	2.7	-0.15	0.19	-0.11	-0.08	0.01
		100	184	0.4	7.4	---	5.1	12.2	--	54.1	4.9	-1.17	0.39	-0.32	-0.08	0.04
		200	148	4.6	12.5	3.92	8.1	10.3	15.2	54.1	5.6	-1.46	0.45	-0.39	-0.061	-0.05
		400	80	10.6	11.5	---	11.5	8.6	--	54.1	11.6	4.73	0.44	-0.36	-0.08	0.17
		550	77	21.5	12.5	5.3	9.2	6.6	26.0	55.5	12.1	1.96	0.63	-0.43	-0.20	0.07
H-0660	2.1	50	165	1.4	12.0	5.0	9.5	10.8	--	--	8.1	4.32	0.24	-0.30	--	0.16
		100	147	2.4	10.0	---	8.4	9.7	--	--	8.5	3.48	0.32	-0.34	-0.02	0.13
		200	123	5.6	12.3	5.6	10.2	8.9	--	--	10.5	3.90	0.42	-0.35	-0.07	0.14
		400	94	13.3	9.1	---	9.3	7.6	--	--	11.6	3.08	0.54	-0.37	-0.02	0.11
		550	79	22.7	10.2	5.6	10.3	6.0	--	--	16.9	7.20	0.62	-0.37	-0.25	0.26
H-0042	0.5	50	116	15.5	12.8	5.7	15.2	6.4	40.4	55.8	16.3	8.30	0.49	-0.40	-0.1	0.31
		100	120	19.4	--	---	--	---	--	55.9	16.2	6.58	0.59	-0.41	-0.15	0.25
		200	73	55.1	17.4	8.0	16.4	4.0	43.4	57.2	18.8	3.79	0.90	-0.48	-0.43	0.15
		400	41	95.6	30.2	---	20.7	5.3	--	57.4	19.3	4.12	0.91	-0.48	-0.44	0.16
		550	38	17.0	25.3	11.3	19.6	3.5	40	57.4	19.9	4.73	0.91	-0.48	-0.44	0.19
T-0900	2.1	50	220	0.3	10.0	3.4	6.9	13.3	14.6	53.8	4.4	-1.74	0.39	-0.31	-0.08	-0.06
		100	165	1.4	11.1	---	7.0	10.5	--	53.8	6.2	-0.56	0.44	-0.38	-0.06	-0.02
		200	113	3.8	7.7	4.0	8.2	9.3	2 .0	53.8	10.0	2.56	0.47	-0.41	-0.07	0.09
		400	97	23.7	10.6	---	7.8	6.7	25.0	55.5	17.4	--	--	--	--	--
T-0.255	2.1	50	222	0.3	4.2	2.0	4.8	8.3	18.4	53.1	5.8	-0.15	0.38	-0.31	-0.08	-0.01
		100	180	3.2	6.7	---	6.5	---	--	53.8	8.0	0.87	0.45	-0.40	-0.05	0.032
		200	132	12.0	16.5	6.5	15.0	6.4	28.5	52.7	10.3	2.43	0.51	-0.42	-0.10	0.09

TABLE VIII

EXPERIMENTAL DATA ON DRAWN POLYPROPYLENE FIBERS

Sample	Spinline Stress x 10^{-9} dynes/cm^2	Draw Ratio	Modulus x 10^{-10} Dynes/cm^2		Tensile Strength x 10^{-9} Dynes/cm^2		Percent Elongation to Break		Birefringence x 10^3	
			Cold Drawn Annealed	Hot Drawn	Cold Drawn Annealed	Hot Drawn	Cold Drawn Annealed	Hot Drawn	Cold Drawn Annealed	Hot Drawn
H-1200-200	4.6	4.0	4.1	3.1	2.6	2.4	172	98	28.5	26.9
		6.8	3.5	3.9	3.5	4.2	52	51	34.7	33.0
		9.5	9.2	9.0	6.5	6.3	39	28	37.8	36.0
H-1200-550	21.5	2.5	3.1	2.4	1.7	2.3	522	150	20.6	25.1
		4.9	3.9	6.5	3.6	4.4	40	43	32.8	32.5
		6.2	9.0	6.0	4.8	5.8	18	25	35.1	40.2
H-0042-50	15.5	2.0	1.5	1.9	1.7	2.6	385	198	22.4	27.1
		4.1	2.2	3.2	3.7	4.8	108	62	32.4	33.5
		6.2	7.1	5.9	6.3	7.4	45	35	35.9	35.0
H-0042-550	170	2.0	2.5	2.9	1.6	2.9	338	127	21.7	29.6
		2.9	2.0	3.5	3.3	4.7	120	67	27.0	31.5
		3.8	3.3	4.1	5.5	5.4	64	41	36.0	35.2

VITA

Hari Prasad Nadella was born in Guntur, A.P., India, on July 1, 1950. He graduated from higher secondary school at Repalle, Guntur in 1967. The same year he entered the Osmania University Hyderabad and graduated in 1970 with a B.S. Special Chemistry. The following year he came to the United States and entered in the B.S. Chemical Engineering program at the University of Akron, Akron, Ohio. Upon graduation, he entered the Graduate School of the University of Tennessee in September 1973 and received the M.S. degree with a major in Chemical Engineering in August 1976. He is currently pursuing a Doctor of Philosophy degree at the same institution.